İSTANBUL TECHNICAL UNIVERSITY ★ INSTITUTE OF SCIENCE AND TECHNOLOGY

AN ASYMPTOTIC MEMBRANE THEORY OF NONLINEARLY ELASTIC TUBES AND A GODUNOV TYPE FINITE VOLUME METHOD FOR AN IMPACT PROBLEM

T.C. YÜKSEKÖĞRETİM KURULU
DOKÜMANTASYON MERKEZİ

M.Sc. Thesis by
Vasfiye Hande METİN, B.Sc.
(509991046)

101332

Date of submission : 18 June 2001

Date of defence examination: 26 June 2001

Supervisor (Chairman): Prof. Dr. Hüsnü Ata ERBAY

Members of the Examining Committee Assoc. Prof. Dr. Faruk GÜNGÖR (İ.T.Ü.)

Prof. Dr. Hilmi DEMİRAY (I.Ü.)

JUNE 2001

İSTANBUL TEKNİK ÜNİVERSİTESİ ★ FEN BİLİMLERİ ENSTİTÜSÜ

NONLİNEER ELASTİK TÜPLERİN BİR ASİMPTOTİK MAMBRAN TEORİSİ VE ÇARPMA PROBLEMİ İÇİN BİR GODUNOV TİPİ SONLU HACİM METODU

T.C. YÜKSEKÖĞRETİM KURULU
DOKÜMANTASYON MERKEZİ

YÜKSEK LİSANS TEZİ

Müh. Vasfiye Hande METİN
(509991046)

Tezin Enstitüye Verildiği Tarih : 18 Haziran 2001
Tezin Savunulduğu Tarih : 26 Haziran 2001

Tez Danışmanı :	**Prof. Dr. Hüsnü Ata ERBAY**
Diğer Jüri Üyeleri	**Doç. Dr. Faruk GÜNGÖR (İ.T.Ü.)**
	Prof. Dr. Hilmi DEMİRAY (I.Ü.)

HAZİRAN 2001

ACKNOWLEDGEMENTS

I acknowledge greatfully my debt to Prof. Hüsnü Ata Erbay who instilled in me a love of mathematics and gave me unfailing encouregement and support over a number of years. He kindly provided me the motivation needed during the preparation of this thesis.

June, 2001 Vasfiye Hande Metin

CONTENTS

LIST OF FIGURES

T.C. YÜKSEKÖĞRETİM KURULU DOKÜMANTASYON MERKEZİ

AN ASYMPTOTIC MEMBRANE THEORY OF NONLINEARLY ELASTIC TUBES AND A GODUNOV-TYPE FINITE VOLUME METHOD FOR AN IMPACT PROBLEM

SUMMARY

In the first part of the present study, an asymptotic membrane theory for finite axially symmetric deformations of nonlinearly elastic circular cylindrical tubes is derived. In the second part, a Godunov-type finite volume method is used to solve numerically an impact problem defined for a circular cylindrical nonlinearly elastic membrane tube. In Chapter 2, a brief introduction to the basic equations of finite elasticity theory is given and the three-dimensional problem for a hollow circular cylinder made of a general homogeneous isotropic nonlinearly elastic material is described. In Chapter 3, an asymptotic expansion theory is used to obtain an asymptotic membrane theory of a thin-walled circular cylindrical tube composed of an incompressible hyperelastic material. The tube is subjected to both tangential and normal tractions on its inner surface while the outer surface is free of tractions. The equations governing dynamic axially symmetric deformations of the membrane tube are obtained for an arbitrary form of the strain-energy function. The analysis is also extended to the case of a compressible hyperelastic tube. Chapter 4 is devoted to a study of the Godunov-type second-order finite volume method proposed for the numerical solution of one dimensional systems of nonlinear conservation laws with source terms. The numerical method is used in Chapter 5 to solve the equations governing dynamic deformations of a nonlinear elastic membrane tube when it is subjected to a dynamic extension. Numerical results are given for the Mooney-Rivlin and neo-Hookean incompressible materials. The question how the present numerical results are related to those obtained in the literature is discussed. The same problem is also studied for both the neo-Hookean compressible material and the Blatz-Ko compressible material. Conclusions are drawn in Chapter 6.

NONLİNEER ELASTİK TÜPLERİN BİR ASİMPTOTİK MAMBRAN TEORİSİ VE ÇARPMA PROBLEMİ İÇİN BİR GODUNOV TİPİ SONLU HACİM METODU

ÖZET

Bu çalışmanın ilk kısmında, nonlineer elastik dairesel silindirik tüplerin sonlu eksenel simetrik deformasyonları için bir asimptotik mambran teorisi türetilir. Çalışmanın ikinci kısmında, bir nonlineer elastik dairesel silindirik mambran tüp için tanımlanmış çarpma problemi sayısal olarak çözülür. Bölüm 2'de sonlu elastisite teorisinin temel denklemlerine bir kısa giriş verilir ve bir genel homojen izotrop nonlineer elastik malzemeden yapılmış, içi boş dairesel silindir için üç boyutlu problem tanımlanır. Bölüm 3'de, sıkışmaz hiperelastik malzemeden oluşmuş, ince-kalınlıklı dairesel silindirik bir tüpün bir asimptotik mambran teorisini elde etmek için asimptotik açılım teorisi kullanılır. Tüpün iç yüzeyi hem normal hem de teğetsel sınır gerilmelerine maruz iken, dış yüzeyi herhangi bir sınır gerilmesine maruz değildir. Mambran tüpün dinamik eksenel simetrik deformasyonlarını yöneten denklemler, şekil değiştirme enerjisinin keyfi bir formu için elde edilir. İnceleme sıkışabilir hiperelastik tüp durumuna da genişletilir. Bölüm 4, kaynak terimleri de içeren nonlineer korunum yasalarından oluşan bir boyutlu sistemlerin sayısal çözümü için önerilmiş olan Godunov tipindeki bir ikinci-mertebe sonlu hacim metodunun çalışmasına ayrılmıştır. Sayısal metod, Bölüm 5'de, bir dinamik uzamaya maruz nonlineer elastik mambran tüpün dinamik deformasyonlarını yöneten denklemleri çözmek için kullanılır. Sayısal sonuçlar Mooney-Rivlin ve neo-Hookyen sıkışmaz malzemeleri için verilir. Şimdiki sayısal sonuçların literatürde elde edilmiş olanlar ile nasıl bağlantılı olduğu sorusu tartışılır. Aynı problem hem neo-Hookyen sıkışabilir malzeme hem de Blatz-Ko sıkışabilir malzeme için de çalışılır. Değerlendirmeler Bölüm 6'da yapılır.

1. INTRODUCTION

An *elastic solid* tends to return to its initial shape when a load is applied and then removed. Often such an elastic solid is called a *nonlinear* elastic solid in the sense that the deflection at a given point in the solid is not proportional to the magnitude of the applied load.

Substantial theoretical and analytical results in the area of nonlinear elasticity have been obtained in the last four decades. One question addressed in a number of papers is to determine all possible solutions of the *equilibrium equations* for a particular class of materials. The accompanying mathematical complexities in solving the equations of nonlinear elastostatics impose specification of the strain energy function to consider deformations for a particular class of materials. Solutions in this context have been crucial to the understanding of material behavior under various loading scenarios. However, even for specific forms of the strain energy function, there has been little progress in our ability to analyze deformations. For *compressible* nonlinear elastic solids, there are relatively few boundary-value problems for which closed form solutions have been found. For such materials, in contrast to the incompressible case, volume changes usually occur. The resulting boundary-value problems are generally much more difficult to solve than their counterparts for incompressible materials. In regard to *dynamic deformations*, only a few exact solutions have been found for both compressible and incompressible nonlinearly elastic solids. We refer the reader to [1] for a discussion on exact solutions and comprehensive list of references.

The difficulties in obtaining the exact solutions of nonlinear elasticity problems have stimulated considerable research effort on the derivation of approximate theories which are based on the introduction of some simplifying approximation.

Nonlinear elastic *shell* theories and nonlinear *membrane* theories among the others are the most common examples of these approximate theories. Shell and membranes are physically three dimensional bodies. But they are curved, thin-walled structures. Membranes are thinner than shells. Approaches to membrane theories range from the purely *direct* to the purely *derived.* A direct theory regards a membrane, *from the start*, as a two dimensional continuum. However, the derived approach recognizes a membrane as a three-dimensional elastic body and derives a system of two-dimensional equations from the three-dimensional elasticity theory by asymptotic analysis. Of course, there is the fundamental and difficult problem of justifying the adequacy and accuracy of membrane theory solutions as approximations of the exact solutions of nonlinear elasticity. The extreme thinness of membrane structures generates two fundamental assumptions:(i) Membrane stiffness is much, much greater than bending stiffness; thus, stress couple effects may be disregarded. (ii) The ratio of thickness to the smallest radius of curvature is much, much less than one; thus terms of the order of this ratio may be disregarded. We refer the reader to [2] for both a recent review on elastic membranes and a comparison of the direct and derived theories from a constitutive point of view.

One must be careful to distinguish between the membrane response of an idealized structure and the response of a true membrane. For instance, a plate or a shell structure may be idealized to respond as a membrane away from its boundaries and consequently the stress couples may be neglected in the interior part of the structure. On the other hand, structure models that cannot support stress couples *anywhere* are by definition true membranes. We refer the reader to [3] for a discussion of a nonlinear elastic plate from these two different perspectives.

The present study has several purposes. The first one is to derive a nonlinear membrane theory for finite axially symmetric dynamic deformations of an *incompressible* nonlinearly elastic circular cylindrical tube. The asymptotic expansion technique is used to obtain the equations of the nonlinear membrane theory by starting from the three-dimensional elasticity theory outlined in Chapter 2. It is assumed that the inner surface of the tube is subjected to both normal and tangential tractions, while the outer surface is free of tractions. Chapter 3 is devoted to the derivation of the reduced equations of motion for an incompressible nonlinearly elastic circular cylindrical membrane. It will be seen in the sequel that the analysis contained in Chapter 3 parallels quite closely that described in [4]. The present discussion of membrane theory is set in a framework which differs in three aspects from that presented in [4]. First we are concerned with finite *dynamic* deformations of nonlinear elastic membranes here whereas the membrane theory derived in [4] is valid only for finite static deformations. Another interesting difference between [4] and the present study arises in consideration of the incompressible material. We consider a circular cylindrical tube composed of an *arbitrary* incompressible elastic material. However, in [4] a circular cylindrical tube made of a neo-Hookean elastic material is considered. Finally, here we prefer to use the *nominal stress tensor* instead of the Cauchy stress tensor used in [4].

The second purpose of the present study is to derive a nonlinear membrane theory for finite axially symmetric dynamic deformations of a circular cylindrical tube made of an arbitrary *compressible* elastic material. For this aim we also consider the case of a compressible elastic tube in Chapter 3 and develope a nonlinear membrane theory.

The next purpose of the present study is to consider wave propagation in a circular cylindrical nonlinear elastic tube when the tube is subjected to dynamic extension. One end of the tube is fixed and the other end is subjected to a dynamic extension. The same problem has been studied by Tait and Zhong [5]. They have considered the tube as an isotropic, homogeneous incompressible membrane and used the membrane theory obtained using the direct approach. They have employed a numerical technique based on the method of characteristics and presented the numerical results for the Mooney-Rivlin material. In another study [6], Tait and Zhong have also considered the same tube and, in addition to the extension, imposed a dynamical twist at the moving end. They have presented the numerical results for the neo-Hookean material. The present discussion of the problem is set in a framework which differs in two aspects from that studied by Tait and Zhong [5]. First, we use the membrane theory obtained by using an asymptotic expansion technique. Second, we use a second-order Godunov method for the numerical solution of the governing equations. In Chapter 4 we shortly summarize mathematical theory of hyperbolic systems and introduce the second-order Godunov method used in our numerical simulations. In Chapter 5 we formulate the problem of dynamic extension of a membrane tube made of an incompressible hyperelastic material and present the numerical results corresponding to both neo-Hookean and Mooney -Rivlin materials. Also we discuss how the results obtained in the present study are related to those obtained in [5]. The same problem is also studied for both neo-Hookean compressible material and the Blatz-Ko compressible material. Finally, in Chapter 6 we conclude the thesis with a discussion of possible extensions of the present study.

We shall cite here only the literature most directly related to the present study and refer the reader to the references in the bibliography at the end of the thesis for a comprehensive list of references.

2. BASIC EQUATIONS

2.1 Introduction

In this chapter a brief introduction to the basic equations of finite elasticity theory is given. The coverage is not intended to be exhaustive and more attention is paid to those part of the theory, which are related to the scope of the thesis. More detail can be found in [1] and [7]. The purpose of Section 2.2 is to briefly summarize the basic equations of finite elasticity theory. The specializations appropriate for cylindrical coordinates are also noted in Section 2.2. The three-dimensional problem for a hollow circular cylinder made of a general homogeneous isotropic nonlinearly elastic material having a natural state is briefly described in Section 2.3. The equations governing finite axisymmetric deformations of the tube are derived in the same section.

In this paragraph some formulae which are used in the subsequent sections are given. A vector $\mathbf{d}$ is called an *eigenvector* of a second-order tensor $\mathbf{D}$ if there is a scalar, d say, such that $\mathbf{D}\mathbf{d} = d\mathbf{d}$. In such a case d is called the *eigenvalue* of $\mathbf{D}$ corresponding to the eigenvector $\mathbf{d}$. The equation det $(\mathbf{D} - d\mathbf{I}) = 0$ is called the *characteristic equation* for $\mathbf{D}$ and it can be written as

$$d^3 - I_1(\mathbf{D})d^2 + I_2(\mathbf{D})d - I_3(\mathbf{D}) = 0$$

where $I_1(\mathbf{D})$, $I_2(\mathbf{D})$ and $I_3(\mathbf{D})$ are called the *principal invariants* of $\mathbf{D}$ and are defined by

$$\begin{aligned}
I_1(\mathbf{D}) &= \operatorname{tr}\mathbf{D}, \\
I_2(\mathbf{D}) &= \frac{1}{2}\left[(\operatorname{tr}\mathbf{D})^2 - \operatorname{tr}\mathbf{D}^2\right], \\
I_3(\mathbf{D}) &= \det\,\mathbf{D} = \frac{1}{6}\left[(\operatorname{tr}\mathbf{D})^3 - 3(\operatorname{tr}\mathbf{D})(\operatorname{tr}\mathbf{D}^2) + 2\operatorname{tr}\mathbf{D}^3\right].
\end{aligned}$$

Here the notations tr and det refer to trace and determinant, respectively. Suppose that d_1, d_2 and d_3 are the eigenvalues of a symmetric second-order tensor $\mathbf{D}$. Then the principal invariants of $\mathbf{D}$ can be expressed in terms of d_1, d_2 and d_3 as follows

$$I_1(\mathbf{D}) = d_1 + d_2 + d_3 \ , \quad I_2(\mathbf{D}) = d_1 d_2 + d_2 d_3 + d_3 d_1 \ , \quad I_3(\mathbf{D}) = d_1 d_2 d_3$$

(see [1] or [7]).

Throughout this chapter we use the notation adopted by Ogden in [1] with a few exceptions: For instance we use $\mathbf{F}$ instead of $\mathbf{A}$ to denote the deformation gradient tensor. Additional references for the topics discussed in the present chapter can be found in the books and papers listed in the references of [1].

2.2 Preliminaries: Equations of Finite Elasticity

Consider a body composed of elastic material. A particular state of the body at some time t_0 is chosen as the reference or undeformed state. Suppose that the body occupies a region $\mathcal{B}_0$ of space in its reference state. Also suppose that the body occupies a region $\mathcal{B}$ of space at current time t. We use fixed rectangular Cartesian coordinate systems to describe the locations of particles in the body for both the reference (Lagrangean) and current (Eulerean) states. Let $\{X_1, X_2, X_3\}$ represent rectangular Cartesian Lagrangean coordinates with orthonormal basis vectors $\{\mathbf{E}_1, \mathbf{E}_2, \mathbf{E}_3\}$ and origin $\mathbf{O}$. Similarly, let $\{x_1, x_2, x_3\}$ represent rectangular Cartesian Eulerean coordinates with orthonormal basis vectors $\{\mathbf{e}_1, \mathbf{e}_2, \mathbf{e}_3\}$ and origin $\mathbf{o}$. We identify a generic material point of the body by the label X. Suppose that the vector $\mathbf{X}$ represents the place occupied by the particle X in the reference configuration and that the vector $\mathbf{x}$ represents the place occupied by the particle X in the current configuration so that

$$\mathbf{X} = X_K \mathbf{E}_K, \qquad \mathbf{x} = x_k \mathbf{e}_k \tag{2.1}$$

where summation convention is used. The equation

$$\mathbf{x} = \boldsymbol{\chi}(\mathbf{X}, t) \tag{2.2}$$

specifies a one-parameter family of deformations and for any fixed t, $\boldsymbol{\chi}$ is called a deformation from the reference configuration. The component form of (2.2) is

$$x_k = \chi_k(X_K, t), \qquad k, K = 1, 2, 3 \tag{2.3}$$

On taking the differential of (2.2) we obtain

$$\mathbf{dx} = \mathbf{F}\ \mathbf{dX}\ . \tag{2.4}$$

where $\mathbf{F}$ is a second-order tensor defined by

$$\mathbf{F} = \mathrm{Grad}\,\boldsymbol{\chi}(\mathbf{X}, t) \equiv \nabla \otimes \boldsymbol{\chi}(\mathbf{X}, t)\ . \tag{2.5}$$

Here the notation Grad (with upper-case G) refers to the gradient operation taken with respect to $\mathbf{X}$ and the symbol $\otimes$ refers to the tensor product (see [1]). The specialization of the above representation to the case of curvilinear coordinates if required can be easily given. An alternative notation for $\mathbf{F}$ is $\partial\mathbf{x}/\partial\mathbf{X} \equiv \partial\boldsymbol{\chi}(\mathbf{X}, t)/\partial\mathbf{X}$. Suppose that $\mathbf{F}$ have components F_{kK} with respect to bases $\{\mathbf{e}_k\}$ and $\{\mathbf{E}_K\}$: $\mathbf{F} = F_{kK}\mathbf{e}_k \otimes \mathbf{E}_K$. Then it follows from (2.5) that $F_{kK} = \partial x_k/\partial X_K$. Equation (2.4) describes how an arbitrary line element $\mathbf{dX}$ at $\mathbf{X}$ transforms under the deformation to the line element $\mathbf{dx}$ at the point $\mathbf{x}$ in the configuration $\mathcal{B}$. The second-order tensor $\mathbf{F}$ is called the *deformation gradient* relative to the reference configuration $\mathcal{B}_0$. Since any line element of material in the reference configuration cannot be reduced to zero by the deformation, $\mathbf{F}$ is a *non-singular* tensor, that is, $\det\mathbf{F} \neq 0$. For convenience we introduce the standard notation

$$J \equiv \det\mathbf{F}\ . \tag{2.6}$$

In components J represents the Jacobian determinant of the transformation of (2.2). If the current and reference configurations coincide or if the deformation is just a rigid rotation, we have $J = 1$.

Since $\mathbf{F}$ is non-singular, it has an inverse $\mathbf{F}^{-1}$, and for convenience we write $\mathbf{B} = (\mathbf{F}^{-1})^{\mathrm{T}}$ where the superscript T denotes transpose. Hence one can write the inverse of (2.4) as $\mathbf{dX} = \mathbf{B}^{\mathrm{T}}\mathbf{dx}$.

From (2.4) we can easily obtain

$$|\mathbf{dx}|^2 - |\mathbf{dX}|^2 = \mathbf{dX}\cdot(\mathbf{F}^{\mathrm{T}}\mathbf{F} - \mathbf{I})\mathbf{dX}, \tag{2.7}$$

which represents the difference between the squared lengths of a line element in the current and reference configurations. The notation $\cdot$ denotes the scalar product. Note that $(\mathbf{F}^{\mathrm{T}}\mathbf{F})^{\mathrm{T}} = \mathbf{F}^{\mathrm{T}}(\mathbf{F}^{\mathrm{T}})^{\mathrm{T}} = \mathbf{F}^{\mathrm{T}}\mathbf{F}$. Therefore it follows that $\mathbf{F}^{\mathrm{T}}\mathbf{F}$ is symmetric. The tensor $\mathbf{F}^{\mathrm{T}}\mathbf{F}$ is called the *right Cauchy-Green deformation* tensor and it is denoted by $\mathbf{C}$. It follows from (2.7) that the material is unstrained at $\mathbf{X}$ if $\mathbf{C} = \mathbf{I}$ where $\mathbf{I}$ is the identity tensor.

The relationship between the volume element $\mathrm{d}V$ in the reference configuration and the corresponding volume element $\mathrm{d}v$ in the deformed configuration is given by

$$\mathrm{d}v = (\det \mathbf{F})\mathrm{d}V \equiv J\mathrm{d}V \tag{2.8}$$

(see [1]). That is, J is the local ratio of current to reference volume of a material volume element. Since we require volume elements to be positive, it follows from the above equation that

$$J \equiv \det \mathbf{F} > 0\ . \tag{2.9}$$

If the volume does not change locally during the deformation, then we have

$$J = 1 \tag{2.10}$$

at $\mathbf{X}$. Such a deformation is said to be *isochoric* (volume preserving) at $\mathbf{X}$. A material subject to the constraint in which the deformation is volume preserving is called an *incompressible material.*

The velocity of the material particle which occupies the place $\mathbf{X}$ in the reference configuration is denoted by $\mathbf{V}(\mathbf{X}, t)$ in the Lagrangean (referential) specification and is defined by

$$\mathbf{V}(\mathbf{X}, t) = \frac{\partial \boldsymbol{\chi}}{\partial t}(\mathbf{X}, t). \tag{2.11}$$

In the Eulerian (current) specification we write $\mathbf{v}(\mathbf{x}, t)$ for the velocity of the material particle which occupies the place $\mathbf{x}$ at time t, where

$$\mathbf{V}(\mathbf{X}, t) = \mathbf{v}(\boldsymbol{\chi}(\mathbf{X}, t), t). \tag{2.12}$$

For convenience we sometimes use a superposed dot to represent $\partial/\partial t$ at fixed $\mathbf{X}$.

The global forms of the conservation of mass, the balance of linear momentum and the balance of rotational momentum are

$$\frac{\mathrm{d}}{\mathrm{d}t}\int_{\mathcal{B}} \rho(\mathbf{x},t)\mathrm{d}v = 0 \tag{2.13}$$

$$\frac{\mathrm{d}}{\mathrm{d}t}\int_{\mathcal{B}} \rho(\mathbf{x},t)\mathbf{v}(\mathbf{x},t)\mathrm{d}v = \int_{\mathcal{B}} \rho(\mathbf{x},t)\mathbf{b}(\mathbf{x},t)\mathrm{d}v + \int_{\partial\mathcal{B}} \mathbf{t}_{(\mathbf{n})}(\mathbf{x})\mathrm{d}a \tag{2.14}$$

$$\frac{\mathrm{d}}{\mathrm{d}t}\int_{\mathcal{B}} \rho(\mathbf{x},t)(\mathbf{x}-\mathbf{x}_0)\times\mathbf{v}(\mathbf{x},t)\mathrm{d}v = \int_{\mathcal{B}} \rho(\mathbf{x},t)(\mathbf{x}-\mathbf{x}_0)\times\mathbf{b}(\mathbf{x},t)\mathrm{d}v + \int_{\partial\mathcal{B}} (\mathbf{x}-\mathbf{x}_0)\times\mathbf{t}_{(\mathbf{n})}(\mathbf{x})\mathrm{d}a \tag{2.15}$$

where ρ is the mass density of the material of the body in the current configuration, the symbol $\times$ denotes the vector product, $\mathbf{b}$ is the body force density, $\mathbf{t}_{(\mathbf{n})}$ is the stress vector field per unit area of surface (the contact force density), da is the surface area element and $\mathbf{x}_0$ is an arbitrary point (see [1]). The stress vector $\mathbf{t}_{(\mathbf{n})}$ depends on the boundary $\partial\mathcal{B}$, of $\mathcal{B}$, over which it acts. It is assumed that the stress vector $\mathbf{t}_{(\mathbf{n})}$ at a point $\mathbf{x}$ depends on the surface only through the (unit) normal $\mathbf{n}$ to the considered surface at $\mathbf{x}$. Therefore we use the notation $\mathbf{t}_{(\mathbf{n})}(\mathbf{x})$ above to make the dependence on $\mathbf{n}$ explicit. According to the Cauchy theorem (see [1, p.146] for example), the stress vector $\mathbf{t}_{(\mathbf{n})}(\mathbf{x})$ depends linearly on $\mathbf{n}$ provided it is continuous in $\mathbf{x}$. In other words, there exist a second-order tensor field $\boldsymbol{\sigma}$ independent of $\mathbf{n}$ such that

$$\mathbf{t}_{(\mathbf{n})}(\mathbf{x}) = \boldsymbol{\sigma}(\mathbf{x})\mathbf{n}\ , \tag{2.16}$$

for all $\mathbf{x}$ in the current configuration of the body and for arbitrary unit vectors $\mathbf{n}$. The second-order tensor $\boldsymbol{\sigma}(\mathbf{x})$ is called the *Caucy stress tensor*. The *normal stress component* σ_n in the direction of the unit normal vector $\mathbf{n}$ and the *tangential stress component* σ_t in the direction of the unit tangent vector $\mathbf{t}$ are defined in the form

$$\sigma_n = \mathbf{n}\cdot\mathbf{t}_{(\mathbf{n})}(\mathbf{x}) \equiv \mathbf{n}\cdot[\boldsymbol{\sigma}(\mathbf{x})\mathbf{n}], \quad \sigma_t = \mathbf{t}\cdot\mathbf{t}_{(\mathbf{n})}(\mathbf{x}) \equiv \mathbf{t}\cdot[\boldsymbol{\sigma}(\mathbf{x})\mathbf{n}]\ . \tag{2.17}$$

The local forms of the conservation of mass, the balance of linear momentum and the balance of rotational momentum are

$$\dot{\rho} + \text{div } \mathbf{v} = 0 \tag{2.18}$$

$$\text{div } \boldsymbol{\sigma} + \rho\mathbf{b} = \rho\dot{\mathbf{v}} \tag{2.19}$$

$$\boldsymbol{\sigma}^{\mathrm{T}} = \boldsymbol{\sigma} \tag{2.20}$$

(see [1]). Equation (2.18) is the dynamic local form of mass conservation. The equation given by

$$\rho J = \rho_0 \tag{2.21}$$

is another local form of the mass conservation law. Equation (2.19) is known as Cauchy's first law of motion. Equation (2.20) is known as Cauchy's second law of motion, which implies that the Cauchy stress tensor is symmetric.

The linear momentum balance equation (2.14) can be written in terms of integrals over $\mathcal{B}_0$ and $\partial\mathcal{B}_0$ as follows

$$\int_{\mathcal{B}_0} \rho_0(\mathbf{X})\mathbf{b}_0(\mathbf{X},t)\mathrm{d}V + \int_{\partial\mathcal{B}_0} \mathbf{S}^{\mathrm{T}}(\mathbf{X},t)\mathbf{N}\mathrm{d}A = \int_{\mathcal{B}_0} \rho_0(\mathbf{X})\ddot{\boldsymbol{\chi}}(\mathbf{X},t)\mathrm{d}V \tag{2.22}$$

where $\mathbf{b}_0(\mathbf{X},t) = \mathbf{b}(\boldsymbol{\chi}(\mathbf{X},t),t)$, and $\mathbf{N}$ is the unit (outward) normal to the boundary $\partial\mathcal{B}_0$ of the reference configuration $\mathcal{B}_0$. The tensor field $\mathbf{S}$ is given by

$$\mathbf{S} = J\mathbf{B}^{\mathrm{T}}\boldsymbol{\sigma} \tag{2.23}$$

and it is called the *nominal stress tensor* (see [1]). The transpose of $\mathbf{S}$ is sometimes referred to as the first Piola-Kirchhoff stress tensor. The equation

$$\mathbf{n}\mathrm{d}a = J\mathbf{B}\mathbf{N}\mathrm{d}A \tag{2.24}$$

relating current and reference elements of surface area is known as Nanson's formula (see [1]). It is used to transform the linear momentum balance equation (2.14) into the above form given in (2.22). The local form of (2.22) is called the *Lagrangean equation of motion* and it is given by

$$\text{Div } \mathbf{S} + \rho_0\mathbf{b}_0 = \rho_0\ddot{\boldsymbol{\chi}}\,. \tag{2.25}$$

Note that in this equation the independent variables are $\mathbf{X}$ and t although the vectors involved are actually Eulerian. In the rest of this thesis we assume that there are no body forces: $\mathbf{b}(\mathbf{x}, t) \equiv \mathbf{0}$ for all $\mathbf{x} \in \mathcal{B}$. Using (2.23) in (2.20) we observe that the symmetry of $\boldsymbol{\sigma}$ is equivalent to

$$\mathbf{F}\mathbf{S} = \mathbf{S}^{\mathrm{T}}\mathbf{F}^{\mathrm{T}} \, . \tag{2.26}$$

The set of Lagrangean field equations are (2.21), (2.25) and (2.26). This set is completed by use of a *constitutive law* which describes the nature of material behaviour. To describe distinct types of material behaviour different constitutive laws are proposed. For a homogeneous elastic material the set of equations is completed by specifying $\mathbf{S}$ as a function of $\mathbf{F}$. An elastic material for which a strain-energy function $W(\mathbf{F})$ exists and the (nominal) stress-deformation relation is given by

$$\mathbf{S} = \frac{\partial W}{\partial \mathbf{F}}(\mathbf{F}) \, , \tag{2.27}$$

is called a *hyperelastic* material. W is a measure of the energy stored in the material as a result of deformation. If a natural configuration is taken as the reference configuration (so that $\mathbf{F} = \mathbf{I}$ and $\mathbf{S} = \mathbf{0}$ in that configuration), then it may be convenient to set $W(\mathbf{I}) = 0$. An incompressible material is subject to the constraint $\det \mathbf{F} = 1$. The analogue of (2.27) is

$$\mathbf{S} = \frac{\partial W}{\partial \mathbf{F}}(\mathbf{F}) - p\mathbf{B}^{\mathrm{T}} \, . \tag{2.28}$$

where p is called the *arbitrary hydrostatic pressure* and it has the role of a Lagrange multiplier. We now introduce a second-order tensor $\mathbf{T}$, which is called the Biot stress tensor, through the relation

$$\mathbf{T}^2 = \mathbf{S}\mathbf{S}^{\mathrm{T}} \, . \tag{2.29}$$

We shall devote some attention to it in the subsequent chapters. A detailed discussion of the Biot stress tensor is given by Ogden [1].

An elastic material is an *isotropic elastic material* if the mechanical response of the material exhibits no preferred direction in a reference configuration (see [1]).

The strain energy function of a homogeneous isotropic hyperelastic material is a function of the principal invariants of $\mathbf{C}$: $W = W(I_1, I_2, I_3)$ where I_1, I_2, I_3 are the principal invariants of $\mathbf{C}$. Then the nominal stress tensor of a homogeneous isotropic hyperelastic material is given by

$$\mathbf{S} = 2\frac{\partial W}{\partial I_1}\mathbf{F}^{\mathrm{T}} + 2\frac{\partial W}{\partial I_2}\left(I_1\mathbf{I} - \mathbf{F}^{\mathrm{T}}\mathbf{F}\right)\mathbf{F}^{\mathrm{T}} + 2I_3\frac{\partial W}{\partial I_3}\mathbf{B}^{\mathrm{T}}\,, \tag{2.30}$$

(see [1]). Suppose that Λ_1^2, Λ_2^2 and Λ_3^2 are the eigenvalues of the right Cauchy-Green deformation tensor $\mathbf{C}$ which is a symmetric second-order tensor. In other words, we assume that they satisfy the characteristic equation

$$\det\left(\mathbf{F}^{\mathrm{T}}\mathbf{F} - \Lambda^2\mathbf{I}\right) = 0 \tag{2.31}$$

Then the principal invariants of $\mathbf{C}$ can be expressed in terms of Λ_1^2, Λ_2^2, Λ_3^2 as follows

$$I_1(\mathbf{C}) = \Lambda_1^2 + \Lambda_2^2 + \Lambda_3^2\,, \quad I_2(\mathbf{C}) = \Lambda_1^2\Lambda_2^2 + \Lambda_2^2\Lambda_3^2 + \Lambda_3^2\Lambda_1^2\,, \quad I_3(\mathbf{C}) = \Lambda_1^2\Lambda_2^2\Lambda_3^2\,. \tag{2.32}$$

The scalars Λ_1, Λ_2 and Λ_3 are also called the *principal stretches* (see [1]). Note that $\Lambda_1^2 = \Lambda_2^2 = \Lambda_3^2 = 1$ if a natural configuration is taken as the reference configuration. Also note that $I_1 = I_2 = 3$ and $I_3 = 1$ in the reference configuration. We may regard W as a function of the principal stretches Λ_1, Λ_2 and Λ_3 and we may write $W = W(\Lambda_1, \Lambda_2, \Lambda_3)$. Note that we use the same letter to indicate the revised functional dependence. For an isotropic strain-energy function we have

$$\frac{\partial W}{\partial \Lambda_1} = 2\Lambda_1[\frac{\partial W}{\partial I_1} + (\Lambda_2^2 + \Lambda_3^2)\frac{\partial W}{\partial I_2} + \Lambda_2^2\Lambda_3^2\frac{\partial W}{\partial I_3}], \tag{2.33}$$

$$\frac{\partial W}{\partial \Lambda_2} = 2\Lambda_2[\frac{\partial W}{\partial I_1} + (\Lambda_1^2 + \Lambda_3^2)\frac{\partial W}{\partial I_2} + \Lambda_1^2\Lambda_3^2\frac{\partial W}{\partial I_3}], \tag{2.34}$$

$$\frac{\partial W}{\partial \Lambda_3} = 2\Lambda_3[\frac{\partial W}{\partial I_1} + (\Lambda_1^2 + \Lambda_2^2)\frac{\partial W}{\partial I_2} + \Lambda_1^2\Lambda_2^2\frac{\partial W}{\partial I_3}], \tag{2.35}$$

where (2.32) is used.

For an incompressible material for which $I_3 = 1$, the strain energy function W depends on only two principal invariants: $W = W(I_1, I_2)$. Then the corresponding expression of (2.30) for the nominal stress tensor of an incompressible material takes the form

$$\mathbf{S} = 2\frac{\partial W}{\partial I_1}\mathbf{F}^{\mathrm{T}} + 2\frac{\partial W}{\partial I_2}\left(I_1\mathbf{I} - \mathbf{F}^{\mathrm{T}}\mathbf{F}\right)\mathbf{F}^{\mathrm{T}} - p\mathbf{B}^{\mathrm{T}} . \tag{2.36}$$

where p is the arbitrary hydrostatic pressure to be determined. Since $I_3 = 1$ and consequently $\Lambda_1^2\Lambda_2^2\Lambda_3^2 = 1$ for an incompressible material, we can rewrite the principal invariants given by (2.32) in the form

$$I_1 = \Lambda_1^2 + \Lambda_2^2 + \frac{1}{\Lambda_1^2\Lambda_2^2} , \quad I_2 = \Lambda_1^2\Lambda_2^2 + \frac{1}{\Lambda_1^2} + \frac{1}{\Lambda_2^2} \tag{2.37}$$

from which we deduce that

$$\frac{\partial W}{\partial \Lambda_1} = 2\Lambda_1\left(1 - \frac{1}{\Lambda_1^4\Lambda_2^2}\right)\left(\frac{\partial W}{\partial I_1} + \Lambda_2^2\frac{\partial W}{\partial I_2}\right) \tag{2.38}$$

$$\frac{\partial W}{\partial \Lambda_2} = 2\Lambda_2\left(1 - \frac{1}{\Lambda_1^2\Lambda_2^4}\right)\left(\frac{\partial W}{\partial I_1} + \Lambda_1^2\frac{\partial W}{\partial I_2}\right) \tag{2.39}$$

$$\frac{\partial W}{\partial \Lambda_3} \equiv 0 . \tag{2.40}$$

We now present a few specific forms of strain energy functions for future reference. A variety of constitutive laws have been proposed in the literature; some examples are provived in [1]. Two material models which have also received much attention in the literature are the *compressible neo-Hookean* material,

$$W(I_1, I_2, I_3) = \frac{\mu}{2}(I_1 + I_3^{-1} - 4) , \tag{2.41}$$

and the *Blatz-Ko* material,

$$W(I_1, I_2, I_3) = \frac{\mu}{2}(I_2 I_3^{-1} + 2I_3^{1/2} - 5) , \tag{2.42}$$

respectively. In these equations, the constant μ is the shear modulus for infinitesimal deformations so that $\mu > 0$. The strain energy functions corresponding to the compressible neo-Hookean and Blatz-Ko materials may be written in terms of the principal stretches in the form

$$W(\Lambda_1, \Lambda_2, \Lambda_3) = \frac{\mu}{2}(\Lambda_1^2 + \Lambda_2^2 + \Lambda_3^2 + \Lambda_1^{-2}\Lambda_2^{-2}\Lambda_3^{-2} - 4) , \tag{2.43}$$

and

$$W(\Lambda_1, \Lambda_2, \Lambda_3) = \frac{\mu}{2}(\Lambda_1^{-2} + \Lambda_2^{-2} + \Lambda_3^{-2} + 2\Lambda_1\Lambda_2\Lambda_3 - 5) \ , \tag{2.44}$$

respectively. Finally we conclude with two examples of incompressible materials which have received much attention in the literature. These are the *neo-Hookean* material,

$$W(I_1, I_2) = \frac{\mu}{2}(I_1 - 3) \ , \tag{2.45}$$

and the *Mooney-Rivlin* material,

$$W(I_1, I_2) = \frac{\mu}{2}[\gamma(I_1 - 3) + (1 - \gamma)(I_2 - 3)], \tag{2.46}$$

respectively. In these equations, μ and γ are constants with $\mu > 0$ and $0 \leq \gamma \leq 1$. If $\gamma = 1$, then the Mooney-Rivlin strain energy function (2.46) reduces to the neo-Hookean strain energy function (2.45). The strain energy functions corresponding to the neo-Hookean and Mooney-Rivlin materials may also be written in terms of the principal stretches in the form

$$W(\Lambda_1, \Lambda_2, \Lambda_3) = \frac{\mu}{2}(\Lambda_1^2 + \Lambda_2^2 + \Lambda_3^2 - 3) \ , \tag{2.47}$$

and

$$W(\Lambda_1, \Lambda_2, \Lambda_3) = \frac{\mu}{2}[\gamma(\Lambda_1^2 + \Lambda_2^2 + \Lambda_3^2 - 3) + (1 - \gamma)(\Lambda_1^2\Lambda_2^2 + \Lambda_1^2\Lambda_3^2 + \Lambda_2^2\Lambda_3^2 - 3)] \ , \tag{2.48}$$

respectively.

In the subsequent chapters, we wish to study the equations governing axisymmetric deformations of a thin-walled circular cylindrical tube of homogeneous isotropic nonlinearly elastic material. For this aim, we now derive the cylindrical coordinates form of (2.25) in the absence of body forces. We introduce the cylindrical coordinates

$$\{X_1, X_2, X_3\} = \{R\cos\Theta, R\sin\Theta, Z\} \tag{2.49}$$

and

$$\{x_1, x_2, x_3\} = \{r\cos\theta, r\sin\theta, z\} \ . \tag{2.50}$$

T.C. YÜKSEKÖĞRETİM KURULU
DOKÜMANTASYON MERKEZİ

for $\mathbf{X}$ and $\mathbf{x}$, respectively. The corresponding orthonormal basis vectors are

$$\mathbf{E}_R = \cos\Theta\mathbf{E}_1 + \sin\Theta\mathbf{E}_2, \quad \mathbf{E}_\Theta = -\sin\Theta\mathbf{E}_1 + \cos\Theta\mathbf{E}_2, \quad \mathbf{E}_Z = \mathbf{E}_3, \tag{2.51}$$

and

$$\mathbf{e}_r = \cos\theta\mathbf{e}_1 + \sin\theta\mathbf{e}_2, \quad \mathbf{e}_\theta = -\sin\theta\mathbf{e}_1 + \cos\theta\mathbf{e}_2, \quad \mathbf{e}_z = \mathbf{e}_3\ . \tag{2.52}$$

With respect to the orthonormal bases (2.51) and (2.52), the nominal stress tensor $\mathbf{S}$ has the following component form

$$\begin{aligned}\mathbf{S} = {} & S_{Rr}\mathbf{E}_R\otimes\mathbf{e}_r + S_{R\theta}\mathbf{E}_R\otimes\mathbf{e}_\theta + S_{Rz}\mathbf{E}_R\otimes\mathbf{e}_z + S_{\Theta r}\mathbf{E}_\Theta\otimes\mathbf{e}_r + S_{\Theta\theta}\mathbf{E}_\Theta\otimes\mathbf{e}_\theta \\ & + S_{\Theta z}\mathbf{E}_\Theta\otimes\mathbf{e}_z + S_{Zr}\mathbf{E}_Z\otimes\mathbf{e}_r + S_{Z\theta}\mathbf{E}_Z\otimes\mathbf{e}_\theta + S_{Zz}\mathbf{E}_Z\otimes\mathbf{e}_z\end{aligned} \tag{2.53}$$

where S_{Rr}, $S_{R\theta}$, S_{Rz}, $S_{\Theta r}$, $S_{\Theta\theta}$, $S_{\Theta z}$, S_{Zr}, $S_{Z\theta}$, S_{Zz} are the physical components of the nominal stress tensor. In the matrix notation the nominal stress tensor will be expressed in the form

$$[\mathbf{S}] = \begin{bmatrix} S_{Rr} & S_{R\theta} & S_{Rz} \\ S_{\Theta r} & S_{\Theta\theta} & S_{\Theta z} \\ S_{Zr} & S_{Z\theta} & S_{Zz} \end{bmatrix}. \tag{2.54}$$

The divergence of the nominal stress tensor, $\nabla\cdot\mathbf{S}$, is defined according to a contraction between ∇ and $\mathbf{S}$ applied to $\nabla\otimes\mathbf{S}$. This contraction defines $\nabla\cdot\mathbf{S}$ such that

$$\begin{aligned}\nabla\cdot\mathbf{S} = {} & \left[\frac{\partial S_{Rr}}{\partial R} + \frac{1}{R}\left(\frac{\partial S_{\Theta r}}{\partial\Theta} + S_{Rr} - S_{\Theta\theta}\frac{\partial\theta}{\partial\Theta}\right) + \frac{\partial S_{Zr}}{\partial Z} - S_{R\theta}\frac{\partial\theta}{\partial R} - S_{Z\theta}\frac{\partial\theta}{\partial Z}\right]\mathbf{e}_r \\ & + \left[\frac{\partial S_{R\theta}}{\partial R} + \frac{1}{R}\left(\frac{\partial S_{\Theta\theta}}{\partial\Theta} + S_{R\theta} + S_{\Theta r}\frac{\partial\theta}{\partial\Theta}\right) + \frac{\partial S_{Z\theta}}{\partial Z} + S_{Rr}\frac{\partial\theta}{\partial R} + S_{Zr}\frac{\partial\theta}{\partial Z}\right]\mathbf{e}_\theta \\ & + \left[\frac{\partial S_{Rz}}{\partial R} + \frac{1}{R}\left(\frac{\partial S_{\Theta z}}{\partial\Theta} + S_{Rz}\right) + \frac{\partial S_{Zz}}{\partial Z}\right]\mathbf{e}_z\ .\end{aligned} \tag{2.55}$$

The acceleration field $\ddot{\boldsymbol{\chi}}$ on the right-hand side of (2.25), referred to cylindrical coordinates, are given in the form

$$\ddot{\boldsymbol{\chi}} = \left(\frac{\partial V_r}{\partial t} - \frac{1}{r}{V_\theta}^2\right)\mathbf{e}_r + \left(\frac{\partial V_\theta}{\partial t} + \frac{1}{r}V_r V_\theta\right)\mathbf{e}_\theta + \left(\frac{\partial V_z}{\partial t}\right)\mathbf{e}_z\ , \tag{2.56}$$

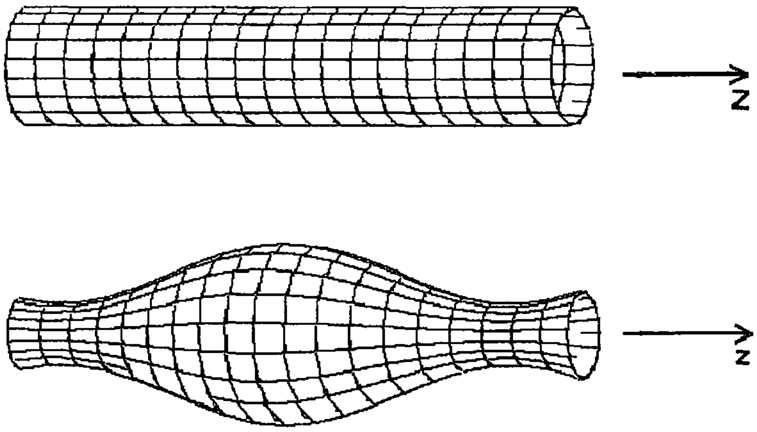

Figure 2.1: Undeformed and deformed configurations of the tube.

where $V_r = \partial r/\partial t$, $V_\theta = \partial\theta/\partial t$, $V_z = \partial z/\partial t$. Thus the equations of motion in the absence of body forces, referred to cylindrical polar coordinates, are given in component form by equating the coefficients of $\mathbf{e}_r$, $\mathbf{e}_\theta$ and $\mathbf{e}_z$ in (2.55) and (2.56), respectively;

$$\left[\frac{\partial S_{Rr}}{\partial R} + \frac{1}{R}\left(\frac{\partial S_{\Theta r}}{\partial\Theta} + S_{Rr} - S_{\Theta\theta}\frac{\partial\theta}{\partial\Theta}\right) + \frac{\partial S_{Zr}}{\partial Z} - S_{R\theta}\frac{\partial\theta}{\partial R} - S_{Z\theta}\frac{\partial\theta}{\partial Z}\right]$$
$$- \rho_0\left(\frac{\partial V_r}{\partial t} - \frac{1}{r}{V_\theta}^2\right) = 0\,, \tag{2.57}$$

$$\left[\frac{\partial S_{R\theta}}{\partial R} + \frac{1}{R}\left(\frac{\partial S_{\Theta\theta}}{\partial\Theta} + S_{R\theta} + S_{\Theta r}\frac{\partial\theta}{\partial\Theta}\right) + \frac{\partial S_{Z\theta}}{\partial Z} + S_{Rr}\frac{\partial\theta}{\partial R} + S_{Zr}\frac{\partial\theta}{\partial Z}\right]$$
$$- \rho_0\left(\frac{\partial V_\theta}{\partial t} + \frac{1}{r}V_r V_\theta\right) = 0\,, \tag{2.58}$$

$$\left[\frac{\partial S_{Rz}}{\partial R} + \frac{1}{R}\left(\frac{\partial S_{\Theta z}}{\partial\Theta} + S_{Rz}\right) + \frac{\partial S_{Zz}}{\partial Z}\right] - \rho_0\left(\frac{\partial V_z}{\partial t}\right) = 0\,. \tag{2.59}$$

2.3 Axisymmetric Deformations

We wish to investigate axisymmetric deformations of a nonlinearly elastic circular cylindrical tube in the subsequent chapters. For this aim we now derive the basic equations corresponding to the case where the deformed tube is assumed to be axisymmetric. We consider a hollow circular cylindrical tube of homogeneous isotropic hyperelastic material which, in its (undeformed, stress-free) natural configuration, is defined by

$$R_i \leq R \leq R_i + H, \quad 0 \leq \Theta \leq 2\pi, \quad 0 \leq Z \leq L \tag{2.60}$$

where R_i is the undeformed radius of the inner surface, H is the (uniform) thickness of the tube, L is the initial length of the tube, $\{R, \Theta, Z\}$ are cylindrical polar coordinates associated with the natural configuration. The axisymmetric deformation of the tube is defined by

$$r = r(R, Z, t)\ ,\ \theta = \Theta\ ,\ z = z(R, Z, t)\ , \tag{2.61}$$

where $\{r, \theta, z\}$ are cylindrical polar coordinates associated with the deformed configuration.

Recall that we restrict attention to the case where the deformed tube is axisymmetric. The deformation gradient tensor $\mathbf{F}$ associated with (2.61), referred to cylindrical polar coordinates, is given by

$$\mathbf{F} = \frac{\partial r}{\partial R}\mathbf{e}_r \otimes \mathbf{E}_R + \frac{\partial r}{\partial Z}\mathbf{e}_r \otimes \mathbf{E}_Z + \frac{r}{R}\mathbf{e}_\theta \otimes \mathbf{E}_\Theta + \frac{\partial z}{\partial R}\mathbf{e}_z \otimes \mathbf{E}_R + \frac{\partial z}{\partial Z}\mathbf{e}_z \otimes \mathbf{E}_Z \tag{2.62}$$

or, in matrix notation,

$$[\mathbf{F}] = \begin{bmatrix} \dfrac{\partial r}{\partial R} & 0 & \dfrac{\partial r}{\partial Z} \\ 0 & \dfrac{r}{R} & 0 \\ \dfrac{\partial z}{\partial R} & 0 & \dfrac{\partial z}{\partial Z} \end{bmatrix} . \tag{2.63}$$

Then, from (2.6) we have

$$J = \frac{r}{R}\left(\frac{\partial r}{\partial R}\frac{\partial z}{\partial Z} - \frac{\partial r}{\partial Z}\frac{\partial z}{\partial R}\right) . \tag{2.64}$$

It follows from (2.63) and $\mathbf{B} = (\mathbf{F}^{-1})^{\mathrm{T}}$ that

$$[\mathbf{B}] = \frac{1}{J}\begin{bmatrix} \dfrac{r}{R}\dfrac{\partial z}{\partial Z} & 0 & -\dfrac{r}{R}\dfrac{\partial z}{\partial R} \\ 0 & \left(\dfrac{\partial r}{\partial R}\dfrac{\partial z}{\partial Z} - \dfrac{\partial r}{\partial Z}\dfrac{\partial z}{\partial R}\right) & 0 \\ -\dfrac{r}{R}\dfrac{\partial r}{\partial Z} & 0 & \dfrac{r}{R}\dfrac{\partial r}{\partial R} \end{bmatrix} . \tag{2.65}$$

The right Cauchy-Green tensor $\mathbf{C}$ is then

$$[\mathbf{C}] = \begin{bmatrix} \left(\frac{\partial r}{\partial R}\right)^2 + \left(\frac{\partial z}{\partial R}\right)^2 & 0 & \left(\frac{\partial r}{\partial R}\frac{\partial r}{\partial Z} + \frac{\partial z}{\partial R}\frac{\partial z}{\partial Z}\right) \\ 0 & \left(\frac{r}{R}\right)^2 & 0 \\ \left(\frac{\partial r}{\partial R}\frac{\partial r}{\partial Z} + \frac{\partial z}{\partial R}\frac{\partial z}{\partial Z}\right) & 0 & \left(\frac{\partial r}{\partial Z}\right)^2 + \left(\frac{\partial z}{\partial Z}\right)^2 \end{bmatrix}. \tag{2.66}$$

Since the principal stretches are associated with the eigenvalues of $\mathbf{C}$, we have

$$\begin{aligned} \Lambda_2^2 &= \left(\frac{r}{R}\right)^2, \\ \Lambda_1^2 + \Lambda_3^2 &= \left(\frac{\partial r}{\partial R}\right)^2 + \left(\frac{\partial r}{\partial Z}\right)^2 + \left(\frac{\partial z}{\partial R}\right)^2 + \left(\frac{\partial z}{\partial Z}\right)^2, \\ \Lambda_1^2\Lambda_3^2 &= \left(\frac{\partial r}{\partial R}\frac{\partial z}{\partial Z} - \frac{\partial r}{\partial Z}\frac{\partial z}{\partial R}\right)^2. \end{aligned} \tag{2.67}$$

Thus, (2.32) gives the principal invariants of $\mathbf{C}$ as

$$\begin{aligned} I_1(\mathbf{C}) &= \left(\frac{\partial r}{\partial R}\right)^2 + \left(\frac{\partial r}{\partial Z}\right)^2 + \left(\frac{\partial z}{\partial R}\right)^2 + \left(\frac{\partial z}{\partial Z}\right)^2 + \left(\frac{r}{R}\right)^2, \\ I_2(\mathbf{C}) &= \left(\frac{r}{R}\right)^2 \left[\left(\frac{\partial r}{\partial R}\right)^2 + \left(\frac{\partial r}{\partial Z}\right)^2 + \left(\frac{\partial z}{\partial R}\right)^2 + \left(\frac{\partial z}{\partial Z}\right)^2\right] \\ &\quad + \left(\frac{\partial r}{\partial R}\frac{\partial z}{\partial Z} - \frac{\partial r}{\partial Z}\frac{\partial z}{\partial R}\right)^2, \\ I_3(\mathbf{C}) &= \left(\frac{r}{R}\right)^2 \left(\frac{\partial r}{\partial R}\frac{\partial z}{\partial Z} - \frac{\partial r}{\partial Z}\frac{\partial z}{\partial R}\right)^2. \end{aligned} \tag{2.68}$$

Under the deformation (2.61), (2.30) gives the physical components of the nominal stress tensor $\mathbf{S}$ for compressible hyperelastic materials as

$$\begin{aligned} S_{Rr} &= 2\left[\frac{\partial W}{\partial I_1}\frac{\partial r}{\partial R} + \frac{\partial W}{\partial I_2}K_{Rr} + \frac{\partial W}{\partial I_3}\left(\frac{r}{R}\right)^2 \frac{\partial z}{\partial Z}\left(\frac{\partial r}{\partial R}\frac{\partial z}{\partial Z} - \frac{\partial z}{\partial R}\frac{\partial r}{\partial Z}\right)\right], \\ S_{Rz} &= 2\left[\frac{\partial W}{\partial I_1}\frac{\partial z}{\partial R} + \frac{\partial W}{\partial I_2}K_{Rz} - \frac{\partial W}{\partial I_3}\left(\frac{r}{R}\right)^2 \frac{\partial r}{\partial Z}\left(\frac{\partial r}{\partial R}\frac{\partial z}{\partial Z} - \frac{\partial z}{\partial R}\frac{\partial r}{\partial Z}\right)\right], \\ S_{\Theta\theta} &= 2\frac{r}{R}\left[\frac{\partial W}{\partial I_1} + \frac{\partial W}{\partial I_2}K_{\Theta\theta} + \frac{\partial W}{\partial I_3}\left(\frac{\partial r}{\partial R}\frac{\partial z}{\partial Z} - \frac{\partial z}{\partial R}\frac{\partial r}{\partial Z}\right)^2\right], \\ S_{Zr} &= 2\left[\frac{\partial W}{\partial I_1}\frac{\partial r}{\partial Z} + \frac{\partial W}{\partial I_2}K_{Zr} - \frac{\partial W}{\partial I_3}\left(\frac{r}{R}\right)^2 \frac{\partial z}{\partial R}\left(\frac{\partial r}{\partial R}\frac{\partial z}{\partial Z} - \frac{\partial z}{\partial R}\frac{\partial r}{\partial Z}\right)\right], \\ S_{Zz} &= 2\left[\frac{\partial W}{\partial I_1}\frac{\partial z}{\partial Z} + \frac{\partial W}{\partial I_2}K_{Zz} + \frac{\partial W}{\partial I_3}\left(\frac{r}{R}\right)^2 \frac{\partial r}{\partial R}\left(\frac{\partial r}{\partial R}\frac{\partial z}{\partial Z} - \frac{\partial z}{\partial R}\frac{\partial r}{\partial Z}\right)\right], \\ S_{\Theta r} &= S_{R\theta} = S_{Z\theta} = S_{\Theta z} = 0 \end{aligned} \tag{2.69}$$

where

$$
\begin{aligned}
K_{Rr} &= \frac{\partial r}{\partial R}\left[\left(\frac{r}{R}\right)^2 + \left(\frac{\partial r}{\partial Z}\right)^2 + \left(\frac{\partial z}{\partial Z}\right)^2\right] - \frac{\partial r}{\partial Z}\left(\frac{\partial r}{\partial R}\frac{\partial r}{\partial Z} + \frac{\partial z}{\partial R}\frac{\partial z}{\partial Z}\right) , \\
K_{Rz} &= \frac{\partial z}{\partial R}\left[\left(\frac{r}{R}\right)^2 + \left(\frac{\partial r}{\partial Z}\right)^2 + \left(\frac{\partial z}{\partial Z}\right)^2\right] - \frac{\partial z}{\partial Z}\left(\frac{\partial r}{\partial R}\frac{\partial r}{\partial Z} + \frac{\partial z}{\partial R}\frac{\partial z}{\partial Z}\right) , \\
K_{\Theta\theta} &= \left(\frac{\partial r}{\partial R}\right)^2 + \left(\frac{\partial z}{\partial R}\right)^2 + \left(\frac{\partial r}{\partial Z}\right)^2 + \left(\frac{\partial z}{\partial Z}\right)^2 , \\
K_{Zr} &= \frac{\partial r}{\partial Z}\left[\left(\frac{r}{R}\right)^2 + \left(\frac{\partial r}{\partial R}\right)^2 + \left(\frac{\partial z}{\partial R}\right)^2\right] - \frac{\partial r}{\partial R}\left(\frac{\partial r}{\partial R}\frac{\partial r}{\partial Z} + \frac{\partial z}{\partial R}\frac{\partial z}{\partial Z}\right) , \\
K_{Zz} &= \frac{\partial z}{\partial Z}\left[\left(\frac{r}{R}\right)^2 + \left(\frac{\partial r}{\partial R}\right)^2 + \left(\frac{\partial z}{\partial R}\right)^2\right] - \frac{\partial z}{\partial R}\left(\frac{\partial r}{\partial R}\frac{\partial r}{\partial Z} + \frac{\partial z}{\partial R}\frac{\partial z}{\partial Z}\right) .
\end{aligned}
\tag{2.70}
$$

Similarly, (2.36) gives the physical components of the nominal stress tensor for incompresibble hyperelastic materials in the form

$$
\begin{aligned}
S_{Rr} &= 2\left(\frac{\partial W}{\partial I_1}\frac{\partial r}{\partial R} + \frac{\partial W}{\partial I_2}K_{Rr}\right) - p\frac{r}{R}\frac{\partial z}{\partial Z} , \\
S_{Rz} &= 2\left(\frac{\partial W}{\partial I_1}\frac{\partial z}{\partial R} + \frac{\partial W}{\partial I_2}K_{Rz}\right) + p\frac{r}{R}\frac{\partial r}{\partial Z} , \\
S_{\Theta\theta} &= 2\frac{r}{R}\left(\frac{\partial W}{\partial I_1} + \frac{\partial W}{\partial I_2}K_{\Theta\theta}\right) - p\left(\frac{\partial r}{\partial R}\frac{\partial z}{\partial Z} - \frac{\partial z}{\partial R}\frac{\partial r}{\partial Z}\right) , \\
S_{Zr} &= 2\left(\frac{\partial W}{\partial I_1}\frac{\partial r}{\partial Z} + \frac{\partial W}{\partial I_2}K_{Zr}\right) + p\frac{r}{R}\frac{\partial z}{\partial R} , \\
S_{Zz} &= 2\left(\frac{\partial W}{\partial I_1}\frac{\partial z}{\partial Z} + \frac{\partial W}{\partial I_2}K_{Zz}\right) - p\frac{r}{R}\frac{\partial r}{\partial R} , \\
S_{\Theta r} &= S_{R\theta} = S_{Z\theta} = S_{\Theta z} = 0
\end{aligned}
\tag{2.71}
$$

where K_{Rr}, K_{Rz}, ... , K_{Zz} are given by (2.70).

Recalling that $S_{R\theta} = S_{\Theta r} = S_{\Theta z} = S_{Z\theta} = 0$, the eigenvalues, (S_1, S_2, S_3), of the nominal stress tensor $\mathbf{S}$ are obtained in the form

$$
S_2 = S_{\Theta\theta} , \quad S_1 + S_3 = S_{Rr} + S_{Zz} , \quad S_1 S_3 = S_{Rr}S_{Zz} - S_{Rz}S_{Zr} , \tag{2.72}
$$

and the principal invariants of $\mathbf{S}$ in the form

$$
I_1(\mathbf{S}) = S_{Rr} + S_{\Theta\theta} + S_{Zz} ,
$$

$$
\begin{aligned}
I_2(\mathbf{S}) &= S_{Rr}S_{\Theta\theta} - S_{Zr}S_{Rz} + S_{Zz}(S_{Rr} + S_{\Theta\theta}) \; , \\
I_3(\mathbf{S}) &= S_{\Theta\theta}(S_{Rr}S_{Zz} - S_{Rz}S_{Zr}) \; . \qquad (2.73)
\end{aligned}
$$

Similarly, using the relationship between the Biot stress tensor and the nominal stress tensor given by (2.29), we observe that the eigenvalues, T_1, T_2, T_3, of the Biot stress tensor $\mathbf{T}$ must satisfy

$$
T_2^2 = S_{\Theta\theta}^2 \; , \quad T_1^2 + T_3^2 = S_{Rr}^2 + S_{Rz}^2 + S_{Zr}^2 + S_{Zz}^2 \; , \quad T_1^2 T_3^2 = (S_{Rr}S_{Zz} - S_{Rz}S_{Zr})^2 \; . \qquad (2.74)
$$

Since $S_{\Theta r} = S_{R\theta} = S_{Z\theta} = S_{\Theta z} = 0$ for both compressible and incompressible hyperelastic materials under the deformation (2.61), we may write $\mathbf{S} = \mathbf{S}(R, Z, t)$. Thus, for the deformation (2.61) of interest here, the general equations of motion reduce to

$$
\frac{\partial S_{Rr}}{\partial R} + \frac{\partial S_{Zr}}{\partial Z} + \frac{1}{R}(S_{Rr} - S_{\Theta\theta}) - \rho_0 \frac{\partial^2 r}{\partial t^2} = 0 \; , \qquad (2.75)
$$

$$
\frac{\partial S_{\Theta\theta}}{\partial \Theta} = 0 \; , \qquad (2.76)
$$

$$
\frac{\partial S_{Rz}}{\partial R} + \frac{\partial S_{Zz}}{\partial Z} + \frac{1}{R} S_{Rz} - \rho_0 \frac{\partial^2 z}{\partial t^2} = 0 \; . \qquad (2.77)
$$

Note that (2.23) gives $\boldsymbol{\sigma} = J^{-1}\mathbf{F}\mathbf{S}$. Then the physical components of the Cauchy stress tensor $\boldsymbol{\sigma}$ are obtained in terms of the components of nominal stress tensor $\mathbf{S}$ as follows

$$
[\boldsymbol{\sigma}] = \frac{1}{J}
\begin{bmatrix}
\frac{\partial r}{\partial R} S_{Rr} + \frac{\partial r}{\partial Z} S_{Zr} & 0 & \frac{\partial r}{\partial R} S_{Rz} + \frac{\partial r}{\partial Z} S_{Zz} \\
0 & \frac{r}{R} S_{\Theta\theta} & 0 \\
\frac{\partial z}{\partial R} S_{Rr} + \frac{\partial z}{\partial Z} S_{Zr} & 0 & \frac{\partial z}{\partial R} S_{Rz} + \frac{\partial z}{\partial Z} S_{Zz}
\end{bmatrix} . \qquad (2.78)
$$

We also observe that, for the deformation (2.61) of interest here, the symmetry property of $\boldsymbol{\sigma}$ given by (2.26) reduces to

$$
\frac{\partial z}{\partial R} S_{Rr} - \frac{\partial r}{\partial R} S_{Rz} = \frac{\partial r}{\partial Z} S_{Zz} - \frac{\partial z}{\partial Z} S_{Zr} \qquad (2.79)
$$

which implies that $\sigma_{rz} = \sigma_{zr}$.

3. AN ASYMPTOTIC MEMBRANE THEORY OF HYPERELASTIC TUBES

3.1 Introduction

In this chapter, the asymptotic expansion technique is used to obtain a nonlinear asymptotic membrane theory of a thin-walled circular cylindrical tube composed of a homogeneous isotropic general hyperelastic material. We restrict attention to the case where the deformed tube is assumed to be axisymmetric. Applying the asymptotic expansion method to the equations presented in Section 2.3, the equations governing the axially symmetric dynamic deformations of a membrane tube are obtained for an arbitrary form of the strain-energy function. Some aspects of the present membrane theory are also discussed.

In Section 3.2, we describe a tube whose thickness is smaller than the radius of its inner surface in the undeformed configuration and we briefly summarize the boundary conditions at the inner and outer surfaces of the tube. In Section 3.3, utilizing an appropriate thickness parameter all the field variables are scaled. In Section 3.4 the non-dimensional form of the governing equations are given. In Section 3.5, the asymptotic expansion method is used to construct an asymptotic membrane theory for thin tubes made of an incompressible hyperelastic material. To this end, the radial and axial cordinates in the deformed configuration and the surface tractions are expanded into a formal power series of the thickness parameter. Without any a priori assumption on the form of the field variables, it is shown that the zeroth-order approximation simultaneously includes both the membrane equations previously presented in the literature and the usual assumptions on the specific forms of the field variables. In Section 3.6, a similar analysis is developed for thin tubes made of a compressible hyperelastic material.

3.2 Formulation of the Problem

We consider a hollow circular cylinder made of a homogeneous, isotropic incompressible hyperelastic material, which, in its natural configuration, is defined by (2.60). The cylinder is subjected to both tangential and normal tractions on its inner surface while the outer surface is free of tractions. The surface tractions may vary axially, but not circumferentially so that an axisymmetric deformation is produced. Thus the deformation is given by (2.61). The inner surface of the deformed tube can be generated by rotating a continuous curve in the rz-plane about the z-axis. It is assumed the curve does not intersect the z-axis. At time t the inner surface of the deformed tube have the parametric equations $r = r(R_i, Z, t)$, $z = z(R_i, Z, t)$. The tangential and normal unit vectors, $\mathbf{t}$ and $\mathbf{n}$, of the deformed inner surface ($R = R_i$) are

$$\mathbf{n} = -\frac{1}{\Phi}\left(\frac{\partial z}{\partial Z}\mathbf{e}_r - \frac{\partial r}{\partial Z}\mathbf{e}_z\right) , \quad \mathbf{t} = \frac{1}{\Phi}\left(\frac{\partial r}{\partial Z}\mathbf{e}_r + \frac{\partial z}{\partial Z}\mathbf{e}_z\right) , \tag{3.1}$$

where

$$\Phi(R, Z) = \left[\left(\frac{\partial r}{\partial Z}\right)^2 + \left(\frac{\partial z}{\partial Z}\right)^2\right]^{\frac{1}{2}} , \tag{3.2}$$

If we denote the tangential and normal tractions on the inner surface of the deformed tube by $P_t(Z, t)$ and $P_n(Z, t)$, then the boundary conditions at the inner and outer surfaces of the deformed tube are given by

$$\sigma_n = -P_n \, , \quad \sigma_t = -P_t \qquad \text{at } R = R_i \tag{3.3}$$

and

$$\sigma_n = 0 \, , \quad \sigma_t = 0 \qquad \text{at } R = R_i + H \tag{3.4}$$

where σ_n and σ_t are the normal and tangential stress components defined by (2.17). For the present problem, using (2.17) and noting that $\sigma_{r\theta} = \sigma_{\theta r} = \sigma_{\theta z} = \sigma_{z\theta} \equiv 0$, σ_n and σ_t can be expressed in terms of the nonzero components of the Cauch stress tensor as follows

$$\sigma_n = \frac{1}{\Phi^2}\left[\left(\frac{\partial r}{\partial Z}\right)^2 \sigma_{zz} + \left(\frac{\partial z}{\partial Z}\right)^2 \sigma_{rr} - \frac{\partial r}{\partial Z}\frac{\partial z}{\partial Z}(\sigma_{rz} + \sigma_{zr})\right] , \tag{3.5}$$

and

$$\sigma_t = \frac{1}{\Phi^2}\left[\left(\frac{\partial r}{\partial Z}\right)^2 \sigma_{rz} - \left(\frac{\partial z}{\partial Z}\right)^2 \sigma_{zr} + \frac{\partial r}{\partial Z}\frac{\partial z}{\partial Z}(\sigma_{zz} - \sigma_{rr})\right] , \tag{3.6}$$

respectively. If we use (2.78) in (3.5) and (3.6), we can express σ_n and σ_t in terms of the nonzero components of nominal stress tensor. If the resulting expression and (2.64), (2.79), (3.2) are used in (3.3) and (3.4), after some straightforward calculations, the boundary conditions at the inner and outer surfaces of the deformed tube are rewritten in the form

$$\frac{1}{\Phi^2}\left(\frac{\partial z}{\partial Z}S_{Rr} - \frac{\partial r}{\partial Z}S_{Rz}\right) = -\frac{r}{R}P_n, \; \frac{1}{\Phi^2}\left(\frac{\partial r}{\partial Z}S_{Rr} + \frac{\partial z}{\partial Z}S_{Rz}\right) = -\frac{r}{R}P_t \quad \text{at } R = R_i \tag{3.7}$$

and

$$\frac{1}{\Phi^2}\left(\frac{\partial z}{\partial Z}S_{Rr} - \frac{\partial r}{\partial Z}S_{Rz}\right) = 0 \, , \; \frac{1}{\Phi^2}\left(\frac{\partial r}{\partial Z}S_{Rr} + \frac{\partial z}{\partial Z}S_{Rz}\right) = 0 \quad \text{at } R = R_i + H. \tag{3.8}$$

Thus, it follows from these equations that the boundary conditions can be stated alternatively in the form

$$S_{Rr} = -\frac{r}{R}\left(\frac{\partial z}{\partial Z}P_n - \frac{\partial r}{\partial Z}P_t\right) \; , \quad S_{Rz} = \frac{r}{R}\left(\frac{\partial r}{\partial Z}P_n + \frac{\partial z}{\partial Z}P_t\right) \quad \text{at } R = R_i \tag{3.9}$$

and

$$S_{Rr} = 0 \, , \quad S_{Rz} = 0 \qquad \text{at } R = R_i + H. \tag{3.10}$$

For the time being, the boundary conditions at two ends of the cylinder will not be specified. This subject will be discussed later.

3.3 Scaling

In this section we define the dimensionless coordinates and scale the unknowns and loads by some particular powers of an appropriate thickness parameter. The thickness parameter ε is defined in the form $\varepsilon = H/R_i$ and the thin tube assumption results in $\varepsilon << 1$. Consequently, we may attempt to study an asymptotic expansion of the basic equations with respect to the small dimensionless parameter ε. We now introduce the following dimensionless coordinates $\bar{R}$, $\bar{Z}$

$$R = R_i(1+\varepsilon\bar{R}), \quad Z = R_i\bar{Z} \tag{3.11}$$

in the undeformed configuration, and $\bar{r}$, $\bar{z}$

$$r(R,Z) = R_i\bar{r}(\bar{R},\bar{Z}), \quad z(R,Z) = R_i\bar{z}(\bar{R},\bar{Z}) \tag{3.12}$$

in the deformed configuration, and the dimensionless time $\bar{t}$

$$t = \left(\frac{\rho_0}{\mu}\right)^{\frac{1}{2}} R_i\bar{t}\,. \tag{3.13}$$

Thus the domain occupied by the thin tube in the undeformed configuration is transformed into a domain of comparable dimensions, which is independent of ε. Since such a transformation introduces the thickness parameter ε into the field equations, the solution of the three-dimensional problem will depend not only on $\bar{R}$, $\bar{Z}$, $\bar{t}$ but also on ε. It is reasonable then to expect the solution of the corresponding problem defined in the dimensionless coordinates to have an expansion with respect to ε. In what follows, all the field variables in the dimensionless coordinates will be scaled by some particular powers of ε such that it reflects the expected behaviour of the tube and then a consistent asymptotic theory for thin nonlinearly elastic tubes will be developed without any additional assumptions. But at this point, note that the asymptotic expansion method is not free from a priori assumptions due to the scaling assertions. Now we define the non-dimensional tangential and surface tractions, i.e., $\bar{P}_t$ and $\bar{P}_n$, as follows:

$$P_t = \mu\varepsilon\bar{P}_t, \quad P_n = \mu\varepsilon\bar{P}_n \tag{3.14}$$

where the common factor of the stress dimension is chosen as μ. To proceed with our analysis further, we define the non-dimensional components of the nominal stress tensor $\mathbf{S}$ in the form

$$S_{Rr} = \mu\varepsilon\bar{S}_{Rr}, \quad S_{Rz} = \mu\varepsilon\bar{S}_{Rz}, \quad S_{Zr} = \mu\bar{S}_{Zr}, \quad S_{Zz} = \mu\bar{S}_{Zz}, \quad S_{\Theta\theta} = \mu\bar{S}_{\Theta\theta} \tag{3.15}$$

where the nominal stress components S_{Rr} and S_{Rz} are scaled such that they are included in the lowest order approximation of (3.9). Similarly, the non-dimensional strain-energy function $\bar{W}$, the non-dimensional principal components of Biot stress, $\bar{T}_i$ $(i = 1, 2, 3)$, and the non-dimensional hydrostatic pressure $\bar{p}$ are defined by

$$W = \mu\bar{W}, \quad T_k = \mu\bar{T}_k \ ; (k = 1, 2, 3) \ , \quad p = \mu\bar{p} \ . \tag{3.16}$$

3.4 Transformed Problem

For future reference we record here the basic equations of the three-dimensional problem in the dimensionless coordinates by using the definitions given in the previous section. For convenience we omit the bars on the non-dimensional equations.

We now briefly summarize the basic equations in the dimensionless coordinates, which are obtained using (3.11)-(3.16) in the equations derived in the previous chapter and in Section 3.2, as follows. The Jacobian J given by (2.64) takes the following form

$$J = \frac{r}{1+\varepsilon R}\left[\frac{1}{\varepsilon}\left(\frac{\partial r}{\partial R}\frac{\partial z}{\partial Z} - \frac{\partial r}{\partial Z}\frac{\partial z}{\partial R}\right)\right] \ . \tag{3.17}$$

The scaled form of the right Cauchy-Green tensor $\mathbf{C}$, given by (2.66), is

$$[\mathbf{C}] = \begin{bmatrix} \frac{1}{\varepsilon^2}\left[\left(\frac{\partial r}{\partial R}\right)^2 + \left(\frac{\partial z}{\partial R}\right)^2\right] & 0 & \frac{1}{\varepsilon}\left[\frac{\partial r}{\partial R}\frac{\partial r}{\partial Z} + \frac{\partial z}{\partial R}\frac{\partial z}{\partial Z}\right] \\ 0 & \left(\frac{r}{1+\varepsilon R}\right)^2 & 0 \\ \frac{1}{\varepsilon}\left[\frac{\partial r}{\partial R}\frac{\partial r}{\partial Z} + \frac{\partial z}{\partial R}\frac{\partial z}{\partial Z}\right] & 0 & \left(\frac{\partial r}{\partial Z}\right)^2 + \left(\frac{\partial z}{\partial Z}\right)^2 \end{bmatrix} . \tag{3.18}$$

Furthermore, in the dimensionless coordinates, the principal stretches Λ_k $(k = 1, 2, 3)$, which satisfy (2.67), and the principal invariants I_k $(k = 1, 2, 3)$ given by (2.68), take the following form

$$\Lambda_2^2 = \left(\frac{r}{1+\varepsilon R}\right)^2 ,$$

$$\Lambda_1^2+\Lambda_3^2=\frac{1}{\varepsilon^2}\left[\left(\frac{\partial r}{\partial R}\right)^2+\left(\frac{\partial z}{\partial R}\right)^2\right]+\left(\frac{\partial r}{\partial Z}\right)^2+\left(\frac{\partial z}{\partial Z}\right)^2,$$

$$\Lambda_1^2\Lambda_3^2=\frac{1}{\varepsilon^2}\left(\frac{\partial r}{\partial R}\frac{\partial z}{\partial Z}-\frac{\partial r}{\partial Z}\frac{\partial z}{\partial R}\right)^2, \tag{3.19}$$

and

$$\begin{aligned}
I_1(C) &= \frac{1}{\varepsilon^2}\left[\left(\frac{\partial r}{\partial R}\right)^2+\left(\frac{\partial z}{\partial R}\right)^2\right]+\left(\frac{\partial r}{\partial Z}\right)^2+\left(\frac{\partial z}{\partial Z}\right)^2+\left(\frac{r}{1+\varepsilon R}\right)^2,\\
I_2(C) &= \left(\frac{r}{1+\varepsilon R}\right)^2\left[\frac{1}{\varepsilon^2}\left[\left(\frac{\partial r}{\partial R}\right)^2+\left(\frac{\partial z}{\partial R}\right)^2\right]+\left(\frac{\partial r}{\partial Z}\right)^2+\left(\frac{\partial z}{\partial Z}\right)^2\right]\\
&+ \frac{1}{\varepsilon^2}\left(\frac{\partial r}{\partial R}\frac{\partial z}{\partial Z}-\frac{\partial r}{\partial Z}\frac{\partial z}{\partial R}\right)^2,\\
I_3(C) &= \left(\frac{r}{1+\varepsilon R}\right)^2\left[\frac{1}{\varepsilon^2}\left(\frac{\partial r}{\partial R}\frac{\partial z}{\partial Z}-\frac{\partial r}{\partial Z}\frac{\partial z}{\partial R}\right)^2\right],
\end{aligned} \tag{3.20}$$

respectively. Noting that

$$S_{\Theta r}=S_{R\theta}=S_{Z\theta}=S_{\Theta z}=0\,, \tag{3.21}$$

it follows from (2.69) that the nonzero components of the nominal stress tensor for a compressible hyperelastic material are given by

$$\begin{aligned}
S_{Rr} &= 2\left[\frac{1}{\varepsilon^2}\frac{\partial W}{\partial I_1}\frac{\partial r}{\partial R}+\frac{1}{\varepsilon}\frac{\partial W}{\partial I_2}K_{Rr}+\frac{1}{\varepsilon^2}\frac{\partial W}{\partial I_3}\left(\frac{r}{1+\varepsilon R}\right)^2\frac{\partial z}{\partial Z}\left(\frac{\partial r}{\partial R}\frac{\partial z}{\partial Z}-\frac{\partial z}{\partial R}\frac{\partial r}{\partial Z}\right)\right],\\
S_{Rz} &= 2\left[\frac{1}{\varepsilon^2}\frac{\partial W}{\partial I_1}\frac{\partial z}{\partial R}+\frac{1}{\varepsilon}\frac{\partial W}{\partial I_2}K_{Rz}-\frac{1}{\varepsilon^2}\frac{\partial W}{\partial I_3}\left(\frac{r}{1+\varepsilon R}\right)^2\frac{\partial r}{\partial Z}\left(\frac{\partial r}{\partial R}\frac{\partial z}{\partial Z}-\frac{\partial z}{\partial R}\frac{\partial r}{\partial Z}\right)\right],\\
S_{\Theta\theta} &= 2\left(\frac{r}{1+\varepsilon R}\right)\left[\frac{\partial W}{\partial I_1}+\frac{\partial W}{\partial I_2}K_{\Theta\theta}+\frac{1}{\varepsilon^2}\frac{\partial W}{\partial I_3}\left(\frac{\partial r}{\partial R}\frac{\partial z}{\partial Z}-\frac{\partial z}{\partial R}\frac{\partial r}{\partial Z}\right)^2\right],\\
S_{Zr} &= 2\left[\frac{\partial W}{\partial I_1}\frac{\partial r}{\partial Z}+\frac{\partial W}{\partial I_2}K_{Zr}-\frac{1}{\varepsilon^2}\frac{\partial W}{\partial I_3}\left(\frac{r}{1+\varepsilon R}\right)^2\frac{\partial z}{\partial R}\left(\frac{\partial r}{\partial R}\frac{\partial z}{\partial Z}-\frac{\partial z}{\partial R}\frac{\partial r}{\partial Z}\right)\right],\\
S_{Zz} &= 2\left[\frac{\partial W}{\partial I_1}\frac{\partial z}{\partial Z}+\frac{\partial W}{\partial I_2}K_{Zz}+\frac{1}{\varepsilon^2}\frac{\partial W}{\partial I_3}\left(\frac{r}{1+\varepsilon R}\right)^2\frac{\partial r}{\partial R}\left(\frac{\partial r}{\partial R}\frac{\partial z}{\partial Z}-\frac{\partial z}{\partial R}\frac{\partial r}{\partial Z}\right)\right].
\end{aligned} \tag{3.22}$$

where the following notation is used

$$K_{Rr}=\frac{1}{\varepsilon}\frac{\partial r}{\partial R}\left[\left(\frac{r}{1+\varepsilon R}\right)^2+\left(\frac{\partial r}{\partial Z}\right)^2+\left(\frac{\partial z}{\partial Z}\right)^2\right]$$

$$
\begin{aligned}
& \qquad -\frac{1}{\varepsilon}\frac{\partial r}{\partial Z}\left(\frac{\partial r}{\partial R}\frac{\partial r}{\partial Z}+\frac{\partial z}{\partial R}\frac{\partial z}{\partial Z}\right), \\
K_{Rz} &= \frac{1}{\varepsilon}\frac{\partial z}{\partial R}\left[\left(\frac{r}{1+\varepsilon R}\right)^2+\left(\frac{\partial r}{\partial Z}\right)^2+\left(\frac{\partial z}{\partial Z}\right)^2\right] \\
& \qquad -\frac{1}{\varepsilon}\frac{\partial z}{\partial Z}\left(\frac{\partial r}{\partial R}\frac{\partial r}{\partial Z}+\frac{\partial z}{\partial R}\frac{\partial z}{\partial Z}\right), \\
K_{\Theta\theta} &= \left(\frac{\partial r}{\partial Z}\right)^2+\left(\frac{\partial z}{\partial Z}\right)^2+\frac{1}{\varepsilon^2}\left[\left(\frac{\partial r}{\partial R}\right)^2+\left(\frac{\partial z}{\partial R}\right)^2\right], \\
K_{Zr} &= \frac{\partial r}{\partial Z}\left[\left(\frac{r}{1+\varepsilon R}\right)^2+\frac{1}{\varepsilon^2}\left[\left(\frac{\partial r}{\partial R}\right)^2+\left(\frac{\partial z}{\partial R}\right)^2\right]\right] \\
& \qquad -\frac{1}{\varepsilon^2}\frac{\partial r}{\partial R}\left(\frac{\partial r}{\partial R}\frac{\partial r}{\partial Z}+\frac{\partial z}{\partial R}\frac{\partial z}{\partial Z}\right), \\
K_{Zz} &= \frac{\partial z}{\partial Z}\left[\left(\frac{r}{1+\varepsilon R}\right)^2+\frac{1}{\varepsilon^2}\left[\left(\frac{\partial r}{\partial R}\right)^2+\left(\frac{\partial z}{\partial R}\right)^2\right]\right] \\
& \qquad -\frac{1}{\varepsilon^2}\frac{\partial z}{\partial R}\left(\frac{\partial r}{\partial R}\frac{\partial r}{\partial Z}+\frac{\partial z}{\partial R}\frac{\partial z}{\partial Z}\right). \qquad (3.23)
\end{aligned}
$$

Similarly, it follows from (2.71) that the nonzero components of the nominal stress tensor for an incompressible hyperelastic material are given by

$$
\begin{aligned}
S_{Rr} &= 2\left(\frac{1}{\varepsilon^2}\frac{\partial W}{\partial I_1}\frac{\partial r}{\partial R}+\frac{1}{\varepsilon}\frac{\partial W}{\partial I_2}K_{Rr}\right)-\frac{p}{\varepsilon}\frac{r}{1+\varepsilon R}\frac{\partial z}{\partial Z}, \\
S_{Rz} &= 2\left(\frac{1}{\varepsilon^2}\frac{\partial W}{\partial I_1}\frac{\partial z}{\partial R}+\frac{1}{\varepsilon}\frac{\partial W}{\partial I_2}K_{Rz}\right)+\frac{p}{\varepsilon}\frac{r}{1+\varepsilon R}\frac{\partial r}{\partial Z}, \\
S_{\Theta\theta} &= 2\frac{r}{1+\varepsilon R}\left(\frac{\partial W}{\partial I_1}+\frac{\partial W}{\partial I_2}K_{\Theta\theta}\right)-\frac{p}{\varepsilon}\left(\frac{\partial r}{\partial R}\frac{\partial z}{\partial Z}-\frac{\partial z}{\partial R}\frac{\partial r}{\partial Z}\right), \\
S_{Zr} &= 2\left(\frac{\partial W}{\partial I_1}\frac{\partial r}{\partial Z}+\frac{\partial W}{\partial I_2}K_{Zr}\right)+\frac{p}{\varepsilon}\frac{r}{1+\varepsilon R}\frac{\partial z}{\partial R}, \\
S_{Zz} &= 2\left(\frac{\partial W}{\partial I_1}\frac{\partial z}{\partial Z}+\frac{\partial W}{\partial I_2}K_{Zz}\right)-\frac{p}{\varepsilon}\frac{r}{1+\varepsilon R}\frac{\partial r}{\partial R}, \qquad (3.24)
\end{aligned}
$$

where K_{Rr}, K_{Rz}, … ,K_{Zz} are given by (3.23). Furthermore, in the dimensionless coordinates, the equations of motion given by (2.75) and (2.77) reduce to

$$
\frac{\partial S_{Rr}}{\partial R}+\frac{\partial S_{Zr}}{\partial Z}+\frac{1}{1+\varepsilon R}\left(\varepsilon S_{Rr}-S_{\Theta\theta}\right)=\frac{\partial^2 r}{\partial t^2}, \qquad (3.25)
$$

$$
\frac{\partial S_{Rz}}{\partial R}+\frac{\partial S_{Zz}}{\partial Z}+\frac{\varepsilon}{1+\varepsilon R}S_{Rz}=\frac{\partial^2 z}{\partial t^2}. \qquad (3.26)
$$

With a similar process, the scaled forms of the boundary conditions given by

(3.9) and (3.10) are obtained in the form

$$S_{Rr} = \frac{r}{1+\varepsilon R}\left(\frac{\partial r}{\partial Z}P_t - \frac{\partial z}{\partial Z}P_n\right)\ , \quad S_{Rz} = \frac{r}{1+\varepsilon R}\left(\frac{\partial z}{\partial Z}P_t + \frac{\partial r}{\partial Z}P_n\right)\ , \quad \text{at } R=0\,. \tag{3.27}$$

and

$$S_{Rr} = 0\ , \quad S_{Rz} = 0 \qquad \text{at } R = 1. \tag{3.28}$$

Finally, we want to point out that the relationship between the principal Biot stresses and the components of the nominal stress tensor, given by (2.74), takes the following form

$$T_2^2 = S_{\Theta\theta}^2\ , \quad T_1^2+T_3^2 = S_{Zr}^2+S_{Zz}^2+\varepsilon^2(S_{Rr}^2+S_{Rz}^2)\ , \quad T_1^2T_3^2 = \varepsilon^2(S_{Rr}S_{Zz}-S_{Rz}S_{Zr})^2\,. \tag{3.29}$$

3.5 Asymptotic Expansion: The Incompressible Problem

Now, recalling the dependence of the basic equations written in the dimensionless coordinates on ε, it is assumed that the deformed radial coordinate r, the deformed axial coordinate z, the nominal stres tensor $\mathbf{S}$ and the hydrostatic pressure p may be expanded in powers of ε in the form

$$r(R,Z,t) = r^{(0)}(R,Z,t) + \varepsilon r^{(1)}(R,Z,t) + \ldots \tag{3.30}$$

$$z(R,Z,t) = z^{(0)}(R,Z,t) + \varepsilon z^{(1)}(R,Z,t) + \ldots \tag{3.31}$$

$$\mathbf{S}(R,Z,t) = \mathbf{S}^{(0)}(R,Z,t) + \varepsilon \mathbf{S}^{(1)}(R,Z,t) + \ldots \tag{3.32}$$

$$p(R,Z,t) = p^{(0)}(Z,R,t) + \varepsilon p^{(1)}(R,Z,t) + \ldots \tag{3.33}$$

where the coefficients of the parameter ε are assumed to be of order unity. The scaling made in (3.11)-(3.16) and the expansion (3.30)-(3.33) are the main assumptions of this section and an asymptotic expansion will be developed without any additional assumptions. It is expected that the leading terms of this expansion will identify the main features of the true solution of the three-dimensional problem.

If we substitute the asymptotic expansion (3.30)-(3.33) in the dimensionless form of the basic equations and equate the coefficients of powers of ε to zero, we get a hierarchy of the basic equations to be satisfied for each order of ε. In what follows, we study the leading order equations of the asymptotic expansion in detail. To this end we do not record information about higher order terms which will not be needed later in the analysis.

Suppose that the expansions of $r(R,Z)$ and $z(R,Z)$ are substituted into the scaled form of the right Cauchy-Green tensor given by (3.18) and that the limit of the resulting components of the right Cauchy-Green tensor is taken as ε tends to zero. Since we require that the components of the right Cauchy-Green tensor $\mathbf{C}$ take finite values, we obtain the following equations

$$\left(\frac{\partial r^{(0)}}{\partial R}\right)^2 + \left(\frac{\partial z^{(0)}}{\partial R}\right)^2 = 0, \qquad \frac{\partial r^{(0)}}{\partial R}\frac{\partial r^{(0)}}{\partial Z} + \frac{\partial z^{(0)}}{\partial R}\frac{\partial z^{(0)}}{\partial Z} = 0\ . \tag{3.34}$$

The first equation implies that the derivatives of $r^{(0)}$ and $z^{(0)}$ with respect to R must vanish, i.e.

$$\frac{\partial r^{(0)}}{\partial R} \equiv 0, \qquad \frac{\partial z^{(0)}}{\partial R} \equiv 0\ . \tag{3.35}$$

Then the second equation is satisfied identically. Now, for the sake of its simplicity in the subsequent analysis, the following notation is introduced

$$r^{(0)} = g(Z,t), \qquad z^{(0)} = f(Z,t)\ . \tag{3.36}$$

If we substitute the asymptotic expansion (3.30)-(3.33) in the dimensionless form of the basic equations, we obtain the function Φ, the Jacobian J, the stretch ratios Λ_k $(k = 1,2,3)$, the principal invariants I_k $(k = 1,2,3)$, the principal Biot stresses T_k $(k = 1,2,3)$, given by (3.2), (3.17), (3.19), (3.20) and (3.29), respectively, and the strain energy function W as a power series in ε

$$\Phi(R,Z,t) = \phi(Z,t) + \mathcal{O}(\varepsilon) \tag{3.37}$$

$$J = j + \mathcal{O}(\varepsilon) \tag{3.38}$$

$$\Lambda_k = \lambda_k + \mathcal{O}(\varepsilon), \qquad (k = 1,2,3) \tag{3.39}$$

$$I_k = i_k + \mathcal{O}(\varepsilon), \qquad (k = 1,2,3), \tag{3.40}$$

T.C. YÜKSEKÖĞRETİM KURULU DOKÜMANTASYON MERKEZİ

$$T_k = T_k^{(0)} + \mathcal{O}(\varepsilon), \quad (k = 1, 2, 3) \tag{3.41}$$

$$W = w + \mathcal{O}(\varepsilon), \quad (k = 1, 2, 3) \tag{3.42}$$

where the zeroth-order approximation, ϕ, of the function Φ is

$$\phi = \left[(f')^2 + (g')^2\right]^{\frac{1}{2}} , \tag{3.43}$$

the zeroth-order Jacobian j is

$$j = g\left(f'\frac{\partial r^{(1)}}{\partial R} - g'\frac{\partial z^{(1)}}{\partial R}\right) , \tag{3.44}$$

the zeroth-order principal stretch ratios λ_k $(k = 1, 2, 3)$ satisfy

$$\lambda_2^2 = g^2, \quad \lambda_1^2 + \lambda_3^2 = \phi^2 + \left(\frac{\partial r^{(1)}}{\partial R}\right)^2 + \left(\frac{\partial z^{(1)}}{\partial R}\right)^2, \quad \lambda_1^2\lambda_3^2 = \left(f'\frac{\partial r^{(1)}}{\partial R} - g'\frac{\partial z^{(1)}}{\partial R}\right)^2 , \tag{3.45}$$

the zeroth-order principal invariants i_k $(k = 1, 2, 3)$ are

$$\begin{aligned} i_1 &= g^2 + \phi^2 + \left(\frac{\partial r^{(1)}}{\partial R}\right)^2 + \left(\frac{\partial z^{(1)}}{\partial R}\right)^2 , \\ i_2 &= \frac{1}{g^2} + g^2\left[\phi^2 + \left(\frac{\partial r^{(1)}}{\partial R}\right)^2 + \left(\frac{\partial z^{(1)}}{\partial R}\right)^2\right] , \\ i_3 &= g^2\left(f'\frac{\partial r^{(1)}}{\partial R} - g'\frac{\partial z^{(1)}}{\partial R}\right)^2 , \end{aligned} \tag{3.46}$$

the zeroth-order principal Biot stresses are

$$T_1^{(0)} = \sqrt{\left(S_{Zr}^{(0)}\right)^2 + \left(S_{Zz}^{(0)}\right)^2} , \quad T_2^{(0)} = S_{\Theta\theta}^{(0)} , \quad T_3^{(0)} = 0 , \tag{3.47}$$

and the zeroth-order strain energy function w is

$$w = w(i_1, i_2, i_3) . \tag{3.48}$$

Note that $i_3 = j^2$ and that the incompressibility condition $J = 1$ takes the following form $j = 1$ (consequently $i_3 = 1$) at the zeroth-order approximation. Then it follows from (3.44) that the incompressibility condition can be rewritten in the form

$$\left(f'\frac{\partial r^{(1)}}{\partial R} - g'\frac{\partial z^{(1)}}{\partial R}\right) = \frac{1}{g} . \tag{3.49}$$

Introducing (3.30)-(3.33) into (3.25) and (3.26), the equations of motion corresponding to the zeroth-order approximation are obtained in the form:

$$\frac{\partial S_{Rr}^{(0)}}{\partial R} + \frac{\partial S_{Zr}^{(0)}}{\partial Z} - S_{\Theta\theta}^{(0)} = \frac{\partial^2 g}{\partial t^2}, \qquad \frac{\partial S_{Rz}^{(0)}}{\partial R} + \frac{\partial S_{Zz}^{(0)}}{\partial Z} = \frac{\partial^2 f}{\partial t^2}, \tag{3.50}$$

With a similar process, using (3.30)-(3.33) in (3.27)-(3.28), the boundary conditions at the zeroth-order approximation are found as

$$S_{Rr}^{(0)} = g\,(g'P_t - f'P_n)\;, \qquad S_{Rz}^{(0)} = g\,(f'P_t + g'P_n) \qquad \text{at } R = 0 \tag{3.51}$$

and

$$S_{Rr}^{(0)} = 0\,, \quad S_{Rz}^{(0)} = 0 \qquad \text{at } R = 1. \tag{3.52}$$

In order to find the constitutive equations corresponding to the zeroth-order approximation we first expand the derivatives of the strain-energy function with respect to the principal invariants, $\frac{\partial W}{\partial I_l}$ $(l = 1, 2)$, appearing in the constitutive relations (3.24). For this purpose the following Taylor's expansion of a general function $F(I_1(\varepsilon), I_2(\varepsilon), I_3(\varepsilon))$

$$F(I_1(\varepsilon), I_2(\varepsilon), I_3(\varepsilon)) = F(I_1, I_2, I_3)\,|_{\varepsilon=0} + \mathcal{O}(\varepsilon)\;. \tag{3.53}$$

Since it follows from (3.40) that

$$I_1\,|_{\varepsilon=0} = i_1, \qquad I_2\,|_{\varepsilon=0} = i_2, \qquad I_3\,|_{\varepsilon=0} = 1 \tag{3.54}$$

for incompressible hyperelastic tubes, we can write the derivatives of the strain-energy function with respect to the principal invariants, $\frac{\partial W}{\partial I_l}$ $(l = 1, 2)$, in the form

$$\frac{\partial W}{\partial I_l} = \left.\frac{\partial W}{\partial I_l}\right|_{I_k = i_k} + \mathcal{O}(\varepsilon), \qquad l = 1, 2\;, \quad k = 1, 2\;. \tag{3.55}$$

Now, for the sake of brevity, we define

$$W_l = \left.\frac{\partial W}{\partial I_l}\right|_{I_k = i_k}, \qquad l = 1, 2\;, \quad k = 1, 2\;. \tag{3.56}$$

Using the above equations in (3.24), we obtain the following constitutive relations for $S_{\Theta\theta}$, S_{Zr} and S_{Zz} at the zeroth-order approximation:

$$S_{\Theta\theta}^{(0)} = 2g\left[W_1 + W_2\left[\phi^2 + \left(\frac{\partial r^{(1)}}{\partial R}\right)^2 + \left(\frac{\partial z^{(1)}}{\partial R}\right)^2\right)\right] - \frac{1}{g}p^{(0)}\,, \tag{3.57}$$

$$\begin{aligned} S_{Zr}^{(0)} = 2g'W_1 - 2W_2&\left[\frac{\partial r^{(1)}}{\partial R}\left(g'\frac{\partial r^{(1)}}{\partial R} + f'\frac{\partial z^{(1)}}{\partial R}\right)\right. \\ &\left. -g'\left[g^2 + \left(\frac{\partial r^{(1)}}{\partial R}\right)^2 + \left(\frac{\partial z^{(1)}}{\partial R}\right)^2\right]\right] + gp^{(0)}\frac{\partial z^{(1)}}{\partial R}\,, \end{aligned} \tag{3.58}$$

$$\begin{aligned} S_{Zz}^{(0)} = 2f'W_1 - 2W_2&\left[\frac{\partial z^{(1)}}{\partial R}\left(g'\frac{\partial r^{(1)}}{\partial R} + f'\frac{\partial z^{(1)}}{\partial R}\right)\right. \\ &\left. -f'\left[g^2 + \left(\frac{\partial r^{(1)}}{\partial R}\right)^2 + \left(\frac{\partial z^{(1)}}{\partial R}\right)^2\right]\right] - gp^{(0)}\frac{\partial r^{(1)}}{\partial R}\,. \end{aligned} \tag{3.59}$$

Also we observe that the expansions corresponding to S_{Rr} and S_{Rz} include the negative powers of ε. Since the expansion (3.32) suggests that the nominal stress tensor components having negative index are zero, some constraints on the deformed radial and axial coordinates are obtained. Now, these constraints will be discussed in detail. The restrictions $S_{Rr}^{(-1)} = 0$ and $S_{Rz}^{(-1)} = 0$ give the following equations

$$W_1\frac{\partial r^{(1)}}{\partial R} + W_2\left[\left(g^2+\phi^2\right)\frac{\partial r^{(1)}}{\partial R} - g'\left(g'\frac{\partial r^{(1)}}{\partial R} + f'\frac{\partial z^{(1)}}{\partial R}\right)\right] - \frac{1}{2}f'gp^{(0)} = 0\,, \tag{3.60}$$

and

$$W_1\frac{\partial z^{(1)}}{\partial R} + W_2\left[\left(g^2+\phi^2\right)\frac{\partial z^{(1)}}{\partial R} - f'\left(g'\frac{\partial r^{(1)}}{\partial R} + f'\frac{\partial z^{(1)}}{\partial R}\right)\right] + \frac{1}{2}g'gp^{(0)} = 0\,, \tag{3.61}$$

respectively. Multiplying these equations by f' and g', and subtracting and adding the resulting equations, we obtain

$$\left(g'\frac{\partial r^{(1)}}{\partial R} + f'\frac{\partial z^{(1)}}{\partial R}\right)\left[W_2\left(f'\frac{\partial r^{(1)}}{\partial R} - g'\frac{\partial z^{(1)}}{\partial R}\right) - \frac{1}{2}gp^{(0)}\right] = 0\,, \tag{3.62}$$

and

$$\left(f'\frac{\partial r^{(1)}}{\partial R} - g'\frac{\partial z^{(1)}}{\partial R}\right)\left[W_1 + W_2\left(g^2+\phi^2\right)\right] - \frac{1}{2}g\phi^2p^{(0)} = 0\,. \tag{3.63}$$

Note that the incompressibility condition (3.49) and (3.62) and (3.63) give sufficient relations to determine the unknown functions $\dfrac{\partial r^{(1)}}{\partial R}$, $\dfrac{\partial z^{(1)}}{\partial R}$ and $p^{(0)}$.

In order to solve these equations, we introduce the incompressibility condition (3.49) into (3.63) and obtain

$$p^{(0)} = \frac{2}{g^2\phi^2}\left[W_1 + W_2\left(g^2 + \phi^2\right)\right] \; . \tag{3.64}$$

Then, substituting this result and (3.49) into (3.62), we get

$$\frac{1}{g\phi^2}\left(g'\frac{\partial r^{(1)}}{\partial R} + f'\frac{\partial z^{(1)}}{\partial R}\right)\left(W_1 + W_2 g^2\right) = 0 \, . \tag{3.65}$$

The above equation (3.65) is satisfied if either the equation

$$W_1 + W_2 g^2 = 0 \, , \tag{3.66}$$

or the equation

$$g'\frac{\partial r^{(1)}}{\partial R} + f'\frac{\partial z^{(1)}}{\partial R} = 0 \tag{3.67}$$

is satisfied. Since we assume that W is an arbitrary function of the principal invariants, it follows that (3.67) is satisfied identically. Note that in the above treatment we have not placed any restriction on the form of the strain energy function. Thus, it follows from (3.67) and (3.49) that

$$\frac{\partial r^{(1)}}{\partial R} = \frac{f'}{g\phi^2} \, , \qquad \frac{\partial z^{(1)}}{\partial R} = -\frac{g'}{g\phi^2} \, . \tag{3.68}$$

We notice that the derivatives of the first-order aproximations of the deformed radial and axial coordinates with respect to R are independent of the dimensionless undeformed radial coordinate R. That is, the first-order approximations of the deformed radial and axial coordinates, $r^{(1)}$ and $z^{(1)}$, vary linearly along the thickness of the tube whereas the zeroth-order deformed radial and axial coordinates f and g are uniform over the thickness.

If we employ (3.68) in (3.45) and (3.46), we obtain the zeroth-order stretch ratios and the zeroth-order principal invariants in the form

$$\lambda_2^2 = g^2 \, , \qquad \lambda_1^2 + \lambda_3^2 = \phi^2 + \frac{1}{g^2\phi^2} \, , \qquad \lambda_1^2\lambda_3^2 = \frac{1}{g^2} \tag{3.69}$$

and,

$$i_1 = \phi^2 + g^2 + \frac{1}{g^2\phi^2} \, , \quad i_2 = \frac{1}{\phi^2} + \frac{1}{g^2} + g^2\phi^2 \, , \quad i_3 = 1 \tag{3.70}$$

respectively. Then we deduce from (3.69) that

$$\lambda_1 = \phi \,, \qquad \lambda_2 = g \,, \qquad \lambda_3 = \frac{1}{g\phi} \,. \tag{3.71}$$

Note that both the zeroth-order stretch ratios and the zeroth-order principal invariants are independent of R. Consequently, W_1 and W_2 are independent of R. By using (3.64) and (3.68) in (3.57)-(3.59), the zeroth-order components of the nominal stress tensor are obtained in the form

$$S^{(0)}_{\Theta\theta} = 2g\left(1 - \frac{1}{g^4\phi^2}\right)\left(W_1 + W_2\phi^2\right) \,, \tag{3.72}$$

$$S^{(0)}_{Zr} = 2g'\left(1 - \frac{1}{g^2\phi^4}\right)\left(W_1 + W_2 g^2\right) \,, \tag{3.73}$$

$$S^{(0)}_{Zz} = 2f'\left(1 - \frac{1}{g^2\phi^4}\right)\left(W_1 + W_2 g^2\right) \,. \tag{3.74}$$

from which we deduce

$$f' S^{(0)}_{Zr} = g' S^{(0)}_{Zz} \,. \tag{3.75}$$

Note that the above zeroth-order components of the nominal stress tensor are independent of R.

Recalling that $S^{(0)}_{Zr}$ and $S^{(0)}_{Zz}$ are independent of R, we now integrate (3.50) with respect to R between the limits 0 and 1. Employing the boundary conditions (3.51) and (3.52), we obtain the following equations

$$\frac{\partial S^{(0)}_{Zr}}{\partial Z} - S^{(0)}_{\Theta\theta} + g(f'P_n - g'P_t) = \frac{\partial^2 g}{\partial t^2} \,, \tag{3.76}$$

$$\frac{\partial S^{(0)}_{Zz}}{\partial Z} - g(g'P_n + f'P_t) = \frac{\partial^2 f}{\partial t^2} \tag{3.77}$$

from which we easily deduce

$$f'\frac{\partial S^{(0)}_{Zr}}{\partial Z} - f' S^{(0)}_{\Theta\theta} + g\phi^2 P_n - g'\frac{\partial S^{(0)}_{Zz}}{\partial Z} = f'\frac{\partial^2 g}{\partial t^2} - g'\frac{\partial^2 f}{\partial t^2} \,, \tag{3.78}$$

$$g'\frac{\partial S^{(0)}_{Zr}}{\partial Z} - g' S^{(0)}_{\Theta\theta} - g\phi^2 P_t + f'\frac{\partial S^{(0)}_{Zz}}{\partial Z} = g'\frac{\partial^2 g}{\partial t^2} + f'\frac{\partial^2 f}{\partial t^2} \,. \tag{3.79}$$

If the zeroth-order constitutive relations given by (3.72)-(3.74) are employed in (3.78)-(3.79), the following system of two coupled second-order nonlinear partial differential equations is obtained:

$$
\begin{aligned}
&f'g'' - g'f'' - \left[\frac{f'\phi^2}{g}\left(1-g^4\phi^2\right)\left(W_1+W_2\phi^2\right)+\frac{g^3\phi^6}{2}P_n\right.\\
&\qquad\left.-\frac{g^2\phi^4}{2}\left(f'\frac{\partial^2 g}{\partial t^2}-g'\frac{\partial^2 f}{\partial t^2}\right)\right]\frac{1}{\left(1-g^2\phi^4\right)\left(W_1+W_2g^2\right)}=0\,, \qquad (3.80)\\
&g'g'' + f'f'' + \left[\frac{g'\phi^2}{g}\left[W_1\left(3-g^4\phi^2\right)+W_2\left(1+g^4\phi^2\right)\phi^2\right]\right.\\
&\qquad -\phi^2\left(1-g^2\phi^4\right)\left(W'_1+W'_2g^2\right)-\frac{g^3\phi^6}{2}P_t\\
&\qquad\left.-\frac{g^2\phi^4}{2}\left(g'\frac{\partial^2 g}{\partial t^2}+f'\frac{\partial^2 f}{\partial t^2}\right)\right]\frac{1}{\left(3+g^2\phi^4\right)\left(W_1+W_2g^2\right)}=0\,. \qquad (3.81)
\end{aligned}
$$

It may be shown that equations (3.80) and (3.81) are in agreement with those derived in the membrane theory. For instance, they are identical to equations (3.37) of [4] when static deformations of membrane tubes made of the neo-Hookean material are considered. That is, equations (3.37) of [4] correspond to a special case of the above equations.

Recalling that ϕ is given by (3.43), we now introduce a new function $\beta(Z,t)$ in order to write the above system as a system of four coupled first-order nonlinear partial differential equations in the form

$$f' = \phi\,\sin\beta\,, \qquad (3.82)$$

$$g' = \phi\,\cos\beta\,, \qquad (3.83)$$

$$
\begin{aligned}
&\beta' + \left[\frac{\phi\,\sin\beta}{g}\left(1-g^4\phi^2\right)\left(W_1+W_2\phi^2\right)+\frac{g^3\phi^4}{2}P_n\right.\\
&\qquad\left.+\frac{g^2\phi^3}{2}\left(\frac{\partial^2 f}{\partial t^2}\cos\beta-\frac{\partial^2 g}{\partial t^2}\sin\beta\right)\right]\frac{1}{\left(1-g^2\phi^4\right)\left(W_1+W_2g^2\right)}=0\,, \qquad (3.84)\\
&\phi' + \left[\frac{\phi^2\cos\beta}{g}\left[W_1\left(3-g^4\phi^2\right)+W_2\left(1+g^4\phi^2\right)\phi^2\right]\right.\\
&\qquad -\phi\left(1-g^2\phi^4\right)\left(W'_1+W'_2g^2\right)-\frac{g^3\phi^5}{2}P_t\\
&\qquad\left.-\frac{g^2\phi^4}{2}\left(\frac{\partial^2 f}{\partial t^2}\sin\beta+\frac{\partial^2 g}{\partial t^2}\cos\beta\right)\right]\frac{1}{\left(3+g^2\phi^4\right)\left(W_1+W_2g^2\right)}=0\,. \qquad (3.85)
\end{aligned}
$$

Here $\beta(Z,t)$ is the angle measured from the outward radius vector to the tangent of the deformed interior generating line. We point out that equations (3.38) of [4] correspond to a special case of the above equations. The above equations may also be written in terms of the principal stretch ratios and the principal Biot stresses. For this purpose, if we employ (3.82) and (3.83) in (3.75) we obtain the following relation

$$S_{Zz}^{(0)} = S_{Zr}^{(0)} \tan\beta \, . \tag{3.86}$$

Then, using this equation and (3.47) we get

$$S_{Zr}^{(0)} = T_1^{(0)} \cos\beta \, , \quad S_{Zz}^{(0)} = T_1^{(0)} \sin\beta \, . \tag{3.87}$$

Thus, introducing the expressions of $S_{\Theta\theta}^{(0)}$, $S_{Zr}^{(0)}$ and $S_{Zz}^{(0)}$ given by (3.47) and (3.87) into the equations of motion given by (3.76) and (3.76) we get

$$\frac{\partial}{\partial Z}\left(T_1^{(0)} \cos\beta\right) - T_2^{(0)} + g\phi\left(P_n \sin\beta - P_t \cos\beta\right) = \frac{\partial^2 g}{\partial t^2} \, , \tag{3.88}$$

$$\frac{\partial}{\partial Z}\left(T_1^{(0)} \sin\beta\right) - g\phi\left(P_n \cos\beta - P_t \sin\beta\right) = \frac{\partial^2 f}{\partial t^2} \, . \tag{3.89}$$

In the remaining part of this section we want to express the principal Biot stress components, $T_1^{(0)}$ and $T_2^{(0)}$, appearing in (3.88) and (3.89) in terms of the derivatives of the strain energy function with respect to the principal stretch ratios. To this end we first point out that the Taylor expansion of a general function $F(\Lambda_1(\varepsilon), \Lambda_2(\varepsilon), \Lambda_3(\varepsilon))$ is

$$F(\Lambda_1(\varepsilon), \Lambda_2(\varepsilon), \Lambda_3(\varepsilon)) = F(\Lambda_1, \Lambda_2, \Lambda_3)\mid_{\varepsilon=0} + \mathcal{O}(\varepsilon) \, . \tag{3.90}$$

Since it follows from (3.39) that

$$\Lambda_1 \mid_{\varepsilon=0} = \lambda_1, \qquad \Lambda_2 \mid_{\varepsilon=0} = \lambda_2, \qquad \Lambda_3 \mid_{\varepsilon=0} = \lambda_3, \tag{3.91}$$

we can write the derivatives of the strain-energy function with respect to the principal stretch ratios, $\dfrac{\partial W}{\partial \Lambda_l}$ $(l = 1, 2)$, in the form

$$\frac{\partial W}{\partial \Lambda_l} = \left.\frac{\partial W}{\partial \Lambda_l}\right|_{\Lambda_k = \lambda_k} + \mathcal{O}(\varepsilon), \qquad l = 1,\, 2 \;\; , \;\; k = 1,\, 2,\, 3 \;\; . \tag{3.92}$$

Now, for the sake of brevity, we define

$$\hat{W}_l = \left.\frac{\partial W}{\partial \Lambda_l}\right|_{\Lambda_k = \lambda_k} \qquad l = 1,\, 2 \;\; , \;\; k = 1,\, 2,\, 3 \;\; . \tag{3.93}$$

We observe that, at the zeroth-order approximation, (2.38) and (2.39) take the following form

$$\hat{W}_1 = 2\lambda_1 \left(1 - \frac{1}{\lambda_1^4 \lambda_2^2}\right) (W_1 + \lambda_2^2 W_2) \tag{3.94}$$

$$\hat{W}_2 = 2\lambda_2 \left(1 - \frac{1}{\lambda_1^2 \lambda_2^4}\right) (W_1 + \lambda_1^2 W_2) \,. \tag{3.95}$$

Then, using these equations in (3.72), (3.73) and (3.74) we obtain

$$S^{(0)}_{\Theta\theta} = \hat{W}_2 \,, \quad S^{(0)}_{Zr} = \hat{W}_1 \cos\beta \,, \quad S^{(0)}_{Zz} = \hat{W}_1 \sin\beta \,. \tag{3.96}$$

It follows from (3.47) and (3.87) that

$$T_1^{(0)} = \hat{W}_1 \,, \quad T_2^{(0)} = \hat{W}_2 \,. \tag{3.97}$$

3.6 Asymptotic Expansion: The Compressible Problem

In this section, the question how the asymptotic expansion method presented in the previous section should be modified for compressible hyperelastic materials is discussed. Recall that the constraint of incompressibility introduces a scalar multiplier, interpreted as a pressure, into the constitutive equations. Therefore, the fundamental difference in applying the asymptotic expansion method to the compressible and incompressible hyperelastic tubes arises from the difference between the constitutive equations. The approach presented in the previous section can be followed mainly. Since we follow the same approach, we briefly summarize the resulting equations here. Note that we use the same notation in both sections unless stated otherwise.

We first point out that (3.45) and (3.46), which give the zeroth-order principal stretch ratios and the zeroth-order principal invariants, respectively, are also valid for the case of compressible hyperelastic materials. For convenience, using (3.44) we prefer to rewrite these equations in the form

$$\lambda_2^2 = g^2 \,, \quad \lambda_1^2 + \lambda_3^2 = \phi^2 + \left(\frac{\partial r^{(1)}}{\partial R}\right)^2 + \left(\frac{\partial z^{(1)}}{\partial R}\right)^2 \,, \quad \lambda_1^2 \lambda_3^2 = \frac{j^2}{g^2} \,, \tag{3.98}$$

and

$$
\begin{aligned}
i_1 &= g^2 + \phi^2 + \left(\frac{\partial r^{(1)}}{\partial R}\right)^2 + \left(\frac{\partial z^{(1)}}{\partial R}\right)^2 , \\
i_2 &= \frac{j^2}{g^2} + g^2 \left[\phi^2 + \left(\frac{\partial r^{(1)}}{\partial R}\right)^2 + \left(\frac{\partial z^{(1)}}{\partial R}\right)^2\right] , \\
i_3 &= j^2 , \qquad (3.99)
\end{aligned}
$$

respectively. Furthermore, we point out that equations (3.50), which are the equations of motion in the zeroth-order approximation for incompressible case, are also valid for the case of compressible hyperelastic materials. Similarly, the boundary conditions in the zeroth-order approximation are given by (3.51) and (3.52).

As in the previous section, we expand the derivatives of the strain-energy function W with respect to the principal invariants (see (3.55)) and set $W_l = \left.\frac{\partial W}{\partial I_l}\right|_{I_k = i_k}$ $(l, k = 1, 2, 3)$. Then, it follows from (3.22) and (3.23) and the equations presented in the previous section that the zeroth-order approximations of $S_{\Theta\theta}$, S_{Zr} and S_{Zz} are

$$
\begin{aligned}
S^{(0)}_{\Theta\theta} &= 2g\left[W_1 + W_2\left[\left(\frac{\partial r^{(1)}}{\partial R}\right)^2 + \left(\frac{\partial z^{(1)}}{\partial R}\right)^2 + \phi^2\right]\right] \\
&\quad + 2gW_3\left(f'\frac{\partial r^{(1)}}{\partial R} - g'\frac{\partial z^{(1)}}{\partial R}\right)^2 , \qquad (3.100) \\
S^{(0)}_{Zr} &= 2W_1 g' - 2W_2\left[\frac{\partial r^{(1)}}{\partial R}\left(g'\frac{\partial r^{(1)}}{\partial R} + f'\frac{\partial z^{(1)}}{\partial R}\right) - g'\left[\left(\frac{\partial r^{(1)}}{\partial R}\right)^2 + \left(\frac{\partial z^{(1)}}{\partial R}\right)^2\right.\right. \\
&\quad \left.\left. + g^2\right]\right] - 2g^2 W_3 \frac{\partial z^{(1)}}{\partial R}\left(f'\frac{\partial r^{(1)}}{\partial R} - g'\frac{\partial z^{(1)}}{\partial R}\right) , \qquad (3.101) \\
S^{(0)}_{Zz} &= 2W_1 f' - 2W_2\left[\frac{\partial z^{(1)}}{\partial R}\left(g'\frac{\partial r}{\partial R} + f'\frac{\partial z^{(1)}}{\partial R}\right) - f'\left[\left(\frac{\partial r^{(1)}}{\partial R}\right)^2 + \left(\frac{\partial z^{(1)}}{\partial R}\right)^2\right.\right. \\
&\quad \left.\left. + g^2\right]\right] + 2g^2 W_3 \frac{\partial r^{(1)}}{\partial R}\left(f'\frac{\partial r^{(1)}}{\partial R} - g'\frac{\partial z^{(1)}}{\partial R}\right) . \qquad (3.102)
\end{aligned}
$$

Also, as in the case of incompressible hyperelastic materials, we observe that the expansions corresponding to S_{Rr} and S_{Rz} include the negative powers of ε. Since the expansion (3.32) suggests that the nominal stress tensor components having negative index are zero, some constraints on the deformed radial and axial coordinates are obtained. Thus, the restrictions $S^{(-1)}_{Rr} = 0$ and $S^{(-1)}_{Rz} = 0$ give the following equations

$$W_1 \frac{\partial r^{(1)}}{\partial R} + W_2 \left[\left(g^2 + \Phi^2\right) \frac{\partial r^{(1)}}{\partial R} - g' \left(g' \frac{\partial r^{(1)}}{\partial R} + f' \frac{\partial z^{(1)}}{\partial R} \right) \right] + W_3 g^2 f' \left(f' \frac{\partial r^{(1)}}{\partial R} - g' \frac{\partial z^{(1)}}{\partial R} \right) = 0 \,, \tag{3.103}$$

$$W_1 \frac{\partial z^{(1)}}{\partial R} + W_2 \left[\left(g^2 + \Phi^2\right) \frac{\partial z^{(1)}}{\partial R} - f' \left(g' \frac{\partial r^{(1)}}{\partial R} + f' \frac{\partial z^{(1)}}{\partial R} \right) \right] - W_3 g^2 g' \left(f' \frac{\partial r^{(1)}}{\partial R} - g' \frac{\partial z^{(1)}}{\partial R} \right) = 0 \,. \tag{3.104}$$

Multiplying these equations by f' and g', and subtracting and adding the resulting equations, we obtain

$$\frac{j}{g} \left(g' \frac{\partial r^{(1)}}{\partial R} + f' \frac{\partial z^{(1)}}{\partial R} \right) \left(W_2 + W_3 g^2\right) = 0 \,, \tag{3.105}$$

and

$$\frac{j}{g} \left[W_1 + W_2 \left(g^2 + \phi^2\right) + W_3 g^2 \phi^2 \right] = 0 \,, \tag{3.106}$$

where (3.44) is used. Since $j \neq 0$, (3.105) and (3.106) reduce to

$$\left(g' \frac{\partial r^{(1)}}{\partial R} + f' \frac{\partial z^{(1)}}{\partial R} \right) \left(W_2 + W_3 g^2\right) = 0 \,, \tag{3.107}$$

and

$$W_1 + \left(g^2 + \phi^2\right) W_2 + g^2 \phi^2 W_3 = 0 \,, \tag{3.108}$$

respectively. The above equation (3.107) is satisfied if either the equation

$$W_2 + W_3 g^2 = 0 \,, \tag{3.109}$$

or the equation

$$g' \frac{\partial r^{(1)}}{\partial R} + f' \frac{\partial z^{(1)}}{\partial R} = 0 \tag{3.110}$$

is satisfied. Since we assume that W is an arbitrary function of the principal invariants, it follows that (3.110) is satisfied identically. Note that in the above treatment, as in the incompressible problem, we have not placed any restriction on the form of the strain energy function. Using (3.44) and (3.110) we determine the unknown functions $\dfrac{\partial r^{(1)}}{\partial R}$ and $\dfrac{\partial z^{(1)}}{\partial R}$ in terms of j as follows

$$\frac{\partial r^{(1)}}{\partial R} = \frac{jf'}{g\phi^2}\,, \qquad \frac{\partial z^{(1)}}{\partial R} = -\frac{jg'}{g\phi^2}\,, \tag{3.111}$$

Note that the restriction (3.108) may be used to eliminate j from the above equations if the strain energy function is specified. If we employ (3.111) in (3.98) we obtain

$$\lambda_2^2 = g^2\,, \quad \lambda_1^2 + \lambda_3^2 = \phi^2 + \frac{j^2}{g^2\phi^2}\,, \quad \lambda_1^2\lambda_3^2 = \frac{j^2}{g^2}\,, \tag{3.112}$$

from which we deduce that

$$\lambda_1 = \phi\,, \quad \lambda_2 = g\,, \quad \lambda_3 = \frac{j}{g\phi}\,. \tag{3.113}$$

Similarly, using (3.111) in (3.99), the zeroth-order principal invariants are obtained in the form

$$i_1 = \phi^2 + g^2 + \frac{j^2}{g^2\phi^2}\,, \quad i_2 = \frac{j^2}{\phi^2} + \frac{j^2}{g^2} + g^2\phi^2\,, \quad i_3 = j^2\,. \tag{3.114}$$

Futhermore, if we employ (3.111) in (3.100)-(3.102) we obtain the zeroth-order components of the nominal stress tensor as follows,

$$S^{(0)}_{\Theta\theta} = 2g\left[W_1 + \left(\frac{j^2}{g^2\phi^2} + \phi^2\right)W_2 + \frac{j^2}{g^2}W_3\right]\,, \tag{3.115}$$

$$S^{(0)}_{Zr} = 2g'\left[W_1 + \left(\frac{j^2}{g^2\phi^2} + g^2\right)W_2 + \frac{j^2}{\phi^2}W_3\right]\,, \tag{3.116}$$

$$S^{(0)}_{Zz} = 2f'\left[W_1 + \left(\frac{j^2}{g^2\phi^2} + g^2\right)W_2 + \frac{j^2}{\phi^2}W_3\right]\,. \tag{3.117}$$

If we use (3.108) to eliminate W_3 from (3.115)-(3.117), we obtain:

$$S^{(0)}_{\Theta\theta} = 2g\left(W_1 + W_2\phi^2\right)\left(1 - \frac{j^2}{g^4\phi^2}\right)\,, \tag{3.118}$$

$$S^{(0)}_{Zr} = 2g'\left(W_1 + W_2 g^2\right)\left(1 - \frac{j^2}{g^2\phi^4}\right)\,, \tag{3.119}$$

$$S^{(0)}_{Zz} = 2f'\left(W_1 + W_2 g^2\right)\left(1 - \frac{j^2}{g^2\phi^4}\right)\,. \tag{3.120}$$

Note that the relation (3.75) is also valid for the present case. If we substitute (3.118)-(3.120) into (3.78)-(3.79) obtained in the previous section, then we obtain the following system of two coupled second-order nonlinear partial differential equations

$$f'g'' - g'f'' - \left[\frac{f'\phi^2}{g}\left(j^2 - g^4\phi^2\right)(W_1 + W_2\phi^2) + \frac{g^3\phi^6}{2}P_n\right.$$
$$\left. - \frac{g^2\phi^4}{2}\left(f'\frac{\partial^2 g}{\partial t^2} - g'\frac{\partial^2 f}{\partial t^2}\right)\right]\frac{1}{(j^2 - g^2\phi^4)(W_1 + W_2 g^2)} = 0\,, \tag{3.121}$$

$$g'g'' + f'f'' + \left[\frac{g'\phi^2}{g}\left[W_1\left(3j^2 - g^4\phi^2\right) + W_2\left(j^2 + g^4\phi^2\right)\phi^2\right]\right.$$
$$- 2jj'\phi^2(W_1 + W_2 g^2) - \phi^2\left(j^2 - g^2\phi^4\right)\left(W_1' + W_2' g^2\right) - \frac{g^3\phi^6}{2}P_t$$
$$\left. - \frac{g^2\phi^4}{2}\left(g'\frac{\partial^2 g}{\partial t^2} + f'\frac{\partial^2 f}{\partial t^2}\right)\right]\frac{1}{(3j^2 + g^2\phi^4)(W_1 + W_2 g^2)} = 0\,. \tag{3.122}$$

Recalling that ϕ is given by (3.43), as in the previous section we now introduce a new function $\beta(Z,t)$ in order to write the above system as a system of four coupled first-order nonlinear partial differential equations in the form

$$f' = \phi \sin\beta\,, \tag{3.123}$$

$$g' = \phi \cos\beta\,, \tag{3.124}$$

$$\beta' + \left[\frac{\phi \sin\beta}{g}\left(j^2 - g^4\phi^2\right)\left(W_1 + W_2\phi^2\right) + \frac{g^3\phi^4}{2}P_n\right.$$
$$\left. + \frac{g^2\phi^3}{2}\left(\frac{\partial^2 f}{\partial t^2}\cos\beta - \frac{\partial^2 g}{\partial t^2}\sin\beta\right)\right]\frac{1}{\left(j^2 - g^2\phi^4\right)\left(W_1 + W_2 g^2\right)} = 0\,, \tag{3.125}$$

$$\phi' + \left[\frac{\phi^2\cos\beta}{g}\left[W_1\left(3j^2 - g^4\phi^2\right) + W_2\left(j^2 + g^4\phi^2\right)\phi^2\right]\right.$$
$$-2jj'\phi(W_1 + W_2 g^2) - \phi\left(j^2 - g^2\phi^4\right)\left(W'_1 + W'_2 g^2\right) - \frac{g^3\phi^5}{2}P_t$$
$$\left. - \frac{g^2\phi^4}{2}\left(\frac{\partial^2 f}{\partial t^2}\sin\beta + \frac{\partial^2 g}{\partial t^2}\cos\beta\right)\right]\frac{1}{\left(3j^2 + g^2\phi^4\right)\left(W_1 + W_2 g^2\right)} = 0\,. \tag{3.126}$$

where $\beta(Z,t)$ is the angle measured from the outward radius vector to the tangent of the deformed interior generating line. It can be easily shown that the relations (3.86)-(3.87) and the equations of motion given by (3.88)-(3.89) are also valid for the present case.

As in the case of incompressible material, in the remaining part of this section we want to express the principal Biot stress components, $T_1^{(0)}$ and $T_2^{(0)}$, appearing in (3.88) and (3.89) in terms of the derivatives of the strain energy function with respect to the principal stretch ratios. For this aim we first state that the Taylor expansion of a general function $F(\Lambda_1(\varepsilon), \Lambda_2(\varepsilon), \Lambda_3(\varepsilon))$ is

$$F(\Lambda_1(\varepsilon), \Lambda_2(\varepsilon), \Lambda_3(\varepsilon)) = F(\Lambda_1, \Lambda_2, \Lambda_3)\mid_{\varepsilon=0} + \mathcal{O}(\varepsilon)\ . \qquad (3.127)$$

Since it follows from (3.39) that

$$\Lambda_1\mid_{\varepsilon=0} = \lambda_1, \qquad \Lambda_2\mid_{\varepsilon=0} = \lambda_2, \qquad \Lambda_3\mid_{\varepsilon=0} = \lambda_3, \qquad (3.128)$$

we can write the derivatives of the strain-energy function with respect to the principal stretch ratios, $\dfrac{\partial W}{\partial \Lambda_l}$ $(l = 1, 2, 3)$, in the form

$$\frac{\partial W}{\partial \Lambda_l} = \left.\frac{\partial W}{\partial \Lambda_l}\right|_{\Lambda_k=\lambda_k} + \mathcal{O}(\varepsilon), \qquad l = 1,\ 2,\ 3\ \ ,\quad k = 1,\ 2,\ 3\ \ , \qquad (3.129)$$

As in the case of incompressible material, for convenience, we define

$$\hat{W}_l = \left.\frac{\partial W}{\partial \Lambda_l}\right|_{\Lambda_k=\lambda_k} \qquad l = 1,\ 2,\ 3\ \ ,\quad k = 1,\ 2,\ 3\ \ , \qquad (3.130)$$

We observe that, at the zeroth-order approximation, (2.33), (2.34) and (2.35) take the following form

$$\hat{W}_1 = 2\lambda_1 \left[W_1 + (\lambda_2^2 + \lambda_3^2)W_2 + \lambda_2^2\lambda_3^2 W_3\right] \qquad (3.131)$$

$$\hat{W}_2 = 2\lambda_2 \left[W_1 + (\lambda_1^2 + \lambda_3^2)W_2 + \lambda_1^2\lambda_3^2 W_3\right] \qquad (3.132)$$

$$\hat{W}_3 = 2\lambda_3 \left[W_1 + (\lambda_1^2 + \lambda_2^2)W_2 + \lambda_1^2\lambda_2^2 W_3\right] \qquad (3.133)$$

Note that the restriction given by (3.108) can be rewritten in the form $\hat{W}_3 = 0$. Then, using these equations in (3.115), (3.116) and (3.117) we obtain

$$S^{(0)}_{\Theta\theta} = \hat{W}_2\ , \quad S^{(0)}_{Zr} = \hat{W}_1 \cos\beta\ , \quad S^{(0)}_{Zz} = \hat{W}_1 \sin\beta\ . \qquad (3.134)$$

It follows from (3.87) that

$$T^{(0)}_1 = \hat{W}_1\ , \quad T^{(0)}_2 = \hat{W}_2\ . \qquad (3.135)$$

4. NUMERICAL METHOD

4.1 Introduction

In this chapter we are concerned with the numerical solution of hyperbolic systems of conservation laws with source terms (also called balance laws). In particular the purpose of this chapter is to present and describe the numerical scheme that we have used to solve the equations governing dynamic deformation of nonlinear elastic membranes. To this end the chapter is organized as follows: In Section 4.2 we shall resume the notions that are necessary for a self-sufficient understanding of this chapter -the classical definitions of hyperbolicity, weak solutions and the Riemann problem- and present a simple example that will be helpfull to explain the above notions. In Section 4.3 we present an overview of the numerical methods for the systems of conservation laws. Section 4.4 is devoted to the study of the first-order Godunov method for one dimensional systems. In Section 4.5 we present the second-order numerical scheme that will be used in the next chapter. Finally, in Section 4.6 we apply the numerical method to a nonlinear scalar conservation law with a source term. For more complete account of the numerical schemes of hyperbolic systems we refer to the recent books by Leveque [8], Godlewski and Raviart [9] and Kröner [10].

4.2 Mathematical Theory of Hyperbolic Systems

4.2.1 Preliminaries

In this section we present the general form of systems of conservation laws with source terms in one space variable. The general form of a system of conservation

T.C. YÜKSEKÖĞRETİM KURULU
DOKÜMANTASYON MERKEZİ

laws in one space variable is the following nonlinear system of partial differential equations:

$$\mathbf{Q}_t + (\mathbf{H}(\mathbf{Q}))_x + \mathbf{B}(\mathbf{Q}) = \mathbf{0} \quad x \in \mathbb{R}, \quad t > 0 \tag{4.1}$$

Here $\mathbf{Q} : \mathbb{R} \times [0, +\infty) \to \mathbb{R}^m$ is a m-dimensional vector of state variables $q_1, q_2, ..., q_m$ and the vector valued function $\mathbf{H}(\mathbf{Q})$ is called the flux function for the system of conservation laws, so $\mathbf{H} : \mathbb{R}^m \to \mathbb{R}^m$. The vector valued function $\mathbf{B}(\mathbf{Q})$ is called the source term for the system of conservation laws, so $\mathbf{B} : \mathbb{R}^m \to \mathbb{R}^m$. The above system can be written in the quasilinear form

$$\mathbf{Q}_t + \mathbf{A}(\mathbf{Q})\mathbf{Q}_x + \mathbf{B}(\mathbf{Q}) = \mathbf{0} \tag{4.2}$$

where

$$\mathbf{A}(\mathbf{Q}) = \partial \mathbf{H}(\mathbf{Q}) / \partial \mathbf{Q} \tag{4.3}$$

is the $m \times m$ Jacobian matrix of the flux function. One can even consider systems of conservation laws more general than (4.1), namely systems of the form

$$\mathbf{Q}_t + (\mathbf{H}(\mathbf{Q}, x, t))_x + \mathbf{B}(\mathbf{Q}, x, t) = \mathbf{0} \quad x \in \mathbb{R}, \quad t > 0 \tag{4.4}$$

where the flux $\mathbf{H}$ and the source term $\mathbf{B}$ are smooth functions from $\mathbb{R}^m \times [0, +\infty) \times \mathbb{R}$ into $\mathbb{R}^m$. However, we shall essentially concentrate in the following on systems of the form (4.1).

Formally, the system (4.1) expresses the conservation of the m quantities $q_1, q_2, ..., q_m$ in the absence of the source term. The source terms in the nonhomogeneous problems are due to physical effects (exterior forces, release of mass or energy, ...) or to geometrical effects (axisymmetric or cylindrical problems, ...) For instance the equations (3.88) and (3.89), together with some compatibility conditions, obtained in the previous chapter form a system of nonlinear hyperbolic partial differential equations with the source terms which are due to geometrical effects. In the following part of this section we shall restrict ourselves to one-dimensional homogeneous systems:

$$\mathbf{Q}_t + (\mathbf{H}(\mathbf{Q}))_x = \mathbf{0} \quad x \in \mathbb{R}, \quad t > 0 \tag{4.5}$$

If we fix an interval $[a, b]$ on the space coordinate and two times t_a and t_b where $t_a < t_b$ and integrate this equation on the rectangle $[a, b] \times [t_a, t_b]$, it follows that

$$\int_a^b [\mathbf{Q}(x, t_b) - \mathbf{Q}(x, t_a)]\mathrm{d}x + \int_{t_a}^{t_b} [\mathbf{H}(\mathbf{Q}(b, t)) - \mathbf{H}(\mathbf{Q}(a, t))]\mathrm{d}t = \mathbf{0}$$

This equation has the following physical meaning. If we denote the integrals in this equation by J_1 and J_2 respectively, then $-J_2$ is the flow difference through b and a during the time interval $[t_a, t_b]$ and J_1 is the change of $\mathbf{Q}$ in the interval $[a, b]$ during the time $[t_a, t_b]$. That is, the above equation means that each component of $\mathbf{Q}$ is conserved. Therefore, this identity is also called the integral form of the system of conservation laws.

The equation (4.5) must be augmented by some initial conditions

$$\mathbf{Q}(x, t = 0) = \mathbf{Q}_0(x) \tag{4.6}$$

where $\mathbf{Q}_0$ is a given function and also possibly by boundary conditions on a bounded spatial domain. Presently we shall study the initial value problem, or *Cauchy problem*: Find a function $\mathbf{Q}(x, t)$ that satisfies both the system (4.5) and the initial condition (4.6).

In the one-dimensional case of the system of conservation laws, when $\mathbf{Q}_0$ has the following particular form,

$$\mathbf{Q}_0(x) = \begin{cases} \mathbf{Q}_L, & x < 0 \\ \mathbf{Q}_R, & x > 0, \end{cases} \tag{4.7}$$

this Cauchy problem with piecewise constant initial data is called the (one-dimensional) *Riemann problem*.

We assume that the system (4.5) is *hyperbolic*. This means that the $m \times m$ Jacobian matrix $\mathbf{A}$ of the flux function has the following property: For each value of $\mathbf{Q}$ the eigenvalues of $\mathbf{A}$ are real, and the matrix diagonalizable, i.e., there is a complete set of m linearly independent eigenvectors. If, in addition, the eigenvalues $c_k(\mathbf{Q})$ $(1 \leq k \leq m)$ of $\mathbf{A}$ are all distinct, the system (4.5) is called *strictly hyperbolic*.

We now consider two elementary cases where the solution of the Cauchy problem can be written explicitly. In the first case we consider the Cauchy problem for the linear scalar conservation law

$$\begin{cases} q_t + cq_x = 0 \quad x \in \mathbb{R}, \quad t > 0, \\ q(x,0) = q_0(x), \end{cases} \tag{4.8}$$

where c is a constant. If the function q_0 is differentiable, one can easily check that the travelling wave

$$q(x,t) = q_0(x - ct) \tag{4.9}$$

provides a classical solution to the Cauchy problem. Note that the initial profile is simply transported to the right at a fixed velocity c (if $c > 0$), its shape unchanged. The solution $q(x,t)$ is constant along each of the rays $x - ct$ =constant, which are known as the characteristic lines of the equation.

In the second case we consider the Cauchy problem for the first-order linear system

$$\begin{cases} \mathbf{Q}_t + \mathbf{A}\mathbf{Q}_x = \mathbf{0} \quad x \in \mathbb{R}, \quad t > 0, \\ \mathbf{Q}(x,0) = \mathbf{Q}_0(x), \end{cases} \tag{4.10}$$

where $\mathbf{A}$ is a $m \times m$ constant matrix. Assume that the system is strictly hyperbolic and that m distinct real eigenvalues of $\mathbf{A}$ are arranged in increasing order as follows

$$c_1 < c_2 < ...... < c_m$$

With each eigenvalue c_k we associate a right eigenvector $\mathbf{r}_k$

$$\mathbf{A}\mathbf{r}_k = c_k\mathbf{r}_k$$

and a left eigenvector $\mathbf{l}_k$

$$\mathbf{l}_k^T\mathbf{A} = c_k\mathbf{l}_k^T$$

i.e. $\mathbf{l}_k$ is an eigenvector of $\mathbf{A}^T$. The eigenvectors form a basis of $\mathbb{R}^m$ and are chosen so that $\mathbf{l}_j^T\mathbf{r}_k = \mathbf{l}_j \cdot \mathbf{r}_k = \delta_{jk}, \quad (1 \le j,k \le m)$ where the Kronecker delta symbol δ_{jk} is used and the dot $\cdot$ denotes the Euclidean inner product on $\mathbb{R}^m$. We can write a vector $\mathbf{Q}$ with respect to the basis of the right eigenvectors in the form $\mathbf{Q} = \sum_{k=1}^{m} V_k \mathbf{r}_k$ where $V_k(x,t) = \mathbf{l}_k^T \mathbf{Q} = \mathbf{l}_k \cdot \mathbf{Q}$. Then we have

$$\mathbf{Q}_t + \mathbf{A}\mathbf{Q}_x = \sum_{k=1}^{m} [(V_k)_t + c_k (V_k)_x] \mathbf{r}_k,$$

That is, the first-order linear system is equivalent to the m independent scalar first-order equations

$$(V_k)_t + c_k (V_k)_x = 0 \tag{4.11}$$

If we set $V_{k0}(x) = \mathbf{l}_k^T \mathbf{Q}_0(x) = \mathbf{l}_k \cdot \mathbf{Q}_0(x)$, we obtain the solutions of these scalar equations in the form

$$V_k(x,t) = V_{k0}(x - c_k t) = \mathbf{l}_k^T \mathbf{Q}_0(x - c_k t), \quad 1 \leq k \leq m$$

Then we observe that the function

$$\mathbf{Q}(x,t) = \sum_{k=1}^{m} V_{k0}(x - c_k t)\mathbf{r}_k = \sum_{k=1}^{m} \mathbf{l}_k^T \mathbf{Q}_0(x - c_k t)\mathbf{r}_k \tag{4.12}$$

is the solution of the Cauchy problem. Note that the initial profile is decomposed as a sum of m waves, each one travelling with one of the characteristic speeds $c_1, c_2, ..., c_m$. The straight lines $x - c_k t$ =constant are known as the characteristics of the linear system.

We now turn to the nonlinear hyperbolic system (4.5). We assume that the system (4.5) is strictly hyperbolic, i.e., for any $\mathbf{Q}$ the Jacobian matrix $\mathbf{A}(\mathbf{Q})$ defined in (4.3) has m distinct real eigenvalues

$$c_1(\mathbf{Q}) < c_2(\mathbf{Q}) < ...... < c_m(\mathbf{Q}).$$

With each eigenvalue $c_k(\mathbf{Q})$ we associate a right eigenvector $\mathbf{r}_k(\mathbf{Q})$ and a left eigenvector $\mathbf{l}_k(\mathbf{Q})$

$$\mathbf{A}(\mathbf{Q})\mathbf{r}_k(\mathbf{Q}) = c_k(\mathbf{Q})\mathbf{r}_k(\mathbf{Q}), \qquad \mathbf{l}_k^T(\mathbf{Q})\mathbf{A}(\mathbf{Q}) = c_k(\mathbf{Q})\mathbf{l}_k^T(\mathbf{Q})$$

i.e, $\mathbf{l}_k(\mathbf{Q})$ is an eigenvector of $\mathbf{A}^T(\mathbf{Q})$. Since the eigenvalues are distinct we have

$$\mathbf{l}_j^T(\mathbf{Q})\mathbf{r}_k(\mathbf{Q}) = \mathbf{l}_j(\mathbf{Q}) \cdot \mathbf{r}_k(\mathbf{Q}) = 0, \qquad j \neq k$$

The kth characteristic field is said to be *genuinely nonlinear* if

$$\nabla c_k(\mathbf{Q}) \cdot \mathbf{r}_k(\mathbf{Q}) \neq 0 \qquad \text{for all} \quad \mathbf{Q}\,, \tag{4.13}$$

where $\nabla c_k(\mathbf{Q}) = (\partial c_k/\partial q_1, \partial c_k/\partial q_2, \ldots.., \partial c_k/\partial q_m)$ is the gradient of $c_k(\mathbf{Q})$. We say that the kth characteristic field is *linearly degenerate* if

$$\nabla c_k(\mathbf{Q}) \cdot \mathbf{r}_k(\mathbf{Q}) \equiv 0 \qquad \text{for all} \quad \mathbf{Q}\,. \tag{4.14}$$

That is, for a nonlinear system if in one of the characteristic fields the eigenvalue $c_k(\mathbf{Q})$ is constant along the integral curves of the vector field $\mathbf{r}_k(\mathbf{Q})$ we say the kth characteristic field is linearly degenerate. On the other hand, (4.13) implies that $c_k(\mathbf{Q})$ is monotonically increasing or decreasing as $\mathbf{Q}$ varies along an integral curve of the vector field $\mathbf{r}_k(\mathbf{Q})$. Note that for a constant coefficient linear system $c_k(\mathbf{Q})$ is constant and hence $\nabla c_k \equiv 0$.

4.2.2 Shock Formation

We shall say that a function $\mathbf{Q}$ is a *classical solution* of the Cauchy problem (4.5)-(4.6) if $\mathbf{Q}$ is a C^1 function that satisfies the equations (4.5)-(4.6) pointwise. An essential feature of the problem (4.5)-(4.6) is that there do not exist in general classical solutions beyond some finite time interval, even when the initial condition $\mathbf{Q_0}$ is a very smooth function. The solution of the system of conservation laws can become singular within finite time. Therefore we have to consider solutions in the distributional sense. We now illustrate this fact by studying the simple case of a one-dimensional scalar equation. To this end we consider the problem

$$q_t + (H(q))_x = 0, \qquad x \in \mathbb{R}, \quad t > 0, \tag{4.15}$$

$$q(x,0) = q_0(x), \qquad x \in \mathbb{R}, \tag{4.16}$$

where $H : \mathbb{R} \to \mathbb{R}$ is a C^1 function and $m = 1$. Let q be a classical solution of this problem. We can rewrite (4.15) in nonconservative form

$$q_t + a(q)q_x = 0, \qquad x \in \mathbb{R}, \quad t > 0\,, \tag{4.17}$$

where $a(q) = H'(q)$. Then $c_1(q) = a(q)$ while $r(q) = 1$ for all q. Consequently, in the scalar case the condition for a genuinely nonlinear field, (4.13), reduces to the convexity requirement $H''(q) \neq 0$, i.e., $a'(q) \neq 0$ for all q. That is, we are in the genuinely nonlinear case if and only if H is a strictly convex or a strictly concave function. Note that we are in the linearly degenerate case if and only if $a(q)$ does not depend on q, which corresponds to the case of a linear hyperbolic equation with constant coefficients.

The *characteristic curves* associated with (4.17) are defined as the integral curves of the differential equation

$$\frac{dx}{dt} = a(q(x(t),t)) .$$

A characteristic curve passing through the point $(x_0, 0)$ is obtained as a solution of the differential system

$$\frac{dx}{dt} = a(q(x(t),t)), \qquad x(0) = x_0 . \tag{4.18}$$

It exists at least on a small time interval $[0, t_0]$. Along such a curve, we have

$$\begin{aligned} \frac{d}{dt}q(x(t),t) &= q_t(x(t),t) + q_x(x(t),t)\frac{dx(t)}{dt} \\ &= (q_t + a(q)q_x)|_{(x(t),t)} = 0. \end{aligned}$$

That is, q is a constant along a characteristic curve. Therefore, it follows from (4.18) that the characteristic curves are straight lines. Because, solving the differential system (4.18), the equation of the characteristic curve passing through the point $(x_0, 0)$ is obtained in the form

$$x = x_0 + a(q(x_0, 0))t = x_0 + a(q_0(x_0))t . \tag{4.19}$$

The constant slopes of the characteristic straight lines depend on the initial data. This important property helps us to construct smooth solutions. Equation (4.19) gives x_0 implicitly as a function of x and t. For each (x, t) we can solve this equation for x_0 and then the solution is

$$q(x,t) = q(x_0(x,t), 0) = q_0(x_0(x,t)) \tag{4.20}$$

This is the so-called *method of characteristics.* We now assume that there exist two points $x_1 < x_2$ such that

$$m_1 = \frac{1}{a(q_0(x_1))} < m_2 = \frac{1}{a(q_0(x_2))}$$

That is, the characteristics C_1 and C_2 drawn from the points $(x_1, 0)$ and $(x_2, 0)$, respectively, have slopes m_1 and m_2 in which $m_1 < m_2$. Then the characteristics C_1 and C_2 intersect necessarily at some point P. At the point P, the solution q should take both values $q_0(x_1)$ and $q_0(x_2)$, which is impossible. Hence, the solution q cannot be continuous at the point P where a *shock wave* occurs and the solution $q(x,t)$ has a jump discontinuity. Note that this phenomenon is independent of the smoothness of the functions q_0 and H. One can determine the critical time up to which a classical solution exists.

There exists a continuous solution $q(x,t)$ throughout the half-plane $t > 0$ if no pair of characteristic lines intersect in this half-plane. This can happen only if a is an increasing function of x: $a(q(x_1)) \leq a(q(x_2))$ for $x_1 \leq x_2$. Such a solution is called an *expansion wave* or *rarefaction wave.*

We observe that in the nonhomogeneous case, the characteristic curves are not straight lines along which the solution q is not necessarily constant.

We also observe that in the linear case $a(q) = a_0$ =constant the characteristic lines have the same slope $m_0 = 1/a_0$. That is, the characteristic lines drawn from the points $(x_1, 0)$ and $(x_2, 0)$ are parallel and consequently they never intersect.

In summary, using the method of characteristics, one can prove that a classical solution of the Cauchy problem exists in a small time interval. On the other hand, we have seen that in the nonlinear case $a'(q) \neq 0$ discontinuities may develop after a finite time. These considerations lead us to introduce *weak solutions.*

4.2.3 Weak Solutions

A natural way to define a generalized solution of the conservation law (4.15) that does not require differentiability is to go back to the integral form of the conservation law, and say that $q(x,t)$ is a generalized solution if the conservation law

$$\int_{t_1}^{t_2}\int_{x_1}^{x_2}[q_t(x,t)+(H(q(x,t)))_x]\mathrm{d}x\mathrm{d}t=0\ , \tag{4.21}$$

is satisfied for all x_1, x_2, t_1, t_2. There is another approach that results in a different integral formulation [8]. The basic idea is to multiply the conservation law (4.15) by a smooth "test function", integrate over some domain, and then use integration by parts to move derivatives of the function q onto the smooth test function. The result is an equation involving fewer derivatives on q. Therefore less smoothness is required to define a "solution". In our case we will use test functions $\phi(x,t)$ with the property that they are differentiable as often as is required with respect to x and t and that they are identically zero outside a bounded domain D of the xt-plane. Now if we multiply the conservation law (4.15) by $\phi(x,t)$ and then integrate over space and time, we obtain

$$\int_0^{\infty}\int_{-\infty}^{+\infty}[\phi q_t+\phi(H(q))_x]\mathrm{d}x\mathrm{d}t=0\ . \tag{4.22}$$

Integration by parts gives

$$\int_0^{\infty}\int_{-\infty}^{+\infty}[\phi_t q+\phi_x H(q)]\mathrm{d}x\mathrm{d}t=-\int_{-\infty}^{+\infty}\phi(x,0)q(x,0)\mathrm{d}x\ . \tag{4.23}$$

Note that nearly all the boundary terms which normally arise through integration by parts drop out due to the requirement that ϕ vanishes identically outside a bounded domain D and hence vanishes at infinity. The remaining boundary term brings in the initial condition of the partial differential equation, which must still play a role in our weak formulation. The function $q(x,t)$ is called a *weak solution* of the conservation law if the above equation, (4.23), holds for all test functions ϕ defined in the half-plane. The advantage of this formulation over the original integral form (4.21) is that the integration in (4.23) is over a fixed domain, all of $\mathbb{R}\times\mathbb{R}^+$. The integral form (4.21) is over an arbitrary rectangle, and to check that q is a solution we must verify that this holds for all choices of x_1, x_2, t_1 and t_2. Of course, our new form (4.23) has a similar feature, we must check that it holds for all test functions ϕ in D, but this turns out to be an easier task. It can be shown by considering special test functions $\phi(x,t)$ that (4.23) reduces to the integral form (4.21) and mathematically the two integral forms are equivalent [8]. That is, one can show that any weak solution satisfies the original integral conservation law.

We can now extend the above definitions to the system of conservation laws as follows. Let us introduce the class of test vectors $\boldsymbol{\phi}(x,t)$ with the property that they are differentiable as often as is required with respect to x and t and that they vanish identically outside a bounded domain D of the xt-plane. If we multiply the system of conservation laws (4.5) by $\boldsymbol{\phi}(x,t)$ and integrate over space and time we get

$$\int_0^\infty \int_{-\infty}^{+\infty} [\mathbf{Q}_t + (\mathbf{H}(\mathbf{Q}))_x] \cdot \boldsymbol{\phi} \, \mathrm{d}x\mathrm{d}t = 0 \, . \tag{4.24}$$

Integration by parts gives

$$\int_0^\infty \int_{-\infty}^{+\infty} [\mathbf{Q} \cdot \boldsymbol{\phi}_t + \mathbf{H}(\mathbf{Q}) \cdot \boldsymbol{\phi}_x] \mathrm{d}x\mathrm{d}t = -\int_{-\infty}^{+\infty} \mathbf{Q}(x,0) \cdot \boldsymbol{\phi}(x,0)\mathrm{d}x \tag{4.25}$$

where the dot $\cdot$ denotes the Euclidean inner product on $\mathbb{R}^m$. We now introduce the following definition. A function $\mathbf{Q}$ is called a *weak solution* of the Cauchy problem (4.5)-(4.6) if $\mathbf{Q}$ satisfies (4.25) for any vector function $\boldsymbol{\phi}$ in D [8]. By construction, a classical solution of the Cauchy problem is also a weak solution. Conversely, it can be shown that, by choosing the test functions $\boldsymbol{\phi}$ properly, any weak solution $\mathbf{Q}$ satisfies the system of conservation laws 4.5 in the sense of distributions on $\mathbb{R} \times \mathbb{R}^+$. Moreover, if $\mathbf{Q}$ is a weak solution with continuous derivatives, then it is a classical solution so that (4.5) holds pointwise. The above argument shows that any distributional solution $\mathbf{Q}$ is a classical solution of (4.5) in any domain where $\mathbf{Q}$ is a function with continuous derivatives [8]. We shall now consider solutions of the system of conservation laws (4.5) in the sense of distributions that are only piecewise smooth and therefore admit discontinuities.

By virtue of the definition of weak solutions, they need not be differentiable and may have discontinuities across some curve in the xt-plane. However, not every type of discontinuity is admissible. That is, there is a connection between the discontinuity curve and the values of the solution on both sides of the discontinuity. Now we assume that the half space $\mathbb{R} \times \mathbb{R}^+$ is seperated by a smooth curve Σ, which is parametrized in the form $\Sigma : t \to (\xi(t), t)$, into two parts D_- and D_+. We also assume that Σ is a discontinuity curve of $\mathbf{Q}$. That is, $\mathbf{Q}$ is a function with continuous derivatives outside of Σ and it has a jump discontinuity across Σ. In other words, $\mathbf{Q}$ is a classical solution of the system of conservation laws in D_- and D_+. The limits of $\mathbf{Q}$ on each side of Σ are denoted by $\mathbf{Q}_\pm$:

$$\mathbf{Q}_\pm = \lim_{\epsilon>0,\ \epsilon\to 0} \mathbf{Q}(\xi(t) \pm \epsilon, t) \tag{4.26}$$

The values of $\mathbf{Q}$ and $\mathbf{H}(\mathbf{Q})$ on each side of Σ are linked by a relation that is hidden in the equations. That is, not every discontinuity is admissible. For all test vectors $\boldsymbol{\phi}$ in D we have

$$\begin{aligned}
0 &= \int_R \int_{R^+} [\mathbf{Q} \cdot \boldsymbol{\phi}_t + \mathbf{H}(\mathbf{Q}) \cdot \boldsymbol{\phi}_x] \mathrm{d}x \mathrm{d}t \\
&= \int_{D_+} [\mathbf{Q} \cdot \boldsymbol{\phi}_t + \mathbf{H}(\mathbf{Q}) \cdot \boldsymbol{\phi}_x] \mathrm{d}x \mathrm{d}t + \int_{D_-} [\mathbf{Q} \cdot \boldsymbol{\phi}_t + \mathbf{H}(\mathbf{Q}) \cdot \boldsymbol{\phi}_x] \mathrm{d}x \mathrm{d}t \\
&= \int_{D_+} [(\mathbf{Q} \cdot \boldsymbol{\phi})_t + (\mathbf{H}(\mathbf{Q}) \cdot \boldsymbol{\phi})_x] \mathrm{d}x \mathrm{d}t - \int_{D_+} [\mathbf{Q}_t + (\mathbf{H}(\mathbf{Q}))_x] \cdot \boldsymbol{\phi} \ \mathrm{d}x \mathrm{d}t \\
&\quad + \int_{D_-} [(\mathbf{Q} \cdot \boldsymbol{\phi})_t + (\mathbf{H}(\mathbf{Q}) \cdot \boldsymbol{\phi})_x] \mathrm{d}x \mathrm{d}t - \int_{D_-} [\mathbf{Q}_t + (\mathbf{H}(\mathbf{Q}))_x] \cdot \boldsymbol{\phi} \ \mathrm{d}x \mathrm{d}t
\end{aligned}$$

Since $\mathbf{Q}$ is a classical solution of the system of conservation laws in D_- and D_+, the second and fourth integrals vanish and we obtain

$$0 = \int_{D_+} [(\mathbf{Q} \cdot \boldsymbol{\phi})_t + (\mathbf{H}(\mathbf{Q}) \cdot \boldsymbol{\phi})_x] \mathrm{d}x \mathrm{d}t + \int_{D_-} [(\mathbf{Q} \cdot \boldsymbol{\phi})_t + (\mathbf{H}(\mathbf{Q}) \cdot \boldsymbol{\phi})_x] \mathrm{d}x \mathrm{d}t$$

Then applying Green's formula in D_- and D_+ gives

$$0 = -\int_\Sigma [(\mathbf{Q}_+ \cdot \boldsymbol{\phi}) n_t + (\mathbf{H}(\mathbf{Q}_+) \cdot \boldsymbol{\phi}) n_x] \mathrm{d}S + \int_\Sigma [(\mathbf{Q}_- \cdot \boldsymbol{\phi}) n_t + (\mathbf{H}(\mathbf{Q}_-) \cdot \boldsymbol{\phi}) n_x] \mathrm{d}S$$

where (n_x, n_t) denotes the unit normal vector to the shock curve, which points in the direction D_+. We can rewrite the above equation in the form

$$\int_\Sigma [(\mathbf{Q}_+ - \mathbf{Q}_-) n_t + (\mathbf{H}(\mathbf{Q}_+) - \mathbf{H}(\mathbf{Q}_-)) n_x] \cdot \boldsymbol{\phi} \ \mathrm{d}S = 0$$

Since this equation holds for arbitrary $\boldsymbol{\phi}$, we obtain the following jump condition

$$-(\mathbf{Q}_+ - \mathbf{Q}_-) n_t = (\mathbf{H}(\mathbf{Q}_+) - \mathbf{H}(\mathbf{Q}_-)) n_x \ .$$

Note that $-n_t/n_x = d\xi/dt = s(t)$ where s is called the propagation speed of the shock. Then the above equation takes the following form

$$s(\mathbf{Q}_+ - \mathbf{Q}_-) = \mathbf{H}(\mathbf{Q}_+) - \mathbf{H}(\mathbf{Q}_-) \,. \tag{4.27}$$

We can rewrite the jump condition in the form

$$s[\mathbf{Q}] = [\mathbf{H}(\mathbf{Q})] \,, \tag{4.28}$$

where the jumps of $\mathbf{Q}$ and $\mathbf{H}(\mathbf{Q})$ across Σ are denoted by

$$[\mathbf{Q}] = \mathbf{Q}_+ - \mathbf{Q}_- \,, \qquad [\mathbf{H}(\mathbf{Q})] = \mathbf{H}(\mathbf{Q}_+) - \mathbf{H}(\mathbf{Q}_-) \,. \tag{4.29}$$

The condition (4.28) is called a jump condition or Rankine-Hugoniot condition. For the scalar conservation law (4.15) the Rankine-Hugoniot condition (4.28) takes the following form

$$s[q] = [H(q)] \,. \tag{4.30}$$

In other words, for a scalar conservation law, the propagation speed s is given by

$$s = \frac{[H(q)]}{[q]} = \frac{H(q_+) - H(q_-)}{q_+ - q_-} \,. \tag{4.31}$$

On the other hand, for the linear system $(4.10)_1$ the Rankine-Hugoniot condition (4.28) becomes

$$s[\mathbf{Q}] = \mathbf{A}[\mathbf{Q}] \,, \tag{4.32}$$

since $\mathbf{H}(\mathbf{Q}) = \mathbf{A}\mathbf{Q}$ where $\mathbf{A}$ is a constant matrix.

4.2.4 The Riemann Problem

The conservation law together with piecewise constant data having a single discontinuity is known as the Riemann problem. We now consider the scalar conservation law (4.15) with piecewise continuous data

$$q(x,0) = q_0(x) = \begin{cases} q_L \,, & x < 0 \\ q_R \,, & x > 0 \,. \end{cases} \tag{4.33}$$

This Cauchy problem is called the (one-dimensional) *Riemann problem.* We assume that the function $H(q)$ is strictly convex ($H''(q) > 0$) and consequently $a'(q) > 0$. We begin by considering classical solutions of the scalar conservation law (4.15) We notice that the scalar conservation law (4.15) has a classical solution in the form $q(x,t) = \psi(x/t)$. Note that the expression

$$\begin{aligned} q_t + a(q)q_x &= -\frac{x}{t^2}\psi'(x/t) + a(\psi(x/t))\frac{1}{t}\psi'(x/t) \\ &= -\frac{1}{t}[\frac{x}{t} - a(\psi(x/t))]\psi'(x/t) \end{aligned}$$

vanishes if

$$a(\psi(x/t)) = x/t \quad \text{or} \quad \psi'(x/t) = 0$$

The second condition gives the trivial solution, $q(x,t)$ =constant, for the scalar conservation law. On the other hand, the first condition implies that the function ψ is the inverse function a^{-1}; $\psi(x/t) = a^{-1}(x/t)$. Note that the existence of the inverse function a^{-1} is guaranteed by the assumption that $a'(q) > 0$. We conclude that the scalar conservation law has a classical solution of the form $q(x,t) = a^{-1}(x/t)$.

It follows from (4.19) that the characteristic straight line passing through the point $(x_0, 0)$ is given by

$$x(x_0,t) = \begin{cases} x_0 + a(q_L)t\,, & x_0 < 0 \\ x_0 + a(q_R)t\,, & x_0 > 0\,. \end{cases} \tag{4.34}$$

That is, the characteristic lines starting in $(-\infty, 0)$ have slope $1/a(q_L)$ and the characteristic lines starting in $(0,\infty)$ have slope $1/a(q_R)$. Note that, since $a(q)$ is an increasing function, the characteristic line emanating from a point in $(-\infty, 0)$ and the characteristic line emanating from a point in $(0,\infty)$ do not intersect if $q_R \geq q_L$. Otherwise, the characteristics intersect at some points and the solution breaks down at those points. Therefore, the form of the solution depends on the relation between q_L and q_R.

Case A: $q_L = q_R$. In such a case the characteristic lines are parallel and the solution is given in the form $q(x,t) = q_L$.

Case B: $q_L > q_R$. In this case the characteristics starting from a point in $(-\infty, 0)$ and from a point in $(0, \infty)$ intersect and the solution becomes multivalued. Note that the characteristic lines starting from a point in $(-\infty, 0)$ are bounded from the right by the straight line $x = a(q_L)t$. Similarly, the characteristic lines starting from a point in $(0, \infty)$ are bounded from the left by the straight line $x = a(q_R)t$. Therefore, the multivalued region starts right at the origin and is bounded by the straight lines $x = a(q_R)t$ and $x = a(q_L)t$. Recall that not any discontinuity is admissible and the Rankine-Hugoniot jump condition (4.30) must hold. Then the solution given in the form

$$q(x,t) = \begin{cases} q_L\ , & x < st \\ q_R\ , & x > st\ , \end{cases} \tag{4.35}$$

where $s = [H(q_R) - H(q_L)]/(q_R - q_L)$, is a weak solution of the Riemann problem. The weak solution in this case is called a *shock wave*.

Case C: $q_L < q_R$. In such a case the chracteristics starting from a point in $(-\infty, 0)$ and from a point in $(0, \infty)$ do not intersect each other. However, the method of chracteristics enables us to determine the solution everywhere except in the region $a(q_L)t < x < a(q_R)t$. In this region the classical solution is valid. Then, it follows from (4.20) that the solution is in the form

$$q(x,t) = \begin{cases} q_L\ , & x < a(q_L)t \\ a^{-1}(x/t)\ , & a(q_L)t \le x \le a(q_R)t \\ q_R\ , & x > a(q_R)t\ . \end{cases} \tag{4.36}$$

Note that this solution is continuous. Therefore we rewrite in the form

$$q(x,t) = \begin{cases} q_L\ , & x \le a(q_L)t \\ a^{-1}(x/t)\ , & a(q_L)t \le x \le a(q_R)t \\ q_R\ , & x \ge a(q_R)t\ . \end{cases} \tag{4.37}$$

The weak solution in this case is called a *rarefaction wave*.

There are infinitely many other weak solutions to the Riemann problem when $q_L < q_R$. One of these is again the weak solution in *Case B* in which the discontinuity propagates with speed s. Note that the characteristics now go out of the shock. Some further examples showing that in general there is no uniqueness for the weak solution are given in [8, p.30], [9, p.19] and [10, p.20].

As it is pointed out above, there are situations in which the weak solution is not unique. Therefore the question arises how we can select a special weak solution among the whole set of weak solutions. In other words, we need an additional condition to select the physically relevant solution. There is an obvious condition for the above Riemann problem. Recall that the multivalued region starts right at the origin and is bounded by the straight lines $x = a(q_R)t$ (from the left) and $x = a(q_L)t$ (from the right) when $q_L > q_R$. That is, the slope of the straight line $x = st$ must be greater than the slope of the straight line $x = a(q_L)t$ and less than the slope of the straight line $x = a(q_R)t$. This gives the the *entropy condition*

$$a(q_R) < s < a(q_L) \ . \tag{4.38}$$

That is, a discontinuity propagating with speed s satisfies the entropy condition if the above inequality is satisfied. It can be shown that weak solutions satisfying the entropy condition are unique [10, p.27]. If we apply this condition to the case of compressible flow, we observe that the physical entropy increases across the discontinuity. That is why it is called the entropy condition. This condition is used to develop numerical methods that they converge to the correct solution.

We now consider the Riemann problem for the linear system $(4.10)_1$ corresponding to the initial condition (4.7) [8, 9]. Recall that the solution of the Cauchy problem (4.10) for the linear system is given by (4.12). For the Riemann problem we decompose $\mathbf{Q}_L$ and $\mathbf{Q}_R$ as

$$\mathbf{Q}_L = \sum_{k=1}^{m} \alpha_k \mathbf{r}_k \ , \qquad \mathbf{Q}_R = \sum_{k=1}^{m} \beta_k \mathbf{r}_k \ , \tag{4.39}$$

to simplify the notation. Then the initial conditions for the m independent scalar first-order equations given by (4.11) are

$$V_{k0}(x) = V_k(x,0) = \begin{cases} \alpha_k \ , & x < 0 \\ \beta_k \ , & x > 0 \ , \end{cases}$$

and the corresponding solutions of the m scalar equations are

$$V_k(x,t) = \begin{cases} \alpha_k \, , & x < c_k t \\ \beta_k \, , & x > c_k t \, , \end{cases}$$

where $1 \leq k \leq m$. Consequently the solution $\mathbf{Q}$ of the Riemann problem for $c_p t < x < c_{p+1} t$ takes the constant value

$$\mathbf{Q}_p = \sum_{k=1}^{p} \beta_k \mathbf{r}_k + \sum_{k=p+1}^{m} \alpha_k \mathbf{r}_k \, , \qquad 0 \leq p \leq m \tag{4.40}$$

with the convention $c_0 = -\infty$, $c_{m+1} = +\infty$. Then the solution of the Riemann problem for the linear system is

$$\mathbf{Q}(x,t) = \begin{cases} \mathbf{Q}_0 = \mathbf{Q}_L \, , & x < c_1 t \\ \mathbf{Q}_1 \, , & c_1 t < x < c_2 t \\ \mathbf{Q}_2 \, , & c_2 t < x < c_3 t \\ \vdots & \vdots \\ \mathbf{Q}_{m-1} \, , & c_{m-1} t < x < c_m t \\ \mathbf{Q}_m = \mathbf{Q}_R \, , & x > c_m t \, . \end{cases} \tag{4.41}$$

This implies that, in general, the initial discontinuity breaks up into m discontinuity waves, which propagate with the characteristic speeds c_k, $1 \leq k \leq m$. Note that the solution is continuous at any point in the wedge between the $x = c_k t$ and $x = c_{k+1} t$ characteristics. As we cross the kth characteristic, the value of $x - c_k t$ passes through 0 and the corresponding V_k jumps from α_k to β_k. The other coefficients V_j $(j \neq k)$ remain constant. It follows from (4.40) that the intermediate states $\mathbf{Q}_k$ satisfy

$$\mathbf{Q}_k - \mathbf{Q}_{k-1} = (\beta_k - \alpha_k) \mathbf{r}_k \, . \tag{4.42}$$

That is, across the kth characteristic the solution jumps with the jump given by

$$[\mathbf{Q}] = (\beta_k - \alpha_k) \mathbf{r}_k \, . \tag{4.43}$$

Note that we have

$$\mathbf{A}[\mathbf{Q}] \;=\; \mathbf{A}(\mathbf{Q}_k - \mathbf{Q}_{k-1})$$

$$
\begin{aligned}
&= (\beta_k - \alpha_k)\mathbf{A}\mathbf{r}_k \\
&= c_k(\beta_k - \alpha_k)\mathbf{r}_k \\
&= c_k(\mathbf{Q}_k - \mathbf{Q}_{k-1}) \\
&= c_k[\mathbf{Q}] \,. \qquad (4.44)
\end{aligned}
$$

This implies that across the line of discontinuity $x = c_k t$, the Rankine-Hugoniot condition (4.32) is satisfied, that the jump $[\mathbf{Q}]$ is an eigenvector of $\mathbf{A}$ and that c_k is precisely the speed of propagation of the jump $[\mathbf{Q}]$. The solution $\mathbf{Q}(x,t)$ can also be written in terms of these jumps as

$$
\begin{aligned}
\mathbf{Q}(x,t) &= \mathbf{Q}_L + \sum_{c_k < x/t} (\beta_k - \alpha_k)\mathbf{r}_k \qquad (4.45) \\
&= \mathbf{Q}_R - \sum_{c_k \geq x/t} (\beta_k - \alpha_k)\mathbf{r}_k \,. \qquad (4.46)
\end{aligned}
$$

As it is seen from the previous paragraph, the Riemann problem for the constant coefficient linear system can be explicitly solved. We solve the Riemann problem for nonlinear systems in much the same way. However, we will not attempt to construct the solution of the Riemann problem for nonlinear systems. More details on the solution of the Riemann problem for nonlinear systems can be found in [8, 9, 10]. The solution to the Riemann problem defined for the nonlinear system (4.5) is quite similar to the structure of the above linear solution. There exists a theorem about the Riemann problem of the nonlinear system (4.5) in [9, p.84] and [10, p.307]. The main results of this theorem are as follows. The Riemann solution has a weak solution that consists of at most $(m+1)$ constant states separated by rarefaction waves, shock waves or contact discontinuities. Moreover, the theorem states that a weak solution with admissible shock waves is unique. We may explain a contact discontunity as follows. If the propagation velocity, s, of the discontinuity and the characteristic speed c_k one side of the discontinuity are the same, in such a case the discontunity is called a contact discontinuity with respect to c_k. That is, for a contact discontunity (from $\mathbf{Q}_L$ to $\mathbf{Q}_R$, say) the propagation speed s is equal to either $c_k(\mathbf{Q}_L)$ or $c_k(\mathbf{Q}_R)$.

We now want to discuss the question of whether a given discontunity is physically relevant for the case of a nonlinear system. Recall that we considered the entropy condition (4.38) for a scalar nonlinear conservation law. We need a similar entropy condition that can be applied directly to a discontinuous weak solution to determine whether the jumps should be allowed. Lax [11] proposed a simple generalization of the entropy condition to systems of equations that are genuinely nonlinear. For a genuinely nonlinear field, Lax's entropy condition says that a jump in the kth field is admissible only if

$$c_k(\mathbf{Q}_R) < s < c_k(\mathbf{Q}_L) \ . \tag{4.47}$$

The weak solution constructed for the Riemann problem will not be the physically correct solution if any of the resulting shocks violate the entropy condition. However, contact discontinuities can occur for systems with both genuinely nonlinear and linearly degenerate fields. Therefore we should modify the entropy condition (4.47) as

$$c_k(\mathbf{Q}_R) \le s \le c_k(\mathbf{Q}_L) \ . \tag{4.48}$$

4.2.5 Burgers Equation

In this subsection the interesting behavior of solutions to conservation laws is illustrated by considering Burgers' equation. In the scalar case (i.e., $m = 1$), the simplest example of a nonlinear conservation law is given by Burgers' equation. The scalar parabolic equation

$$q_t + qq_x - \nu q_{hx} = 0,$$

where ν is a viscosity coefficient, was introduced in particular by Burgers as the simplest differential model for a fluid flow and is therefore often called the (viscous) Burgers equation. Burgers studied the limit equation when ν tends to zero, which we write in conservative form

$$q_t + (\frac{q^2}{2})_x = 0 \ . \tag{4.49}$$

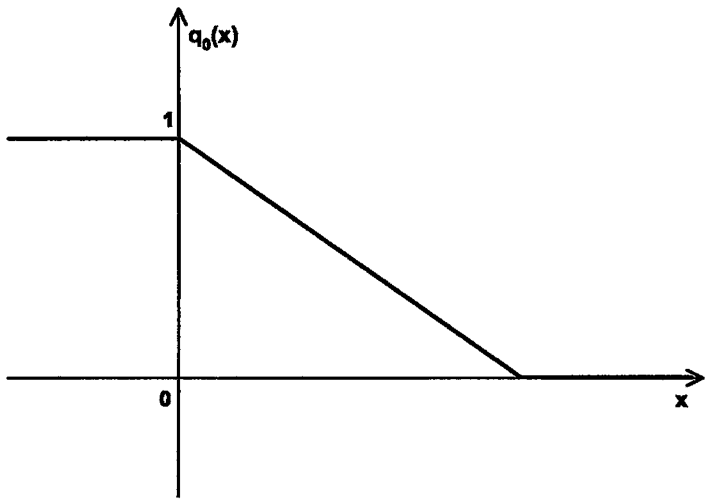

Figure 4.1: Smooth initial data for Cauhy problem of inviscid Burgers equation.

This equation is called the inviscid Burgers equation. It is the simplest conservation law (or nonlinear hyperbolic differential equation). Note that $H(q) = q^2/2$ and $a(q) = q$. Since $a' \neq 0$, the Cauchy problem for the inviscid Burgers equation may have discontinuous weak solutions even for a smooth initial function q_0. This can be explained through the following example. Consider the Cauchy problem for the inviscid Burgers equation with the smooth initial data [9]

$$q(x,0) = q_0(x) = \begin{cases} 1\,, & x \leq 0 \\ 1 - x\,, & 0 \leq x \leq 1 \\ 0\,, & x \geq 1 \end{cases} \tag{4.50}$$

(See Figure 4.1). By using the method of characteristics we can construct the solution up to the time when the characteristics intersect. We already know from (4.19) that the characteristic straight line passing through the point $(x_0, 0)$ is given by

$$x(x_0, t) = x_0 + q_0(x_0)t\,. \tag{4.51}$$

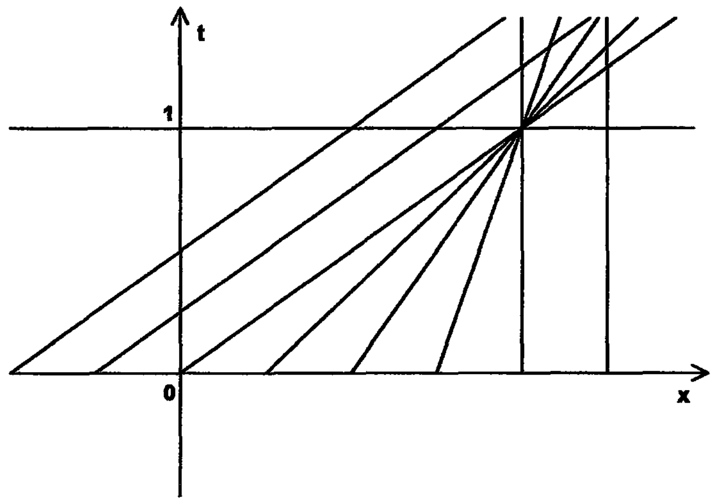

Figure 4.2: The characteristic straight lines passing through the point $(x_0, 0)$.

Then we have

$$x(x_0,t) = \begin{cases} x_0 + t\,, & x_0 \leq 0\,, \\ x_0 + (1-x_0)t\,, & 0 \leq x_0 \leq 1\,, \\ x_0\,, & x_0 \geq 1 \end{cases} \tag{4.52}$$

(See Figure 4.2). For $t < 1$, the characteristics do not intersect. Hence, given a point (x,t) with $t < 1$, we draw the (backward) characteristic passing through this point, and we determine the corresponding point x_0

$$x_0 = \begin{cases} x - t\,, & x \leq t < 1 \\ (x-t)/(1-t)\,, & t \leq x \leq 1 \\ x\,, & x \geq 1\,. \end{cases} \tag{4.53}$$

Using (4.20) we obtain the solution in the form

$$q(x,t) = q_0(x_0(x,t)) = \begin{cases} 1\,, & x \leq t \\ (1-x)/(1-t)\,, & t \leq x \leq 1 \\ 0\,, & x \geq 1 \end{cases} \tag{4.54}$$

(See Figure 4.3). The characteristic lines starting in $(-\infty, 0]$ have slope 1 and $q = 1$ along these lines. The characteristic lines starting in $[1, \infty)$ are vertical

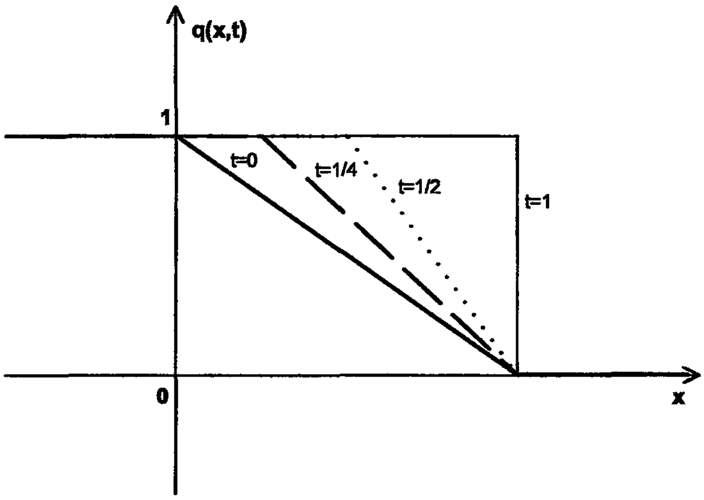

Figure 4.3: Solution of the Cauchy problem for the inviscid Burgers equation.

lines and $q = 0$ along them (See Figure 4.2). However, the characteristic line emanating from a point $(x_0, 0)$, $(0 \leq x_0 \leq 1)$, has slope $1/(1-x_0)$ and $q = 1-x_0$ along it. Furthermore, all of them intersect at the point (1,1). This implies that q is multivalued at (1,1) and hence the solution breaks down at this point. It consists of a front moving to the right and steepening until it becomes a "shock". This discontinuity corresponds to the fact that at time $t = 1$ the characteristics intersect. Also note that the characteristic lines emanating from $(x_0, 0)$ with $x_0 < 0$ intersect those emanating from $(x_0, 0)$ with $x_0 > 1$. In conclusion, even for a continuous initial function $q_0(x)$, the solution of the Riemann problem for the inviscid Burgers equation is either a shock propagating or a rarefaction wave, both being kinds of waves that are involved in the solution of the Riemann problem.

We now consider the Riemann problem for Burgers' equation, in which the piecewise continuous initial data is given by (4.33). If $q_L > q_R$, a weak solution of the Riemann problem is given by (4.35). This represents a shock wave propagating at speed s in which

$$s = (q_L + q_R)/2 \tag{4.55}$$

since $H(q) = q^2/2$. However, if $q_L < q_R$ it follows from (4.36) that a weak solution of the Riemann problem is a rarefaction wave given in the form

$$q(x,t) = \begin{cases} q_L\ , & x < q_L t \\ x/t\ , & q_L t \leq x \leq q_R t \\ q_R\ , & x > q_R t\ . \end{cases} \tag{4.56}$$

4.3 Numerical Solutions of Hyperbolic Systems

Systems of conservation laws are very important and powerful mathematical models for a variety of physical phenomena that appear in fluid mechanics, solid mechanics and several other areas. In general it is not possible to derive exact solutions to the above equations (4.1), and hence we need to devise and study numerical methods for their approximate solutions. There are special difficulties associated with solving these systems (e.g. shock formation). For instance, conservation laws may have discontinuous solutions and therefore they pose a special challenge for both theoretical and numerical analysis. Typically in such systems discontinuos solutions develop and propagate even if the inital data are smooth. For simple cases it is possible to obtain analytical solutions using the method of characteristics. In general, however, the high nonlinearity of the equations and the presence of the source terms rule out analytical solutions using the method of characteristics. For general background on numerical methods for systems of nonlinear partial differential equations, several recent books [8], [9] and [10] are highly recommended. The details of the mathematical proofs concerning the convergence, consistency and stability of the numerical scheme to be presented below are not included here and the reader is referred to the above-mentioned references.

When we attempt to calculate the solutions of systems of conservation laws numerically, we face a new set of problems. We expect a finite difference discretization of the quasilinear system to be inappropriate near discontinuities. Because discontinuous solutions clearly do not satisfy the quasilinear system in the classical sense at all points, since the derivatives are not defined at discontinuities. Instead, if we compute discontinuous solutions to conservation laws using the standard methods developed under the assumption of smooth solutions, we typically obtain numerical results that are very poor.

For conservation laws it is often preferable to use a finite volume method rather than a finite difference method. Because it is important to ensure that the numerical method conserves the appropriate quantitites, such as mass, momentum and energy numerically. This is particularly true when the solution involves shock waves. In a finite volume method the discrete values are viewed as an approximation to the average value of q over a grid cell rather than as an approximation to a pointwise value of q. The cell average is simply the integral of q over the cell divided by its length, so conservation can be maintained by updating this value based on fluxes through the cell edges. Note that the resulting formulas corresponding to finite difference and finite volume methods may be identical in some cases even though their derivations may be quite different from each other.

Ideally we would like to have a numerical method that will produce sharp approximations to discontinuous solutions. If we use a first-order accurate method such as Godunov's method described below, we obtain results that are very smeared in regions near the discontinuities. This is natural because first-order accurate numerical methods have a large amount of "numerical viscosity" that smoothes the solution in much the same way physical viscosity would, but to an extent that is unrealistic by several orders of magnitude. If we attempt to use a second-order method we eliminate this numerical viscosity but now introduce dispersive effects that lead to large oscillations in the numerical solution.

For the homogeneous conservation law, many high-resolution numerical methods have been developed. However, it is not easy task to incorporate source terms into these numerical methods. Because, for some type of problems, they may perform quite poorly. The numerical schemes proposed for conservation laws with source terms are based on a fractional step approach or on the solution of a generalized Riemann problem with stationary data.

Here we are particularly concerned with Godunov-type finite volume methods which require a solution to a Riemann problem with discontinous initial data. It is well known that an exact solution to this problem is non-trivial. See, for example, [8, 9, 10] for a general discussion of such methods that have been used successfully in gas dynamics and shallow water wave problems.

Our goal is to present such a method with good accuracy and resolution properties. A full discussion of the numerical method is beyond the scope of this thesis. In particular, a discussion of the convergence of the method will not be pursued in this thesis.

4.4 Godunov's Method

The Godunov method is the most natural finite volume method to solve numerically the Cauchy problem (4.5)-(4.6). The basic idea of the Godunov method is to compose the global solution by the exact or approximate solutions of local Riemann problems. For nonlinear and/or inhomogoneous problems we will generally not be able to solve the Riemann problems and we will approximate the solution in a sutiable way by using an approximate Riemann solver. Many of the modern high-resolution approximations for nonlinear conservation laws (and related equations) employ the Godunov approach. Godunov's original scheme [12] is the forerunner of all upwind schemes. Its higher-order and multidimensional generalizations were constructed, analyzed and implemented with great succes during the last three decades; consult [8, 9, 10] and the references therein.

To construct a numerical scheme for the quasilinear system of conservation laws, (4.1), the spatial domain $[a, b]$ is discretized by taking an equally spaced grid. Let

$\{x_j : j \in \mathbb{N}\}$ be the nodes of the mesh $x_j = a+(j-1/2)\Delta x$ where $\Delta x = (b-a)/M$ ($M \in \mathbb{N}$). The cell I_j is defined as $I_j = (x_{j-1/2}, x_{j+1/2}) = \{|x - x_j| < \Delta x/2\}$ where Δx denotes its length and is given by $\Delta x = x_j - x_{j-1}$. The cell I_j has interfaces at $x_{j-1/2}$ and $x_{j+1/2}$ which denote the end points of the cell. Let Δt be time step and $t_n = n\Delta t$ ($n \in \mathbb{N}$) be a given time. The approximate solution to $\mathbf{Q}$ at time $t = t_n$ and at the grid point x_j is denoted by $\mathbf{Q}_j^n$. That is, we consider $\mathbf{Q}_j^n$ as an approximation of $\mathbf{Q}(x_j, t_n)$, where $\mathbf{Q}$ is the exact solution of the Cauchy problem (4.5)-(4.6).

The initial condition $\mathbf{Q}(x, 0) = \mathbf{Q}_0(x)$ is projected into the space of piecewise constant functions by

$$\mathbf{Q}_j^0 = \frac{1}{\Delta x}\int_{x_{j-1/2}}^{x_{j+1/2}} \mathbf{Q}_0(x)\mathrm{d}x, \tag{4.57}$$

Now we assume that the discrete function $\mathbf{Q}^n$ for the time level t_n is already computed. In the Godunov method, given an approximation $\mathbf{Q}^n$ of $\mathbf{Q}(., t_n)$, we define the the approximation $\mathbf{Q}^{n+1}$ of $\mathbf{Q}(., t_{n+1})$ as follows. In the first step, the approximate solution $\mathbf{Q}^n$ is considered as a piecewise constant function given by

$$\mathbf{Q}^n(x) = \bar{\mathbf{Q}}_j^n\,, \qquad x_{j-1/2} < x < x_{j+1/2} \tag{4.58}$$

This approach leads to Riemann problems at the cell edges due to jump discontinuities at the cell interfaces $x_{j-1/2}$. Then, in the second step we solve the local Riemann problems

$$\begin{cases} \mathbf{Q}_t + (\mathbf{H}(\mathbf{Q}))_x = \mathbf{0}\,, \quad x \in \mathbb{R}, \quad t > t_n \\ \mathbf{Q}(x, t_n) = \begin{cases} \bar{\mathbf{Q}}_{j-1}^n\,, & x < x_{j-1/2} \\ \bar{\mathbf{Q}}_j^n\,, & x > x_{j-1/2}\,. \end{cases} \end{cases} \tag{4.59}$$

Note that the local Riemann problems are defined for the hyperbolic system (4.1) with the source terms set to zero. An approximate solver based on the pseudo-jump equations (4.28) is used for the Riemann problem. Solving the Riemann problem between $\bar{\mathbf{Q}}_{j-1}^n$ and $\bar{\mathbf{Q}}_j^n$ at the cell interface $x_{j-1/2}$ gives rise to waves which affect both of the cell averages over the next time step. The solution of the local Riemann problem is denoted by $\hat{\mathbf{Q}}_{j-1/2}(\bar{\mathbf{Q}}_{j-1}^n, \bar{\mathbf{Q}}_j^n)$. If the

CFL condition (see below) is satisfied, which provides to avoid two neighbouring Riemann problems interacting, the solutions $\hat{\mathbf{Q}}_{j-1/2}(x,t)$ of the local Riemann problems are now used to define a function $\hat{\mathbf{Q}}$ for all $x \in \mathbb{R}$ such that

$$\hat{\mathbf{Q}}(x,t_{n+1}) = \begin{cases} \hat{\mathbf{Q}}_{j-1/2}(x,t_{n+1}) \,, & x_{j-1/2} < x < x_j \\ \hat{\mathbf{Q}}_{j+1/2}(x,t_{n+1}) \,, & x_j \le x < x_{j+1/2} \end{cases} \tag{4.60}$$

Then in the final step we project the solution $\hat{\mathbf{Q}}(.,t_{n+1})$ onto the piecewise constant functions, i.e., we set

$$\bar{\mathbf{Q}}_j^{n+1} = \frac{1}{\Delta x}\int_{x_{j-1/2}}^{x_{j+1/2}} \hat{\mathbf{Q}}(x,t_{n+1})\mathrm{d}x \tag{4.61}$$

These values are then used to define new piecewise constant function $\mathbf{Q}^{n+1}(x)$ and the process repeats. That is, Godunov's method is based on the assumption that the constant $\bar{\mathbf{Q}}_j^n$ in (4.58) denotes the cell average of the jth grid cell at time t_n.

In order to derive a more explicit form of the scheme, we now integrate the conservation law (4.1) with respect to space and time over the rectangle $(x_{j-1/2},x_{j+1/2}) \times (t_n,t_{n+1})$:

$$\int_{t_n}^{t_{n+1}}\int_{x_{j-1/2}}^{x_{j+1/2}}[\mathbf{Q}_t + (\mathbf{H}(\mathbf{Q}))_x + \mathbf{B}(\mathbf{Q})]\,\mathrm{d}x\mathrm{d}t = \mathbf{0} \tag{4.62}$$

Since the function is piecewise smooth, we obtain

$$\begin{aligned}\int_{x_{j-1/2}}^{x_{j+1/2}}[\mathbf{Q}(x,t_{n+1}) - \mathbf{Q}(x,t_n)]\mathrm{d}x + \int_{t_n}^{t_{n+1}}[\mathbf{H}(\mathbf{Q}(x_{j+1/2}-0,t))& \\ - \mathbf{H}(\mathbf{Q}(x_{j-1/2}+0,t))]\mathrm{d}t + \int_{t_n}^{t_{n+1}}\int_{x_{j-1/2}}^{x_{j+1/2}}\mathbf{B}(\mathbf{Q}(x,t))\mathrm{d}x\mathrm{d}t = \mathbf{0}&\end{aligned}$$

Using (4.58) and (4.61) we get

$$\begin{aligned}\Delta x(\bar{\mathbf{Q}}_j^{n+1} - \bar{\mathbf{Q}}_j^n) + \int_{t_n}^{t_{n+1}}\mathbf{H}(\mathbf{Q}(x_{j+1/2}-0,t))\mathrm{d}t - \int_{t_n}^{t_{n+1}}\mathbf{H}(\mathbf{Q}(x_{j-1/2}+0,t))\mathrm{d}t& \\ + \int_{t_n}^{t_{n+1}}\int_{x_{j-1/2}}^{x_{j+1/2}}\mathbf{B}(\mathbf{Q}(x,t))\mathrm{d}x\mathrm{d}t = \mathbf{0}&\end{aligned} \tag{4.63}$$

We now approximate the integrals in the above equation as follows

$$\int_{t_n}^{t_{n+1}}\mathbf{H}(\mathbf{Q}(x_{j+1/2}-0,t))\mathrm{d}t \;\approx\; \Delta t\mathbf{H}(\hat{\mathbf{Q}}_{j+1/2})\,, \tag{4.64}$$

$$\int_{t_n}^{t_{n+1}}\mathbf{H}(\mathbf{Q}(x_{j-1/2}+0,t))\mathrm{d}t \;\approx\; \Delta t\mathbf{H}(\hat{\mathbf{Q}}_{j-1/2})\,, \tag{4.65}$$

$$\int_{t_n}^{t_{n+1}}\int_{x_{j-1/2}}^{x_{j+1/2}}\mathbf{B}(\mathbf{Q}(x,t))\mathrm{d}x\mathrm{d}t \;\approx\; \Delta t\Delta x\mathbf{B}(\frac{1}{2}(\hat{\mathbf{Q}}_{j+1/2} + \hat{\mathbf{Q}}_{j-1/2}))\,, \tag{4.66}$$

where $\hat{\mathbf{Q}}_{j-1/2}$ is the solution to the Riemann problem between $\bar{\mathbf{Q}}_{j-1}^n$ and $\bar{\mathbf{Q}}_j^n$ at the interface $x_{j-1/2}$ for all $t \in [t_n, t_{n+1}]$. Hence, we have

$$\bar{\mathbf{Q}}_j^{n+1} = \bar{\mathbf{Q}}_j^n - \frac{\Delta t}{\Delta x}[\mathbf{H}(\hat{\mathbf{Q}}_{j+1/2}) - \mathbf{H}(\hat{\mathbf{Q}}_{j-1/2})] - \Delta t \mathbf{B}(\frac{1}{2}(\hat{\mathbf{Q}}_{j+1/2} + \hat{\mathbf{Q}}_{j-1/2})) \quad (4.67)$$

Note that in the above approximation we assume that $\hat{\mathbf{Q}}(x_{j-1/2}, t)$ is constant in time along each cell interface. In the absence of the source terms, $\hat{\mathbf{Q}}(x_{j-1/2}, t)$ is constant at the interface $x_{j-1/2}$ over the time interval $t_n < t \leq t_{n+1}$. This follows from the fact that the solution of the Riemann problem at $x_{j-1/2}$ is a similarity solution, constant along each ray $(x - x_{j-1/2})/t$ =constant. However this is not true when we consider the source terms.

We assume that the condition

$$\max |c_k(\bar{\mathbf{Q}}_j^n)| \leq \frac{\Delta x}{2\Delta t}, \qquad 1 \leq k \leq p, \quad (4.68)$$

is satisfied so that the waves issued from the interfaces $x_{j-1/2}$ and $x_{j+1/2}$ do not interact. Here c_k $(1 \leq k \leq p)$ represent the eigenvalues of the Jacobian matrix $\mathbf{A}(\mathbf{Q})$ and (4.68) gives a restriction on Δx and Δt by using the largest wave speed. This condition is known as the CFL condition after Courant, Friedrichs and Lewy. Shocks form immediately at the points $x_{j-1/2}$, but because of the above time step restriction, these shocks do not reach the cell boundary during the time step Δt. Then the neighbouring solutions $\hat{\mathbf{Q}}_{j-1/2}$ and $\hat{\mathbf{Q}}_{j+1/2}$ cannot influence each other. The CFL condition is only necessary condition for stability, not sufficient.

Equation (4.67) can be rewritten as follows

$$\bar{\mathbf{Q}}_j^{n+1} = \bar{\mathbf{Q}}_j^n - \frac{\Delta t}{\Delta x}[\mathbf{G}(\bar{\mathbf{Q}}_j^n, \bar{\mathbf{Q}}_{j+1}^n) - \mathbf{G}(\bar{\mathbf{Q}}_{j-1}^n, \bar{\mathbf{Q}}_j^n)] - \Delta t \mathbf{B}(\frac{1}{2}(\hat{\mathbf{Q}}_{j+1/2} + \hat{\mathbf{Q}}_{j-1/2})) \quad (4.69)$$

where $\mathbf{G}$ is called the numerical flux for the Godunov method and is given by

$$\mathbf{G}(\bar{\mathbf{Q}}_{j-1}^n, \bar{\mathbf{Q}}_j^n) = \mathbf{H}(\hat{\mathbf{Q}}_{j-1/2}(\bar{\mathbf{Q}}_{j-1}^n, \bar{\mathbf{Q}}_j^n)) \; . \quad (4.70)$$

If we sum $\Delta x \bar{\mathbf{Q}}_j^{n+1}$ from the above equation (4.67) over any set of cells we obtain

$$\Delta x \sum_{j=J}^{K} \bar{\mathbf{Q}}_j^{n+1} = \Delta x \sum_{j=J}^{K} \bar{\mathbf{Q}}_j^n - \Delta t[\mathbf{H}(\hat{\mathbf{Q}}_{K+1/2}) - \mathbf{H}(\hat{\mathbf{Q}}_{J-1/2})]$$

$$- \Delta t \Delta x \sum_{j=J}^{K} \mathbf{B}(\frac{1}{2}(\hat{\mathbf{Q}}_{j+1/2} + \hat{\mathbf{Q}}_{j-1/2})) \tag{4.71}$$

That is, the sum of the flux differences cancels out except for the fluxes at the extreme edges. In the absence of the source term, over the full domain we have exact conservation except for fluxes at the extreme edges. Then the numerical method is said to be in *conservation form*, since it mimics the conservation property of the exact solution.

The concept of total variation plays a central role in computing approximate solutions for scalar conservation laws. In the discrete case we define the total variation for a sequence q^n of discrete values q_j^n $(j = 1, 2, ..., M-1)$ by

$$TV(q^n) = \sum_{j=1}^{M-1} |q_{j+1}^n - q_j^n| \tag{4.72}$$

A numerical scheme which generates approximations q that are nonincreasing in total variation from one time level to the next, $TV(q^{n+1}) \leq TV(q^n)$, is described as *total variation diminishing (TVD).* Entropy solutions of the Cauchy problem (4.5)-(4.6) have decreasing total variation, and so TVD schemes produce approximations that mimic an important property of the desired solution. From a more practical point of view, the TVD property rules out spurious overshoots and oscillations that often appear near steep gradients with the traditional higher order schemes. Finally, the TVD property, when accompanied by some further properties, guarantees that the sequence of approximations converges to a function q as the mesh size shrinks. If the scheme is in conservation form, the Lax-Wendroff [13] theorem guarantees that the limit q is a weak solution of the Cauchy problem of the system of conservation laws. If in addition, the numerical approximations satisfy a set of discrete entropy inequalities, then the whole sequence converges to the physically correct entropy solution. Another important property of the TVD schemes is that they preserve monotonicity [10, p.64]. This property can be explained as follows. Let q_j^n be a grid function defined by a TVD scheme. Assume that q_j^n is a monotone (increasing/decreasing) grid function with respect to j. Then q_j^{n+1} is also a monotone (increasing/decreasing) grid function with respect to j. This property is called the *monotonicity property.* That is, a TVD scheme transforms a monotone sequence into a monotone sequence and oscillations cannot occur. Godunov's scheme for a scalar conservation law is monotone and TVD. Additionally it satisfies a large set of discrete entropy inequalities. This makes it possible to prove that Godunov's scheme converges to the physically unique entropy solution of the Cauchy problem. Unfortunately, both monotonicity and TVD properties are important but purely scalar notions. Furthermore, the solution of an inhomogeneous equation does not posses the TVD property because of the effect of the source term which increases the total variation.

We note that in the Godunov method the solution is not simply an updating from one timestep to another, but includes the solution of the Riemann problem at each cell interface. In attempting to apply this method to a nonlinear problem, the principle difficulty is in the second step, since we typically cannot compute the exact solution to the nonlinear equation with piecewise constant initial data. However, there are various ways to obtain approximate solutions and one of these approaches will be discussed in the next chapter after we introduce a more accurate scheme that is a second-order accurate generalization of the Godunov method.

4.5 A Second-Order Godunov Method

We now introduce a modified Godunov method that is second-order accurate in smooth regions and gives much sharper discontinuities. Algorithms of this type were first introduced by van Leer in a series of papers [14]. Van Leer referred to them as Monotone Upwind Scehemes for Conservation Laws (MUSCL). Sometimes the present method is called van Leer's method [9, p.245]. See [15] for a proof of convergence in the one-dimensional situation. For an application of the method to nonlinear elasticity we refer to [16]. Note that the notation of [16] has been modified here to use $j-1/2$ as the index for the interface between cells I_{j-1} and I_j (rather than using j for this index).

The basic idea of the second-order method is to replace the piecewise constant representation of the solution by a piecewise linear representation. We expect that this generalization of the Godunov method simulates better than the first-order accurate scheme. In this more accurate representation we take

$$\mathbf{Q}^n(x) = \bar{\mathbf{Q}}_j^n + \frac{\mathbf{\Gamma}_j^n}{\Delta x}(x - x_j) , \qquad x_{j-1/2} < x < x_{j+1/2} . \tag{4.73}$$

Here $\mathbf{\Gamma}_j^n$ is a vector of slopes and it is to be detailed later on. Note that taking $\mathbf{\Gamma}_j^n = \mathbf{0}$ for all j and n recovers Godunov's method. More importantly, the cell average of $\mathbf{Q}^n(x)$ over $(x_{j-1/2}, x_{j+1/2})$ is equal to $\bar{\mathbf{Q}}_j^n$ for any choice of $\mathbf{\Gamma}_j^n$.

The distributions in the cells $(x_{j-3/2}, x_{j-1/2})$ and $(x_{j-1/2}, x_{j+1/2})$ at time t_n generally meet, at $x_{j-1/2}$, in a discontinuity. Therefore, as in Godunov's method, the next step involves either an exact or an approximate Riemann solver.

As in the previous section, in order to derive a more explicit form of the scheme, we now integrate the quasilinear system (4.1) with respect to space and time over the rectangle $(x_{j-1/2}, x_{j+1/2}) \times (t_n, t_{n+1})$:

$$\int_{t_n}^{t_{n+1}} \int_{x_{j-1/2}}^{x_{j+1/2}} [\mathbf{Q}_t + (\mathbf{H}(\mathbf{Q}))_x + \mathbf{B}(\mathbf{Q})] \, \mathrm{d}x\mathrm{d}t = \mathbf{0} . \tag{4.74}$$

Since the function is piecewise smooth, we obtain

$$\begin{aligned}\int_{x_{j-1/2}}^{x_{j+1/2}} [\mathbf{Q}(x, t_{n+1}) - \mathbf{Q}(x, t_n)]\mathrm{d}x + \int_{t_n}^{t_{n+1}} [\mathbf{H}(\mathbf{Q}(x_{j+1/2} - 0, t))& \\ - \mathbf{H}(\mathbf{Q}(x_{j-1/2} + 0, t))]\mathrm{d}t + \int_{t_n}^{t_{n+1}} \int_{x_{j-1/2}}^{x_{j+1/2}} \mathbf{B}(\mathbf{Q}(x,t))\mathrm{d}x\mathrm{d}t &= \mathbf{0}\end{aligned}$$

Using (4.73) we get

$$\begin{aligned}\Delta x(\bar{\mathbf{Q}}_j^{n+1} - \bar{\mathbf{Q}}_j^n) + \int_{t_n}^{t_{n+1}} \mathbf{H}(\mathbf{Q}(x_{j+1/2} - 0, t))\mathrm{d}t - \int_{t_n}^{t_{n+1}} \mathbf{H}(\mathbf{Q}(x_{j-1/2} + 0, t))\mathrm{d}t& \\ + \int_{t_n}^{t_{n+1}} \int_{x_{j-1/2}}^{x_{j+1/2}} \mathbf{B}(\mathbf{Q}(x,t))\mathrm{d}x\mathrm{d}t = \mathbf{0}&\end{aligned} \tag{4.75}$$

We now approximate the integrals in the above equation as follows

$$\int_{t_n}^{t_{n+1}} \mathbf{H}(\mathbf{Q}(x_{j+1/2} - 0, t))\mathrm{d}t \;\approx\; \Delta t \mathbf{H}(\hat{\mathbf{Q}}_{j+1/2}) , \tag{4.76}$$

$$\int_{t_n}^{t_{n+1}} \mathbf{H}(\mathbf{Q}(x_{j-1/2}+0,t))\mathrm{d}t \;\approx\; \Delta t\mathbf{H}(\hat{\mathbf{Q}}_{j-1/2}) \,, \tag{4.77}$$

$$\int_{t_n}^{t_{n+1}} \int_{x_{j-1/2}}^{x_{j+1/2}} \mathbf{B}(\mathbf{Q}(x,t))\mathrm{d}x\mathrm{d}t \;\approx\; \Delta t\Delta x\mathbf{B}(\frac{1}{2}(\hat{\mathbf{Q}}_{j+1/2}+\hat{\mathbf{Q}}_{j-1/2})) \,, \tag{4.78}$$

where $\hat{\mathbf{Q}}_{j-1/2}$ is the solution to the Riemann problem between $\mathbf{Q}^{n+1/2}_{j-1/2,-}$ and $\mathbf{Q}^{n+1/2}_{j-1/2,+}$ at the interface $x_{j-1/2}$ for all $t \in [t_{n+1/2}, t_{n+1}]$. Here the data $\mathbf{Q}^{n+1/2}_{j-1/2,+}$ and $\mathbf{Q}^{n+1/2}_{j-1/2,-}$ represent approximations to $\mathbf{Q}(x_{j-1/2}, t_{n+1/2})$ at the midpoint in time, approaching the interface from the right and left, respectively. The construction of the modified states $\mathbf{Q}^{n+1/2}_{j-1/2,-}$ and $\mathbf{Q}^{n+1/2}_{j-1/2,+}$ are to be detailed later on. Then, we have

$$\bar{\mathbf{Q}}^{n+1}_j = \bar{\mathbf{Q}}^n_j - \frac{\Delta t}{\Delta x}[\mathbf{H}(\hat{\mathbf{Q}}_{j+1/2}) - \mathbf{H}(\hat{\mathbf{Q}}_{j-1/2})] - \Delta t\mathbf{B}(\frac{1}{2}(\hat{\mathbf{Q}}_{j+1/2}+\hat{\mathbf{Q}}_{j-1/2})) \,, \tag{4.79}$$

where $\mathbf{H}$ is the numerical flux.

Note that these equations are the same as those obtained in the previous section, except the definition of $\hat{\mathbf{Q}}_{j-1/2}$. In the second order method $\hat{\mathbf{Q}}_{j-1/2}$ will be calculated by using a different approach and the reason of this can be given as follows. If one uses schemes that are higher-order in space, it is necessary to take care of a higher-order time discretization as well. The Godunov scheme presented in the previous section is of first order in time and first order in space. However, the present scheme is second order in space. If the time discretization is also of second order, the scheme may converge to the correct solution. For explicit schemes the CFL condition is necessary for getting a stable scheme. But this means a strong restriction to the size of the timestep when the scheme is of first order in time and second order in space. Therefore we use a predictor-corrector numerical scheme that is also of second order in time. To this end, at the predictor stage the scheme proceeds with a half step in time and the state variables at the cell boundaries at a half time step $t_{n+1/2}$, are calculated. Then, at the corrector stage, the Riemann problems at the interfaces are solved with the initial data obtained at the predictor stage.

As it is mentioned above, $\mathbf{Q}^{n+1/2}_{j-1/2,+}$ and $\mathbf{Q}^{n+1/2}_{j-1/2,-}$ are constructed as approximations to $\mathbf{Q}(x_{j-1/2}, t_{n+1/2})$ at the midpoint in time, approaching the interface from the right and left, respectively. That is, the updated values $\mathbf{Q}^{n+1/2}_{j-1/2,\pm}$ can be interpreted as follows:

$$\mathbf{Q}^{n+1/2}_{j-1/2,+} \approx \mathbf{Q}(x_j - \Delta x/2 + 0, t_n + \Delta t/2) ,$$
$$\mathbf{Q}^{n+1/2}_{j-1/2,-} \approx \mathbf{Q}(x_{j-1} + \Delta x/2 - 0, t_n + \Delta t/2) .$$

If we denote the values at the left and the right side of the interface by $-$ and $+$ at $t = t_n$, respectively we have

$$\mathbf{Q}^n_{j-1/2,+} = \bar{\mathbf{Q}}^n_j - \frac{1}{2}\mathbf{\Gamma}^n_j , \quad \mathbf{Q}^n_{j-1/2,-} = \bar{\mathbf{Q}}^n_{j-1} + \frac{1}{2}\mathbf{\Gamma}^n_{j-1} . \tag{4.80}$$

We now give three different ways for updating $\mathbf{Q}^n_{j-1/2,\pm}$ a half step in time.

Case A: In the first approach, the state variables at the cell boundaries at a half time step are calculated using Taylor series expansions.

$$\mathbf{Q}(x_j - \frac{\Delta x}{2} + 0, t_n + \frac{\Delta t}{2}) \approx \mathbf{Q}(x_j, t_n) + \frac{\Delta t}{2}\mathbf{Q}_t(x_j, t_n) - \frac{\Delta x}{2}\mathbf{Q}_x(x_j, t_n) , \tag{4.81}$$
$$\mathbf{Q}(x_{j-1} + \frac{\Delta x}{2} - 0, t_n + \frac{\Delta t}{2}) \approx \mathbf{Q}(x_{j-1}, t_n) + \frac{\Delta t}{2}\mathbf{Q}_t(x_{j-1}, t_n) + \frac{\Delta x}{2}\mathbf{Q}_x(x_{j-1}, t_n) . \tag{4.82}$$

The linearized forms of the quasilinear system (4.2) about $\mathbf{Q}(x,t) = \mathbf{Q}(x_j, t_n)$ and $\mathbf{Q}(x,t) = \mathbf{Q}(x_{j-1}, t_n)$ are given by

$$\mathbf{Q}_t + \mathbf{A}(\mathbf{Q}(x_j, t_n))\mathbf{Q}_x + \mathbf{B}(\mathbf{Q}(x_j, t_n)) = \mathbf{0} ,$$
$$\mathbf{Q}_t + \mathbf{A}(\mathbf{Q}(x_{j-1}, t_n))\mathbf{Q}_x + \mathbf{B}(\mathbf{Q}(x_{j-1}, t_n)) = \mathbf{0} ,$$

respectively. If we express $\mathbf{Q}_t$ in terms of $\mathbf{Q}_x$ using these relations and substitute the resulting equations into (4.81)-(4.82) we obtain

$$\begin{aligned}\mathbf{Q}(x_j - \frac{\Delta x}{2} + 0, t_n + \frac{\Delta t}{2}) \approx \mathbf{Q}(x_j, t_n) &- \frac{\Delta x}{2}[\mathbf{I} + \frac{\Delta t}{\Delta x}\mathbf{A}(\mathbf{Q}(x_j, t_n))]\mathbf{Q}_x(x_j, t_n) \\ &- \frac{\Delta t}{2}\mathbf{B}(\mathbf{Q}(x_j, t_n)) ,\end{aligned} \tag{4.83}$$

$$\begin{aligned}\mathbf{Q}(x_{j-1} + \frac{\Delta x}{2} - 0, t_n + \frac{\Delta t}{2}) &\approx \mathbf{Q}(x_{j-1}, t_n) \\ &+ \frac{\Delta x}{2}[\mathbf{I} - \frac{\Delta t}{\Delta x}\mathbf{A}(\mathbf{Q}(x_{j-1}, t_n))]\mathbf{Q}_x(x_{j-1}, t_n) \\ &- \frac{\Delta t}{2}\mathbf{B}(\mathbf{Q}(x_{j-1}, t_n)) .\end{aligned} \tag{4.84}$$

T.C. YÜKSEKÖĞRETİM KURULU
DOKÜMANTASYON MERKEZİ

Recall that

$$\mathbf{Q}_x(x_j,t_n) = \mathbf{\Gamma}_j^n/\Delta x\ , \qquad \mathbf{Q}_x(x_{j-1},t_n) = \mathbf{\Gamma}_{j-1}^n/\Delta x\ . \tag{4.85}$$

Then using this result in (4.83)-(4.84) we obtain

$$\begin{aligned}
\mathbf{Q}(x_j - \frac{\Delta x}{2} + 0, t_n + \frac{\Delta t}{2}) &\approx \mathbf{Q}(x_j,t_n) - \frac{1}{2}[\mathbf{I} + \frac{\Delta t}{\Delta x}\mathbf{A}(\mathbf{Q}(x_j,t_n))]\mathbf{\Gamma}_j^n \\
&\quad - \frac{\Delta t}{2}\mathbf{B}(\mathbf{Q}(x_j,t_n))\ , \\
\mathbf{Q}(x_{j-1} + \frac{\Delta x}{2} - 0, t_n + \frac{\Delta t}{2}) &\approx \mathbf{Q}(x_{j-1},t_n) + \frac{1}{2}[\mathbf{I} - \frac{\Delta t}{\Delta x}\mathbf{A}(\mathbf{Q}(x_{j-1},t_n))]\mathbf{\Gamma}_{j-1}^n \\
&\quad - \frac{\Delta t}{2}\mathbf{B}(\mathbf{Q}(x_{j-1},t_n))\ .
\end{aligned}$$

That is, $\mathbf{Q}_{j-1/2,\pm}^{n+1/2}$ are calculated as follows

$$\mathbf{Q}_{j-1/2,+}^{n+1/2} = \bar{\mathbf{Q}}_j^n - \frac{1}{2}[\mathbf{I} + \frac{\Delta t}{\Delta x}\mathbf{A}(\bar{\mathbf{Q}}_j^n)]\mathbf{\Gamma}_j^n - \frac{\Delta t}{2}\mathbf{B}(\bar{\mathbf{Q}}_j^n)\ , \tag{4.86}$$

$$\mathbf{Q}_{j-1/2,-}^{n+1/2} = \bar{\mathbf{Q}}_{j-1}^n + \frac{1}{2}[\mathbf{I} - \frac{\Delta t}{\Delta x}\mathbf{A}(\bar{\mathbf{Q}}_{j-1}^n)]\mathbf{\Gamma}_{j-1}^n - \frac{\Delta t}{2}\mathbf{B}(\bar{\mathbf{Q}}_{j-1}^n)\ . \tag{4.87}$$

The above approach is based on approximating the quasilinear system by a linear system in the neighborhood of each cell center. Because it uses the values at the cell centers since the quasilinear system is linearized about $\bar{\mathbf{Q}}_j^n$. A scheme that linearizes the quasilinear system about $\mathbf{Q}_{j-1/2,\pm}^n$ may be more appropriate and is discussed now.

Case B: In second approach, the state variables at the cell boundaries at a half time step are calculated using Taylor series expansions.

$$\mathbf{Q}(x_{j-1/2} + 0, t_n + \frac{\Delta t}{2}) \approx \mathbf{Q}(x_{j-1/2} + 0, t_n) + \frac{\Delta t}{2}\mathbf{Q}_t(x_{j-1/2} + 0, t_n)\ , \tag{4.88}$$

$$\mathbf{Q}(x_{j-1/2} - 0, t_n + \frac{\Delta t}{2}) \approx \mathbf{Q}(x_{j-1/2} - 0, t_n) + \frac{\Delta t}{2}\mathbf{Q}_t(x_{j-1/2} - 0, t_n)\ . \tag{4.89}$$

The linearized forms of the quasilinear system (4.2) about $\mathbf{Q}(x,t) = \mathbf{Q}(x_{j-1/2} + 0, t_n)$ and $\mathbf{Q}(x,t) = \mathbf{Q}(x_{j-1/2} - 0, t_n)$ are given by

$$\mathbf{Q}_t + \mathbf{A}(\mathbf{Q}(x_{j-1/2} + 0, t_n))\mathbf{Q}_x + \mathbf{B}(\mathbf{Q}(x_{j-1/2} + 0, t_n)) = \mathbf{0}\ ,$$

$$\mathbf{Q}_t + \mathbf{A}(\mathbf{Q}(x_{j-1/2} - 0, t_n))\mathbf{Q}_x + \mathbf{B}(\mathbf{Q}(x_{j-1/2} - 0, t_n)) = Lbf0\ ,$$

respectively. If we express $\mathbf{Q}_t$ in terms of $\mathbf{Q}_x$ using these relations and substitute the resulting equations into (4.88)-(4.89), we obtain

$$\begin{aligned}
\mathbf{Q}(x_{j-1/2}+0, t_n+\frac{\Delta t}{2}) \;&\approx\; \mathbf{Q}(x_{j-1/2}+0, t_n) \\
&\quad - \frac{\Delta t}{2}\mathbf{A}(\mathbf{Q}(x_{j-1/2}+0, t_n))\mathbf{Q}_x(x_{j-1/2}+0, t_n) \\
&\quad - \frac{\Delta t}{2}\mathbf{B}(\mathbf{Q}(x_{j-1/2}+0, t_n)) , \qquad (4.90)\\
\mathbf{Q}(x_{j-1/2}-0, t_n+\frac{\Delta t}{2}) \;&\approx\; \mathbf{Q}(x_{j-1/2}-0, t_n) \\
&\quad - \frac{\Delta t}{2}\mathbf{A}(\mathbf{Q}(x_{j-1/2}-0, t_n))\mathbf{Q}_x(x_{j-1/2}-0, t_n) \\
&\quad - \frac{\Delta t}{2}\mathbf{B}(\mathbf{Q}(x_{j-1/2}-0, t_n)) . \qquad (4.91)
\end{aligned}$$

Recall that

$$\mathbf{Q}_x(x_{j-1/2}+0, t_n) = \mathbf{\Gamma}_j^n/\Delta x \ , \qquad \mathbf{Q}_x(x_{j-1/2}-0, t_n) = \mathbf{\Gamma}_{j-1}^n/\Delta x \ .$$

Then using this result in (4.90)-(4.91) we obtain

$$\begin{aligned}
\mathbf{Q}(x_{j-1/2}+0, t_n+\Delta t/2) \;&\approx\; \mathbf{Q}(x_{j-1/2}+0, t_n) \\
&\quad - \frac{\Delta t}{2\Delta x}\mathbf{A}(\mathbf{Q}(x_{j-1/2}+0, t_n))\mathbf{\Gamma}_j^n \\
&\quad - \frac{\Delta t}{2}\mathbf{B}(\mathbf{Q}(x_{j-1/2}+0, t_n)) , \qquad (4.92)\\
\mathbf{Q}(x_{j-1/2}-0, t_n+\Delta t/2) \;&\approx\; \mathbf{Q}(x_{j-1/2}-0, t_n) \\
&\quad - \frac{\Delta t}{2\Delta x}\mathbf{A}(\mathbf{Q}(x_{j-1/2}-0, t_n))\mathbf{\Gamma}_{j-1}^n \\
&\quad - \frac{\Delta t}{2}\mathbf{B}(\mathbf{Q}(x_{j-1/2}-0, t_n)) . \qquad (4.93)
\end{aligned}$$

That is, $\mathbf{Q}_{j-1/2,\pm}^{n+1/2}$ can be calculated as follows

$$\mathbf{Q}_{j-1/2,+}^{n+1/2} = \mathbf{Q}_{j-1/2,+}^n - \frac{\Delta t}{2\Delta x}\mathbf{A}(\mathbf{Q}_{j-1/2,+}^n)\mathbf{\Gamma}_j^n - \frac{\Delta t}{2}\mathbf{B}(\mathbf{Q}_{j-1/2,+}^n) , \qquad (4.94)$$

$$\mathbf{Q}_{j-1/2,-}^{n+1/2} = \mathbf{Q}_{j-1/2,-}^n - \frac{\Delta t}{2\Delta x}\mathbf{A}(\mathbf{Q}_{j-1/2,-}^n)\mathbf{\Gamma}_{j-1}^n - \frac{\Delta t}{2}\mathbf{B}(\mathbf{Q}_{j-1/2,-}^n) . \qquad (4.95)$$

Using equation (4.80) we can rewrite this equation in the form

$$\mathbf{Q}_{j-1/2,+}^{n+1/2} = \bar{\mathbf{Q}}_j^n - \frac{1}{2}[\mathbf{I} + \frac{\Delta t}{\Delta x}\mathbf{A}(\mathbf{Q}_{j-1/2,+}^n)]\mathbf{\Gamma}_j^n - \frac{\Delta t}{2}\mathbf{B}(\mathbf{Q}_{j-1/2,+}^n) , \qquad (4.96)$$

$$\mathbf{Q}_{j-1/2,-}^{n+1/2} = \bar{\mathbf{Q}}_{j-1}^n + \frac{1}{2}[\mathbf{I} - \frac{\Delta t}{\Delta x}\mathbf{A}(\mathbf{Q}_{j-1/2,-}^n)]\mathbf{\Gamma}_{j-1}^n - \frac{\Delta t}{2}\mathbf{B}(\mathbf{Q}_{j-1/2,-}^n) . \qquad (4.97)$$

If we compare these equations with those obtained using the previous approach, (4.86)-(4.87), we see that the only difference is the evaluation of $\mathbf{A}$ and $\mathbf{B}$ at $\mathbf{Q}^n_{j-1/2,\pm}$ instead of $\bar{\mathbf{Q}}^n_j$.

Case C: The third approach was originally proposed by Hannock [9, p.247] and it does not require the linearization of the quasilinear system about the cell centers or the cell interfaces. As in the second approach, the state variables at the cell boundaries at a half time step are calculated using Taylor series expansions.

$$\mathbf{Q}(x_{j-1/2}+0,t_n+\frac{\Delta t}{2}) \approx \mathbf{Q}(x_{j-1/2}+0,t_n)+\frac{\Delta t}{2}\mathbf{Q}_t(x_{j-1/2}+0,t_n)\ , \tag{4.98}$$

$$\mathbf{Q}(x_{j-1/2}-0,t_n+\frac{\Delta t}{2}) \approx \mathbf{Q}(x_{j-1/2}-0,t_n)+\frac{\Delta t}{2}\mathbf{Q}_t(x_{j-1/2}-0,t_n)\ . \tag{4.99}$$

Then if we express the time derivative $\mathbf{Q}_t$ in terms of $\mathbf{Q}_x$, using the system of conservation laws, in the form $\mathbf{Q}_t = -(\mathbf{H}(\mathbf{Q}))_x - \mathbf{B}(\mathbf{Q})$ and substitute the resulting equation into (4.98)- (4.99) we obtain

$$\begin{aligned}\mathbf{Q}(x_{j-1/2}+0,t_n+\frac{\Delta t}{2}) \approx \mathbf{Q}(x_{j-1/2}+0,t_n) &- \frac{\Delta t}{2}\mathbf{H}_x(\mathbf{Q}(x_{j-1/2}+0,t_n)) \\ &- \frac{\Delta t}{2}\mathbf{B}(\mathbf{Q}(x_{j-1/2}+0,t_n))\ ,\end{aligned} \tag{4.100}$$

$$\begin{aligned}\mathbf{Q}(x_{j-1/2}-0,t_n+\frac{\Delta t}{2}) \approx \mathbf{Q}(x_{j-1/2}-0,t_n) &- \frac{\Delta t}{2}\mathbf{H}_x(\mathbf{Q}(x_{j-1/2}-0,t_n)) \\ &- \frac{\Delta t}{2}\mathbf{B}(\mathbf{Q}(x_{j-1/2}-0,t_n))\ .\end{aligned} \tag{4.101}$$

In the next step the spatial derivaties are approximated using forward and backward differences as follows

$$\mathbf{H}_x(\mathbf{Q}(x_{j-1/2}+0,t_n)) = [\mathbf{H}(\mathbf{Q}(x_{j+1/2}-0,t_n)) - \mathbf{H}(\mathbf{Q}(x_{j-1/2}+0,t_n))]/\Delta x\ , \tag{4.102}$$

$$\mathbf{H}_x(\mathbf{Q}(x_{j-1/2}-0,t_n)) = [\mathbf{H}(\mathbf{Q}(x_{j-1/2}-0,t_n)) - \mathbf{H}(\mathbf{Q}(x_{j-3/2}+0,t_n))]/\Delta x\ . \tag{4.103}$$

Then using this result in equation (4.100)-(4.101) we obtain

$$\begin{aligned}\mathbf{Q}(x_{j-1/2}+0,t_n+\frac{\Delta t}{2}) &\approx \mathbf{Q}(x_{j-1/2}+0,t_n) \\ &\quad - \frac{\Delta t}{2\Delta x}[\mathbf{H}(\mathbf{Q}(x_{j+1/2}-0,t_n)) - \mathbf{H}(\mathbf{Q}(x_{j-1/2}+0,t_n))]\end{aligned}$$

$$
- \frac{\Delta t}{2}\mathbf{B}(\mathbf{Q}(x_{j-1/2}+0,t_n)) \,, \tag{4.104}
$$

$$
\begin{aligned}
\mathbf{Q}(x_{j-1/2}-0,t_n+\frac{\Delta t}{2}) \approx\ & \mathbf{Q}(x_{j-1/2}-0,t_n) \\
& - \frac{\Delta t}{2\Delta x}[\mathbf{H}(\mathbf{Q}(x_{j-1/2}-0,t_n)) - \mathbf{H}(\mathbf{Q}(x_{j-3/2}+0,t_n))] \\
& - \frac{\Delta t}{2}\mathbf{B}(\mathbf{Q}(x_{j-1/2}-0,t_n)) \,.
\end{aligned} \tag{4.105}
$$

Then, $\mathbf{Q}^{n+1/2}_{j-1/2,\pm}$ are calculated as follows

$$
\mathbf{Q}^{n+1/2}_{j-1/2,+} = \mathbf{Q}^{n}_{j-1/2,+} - \frac{\Delta t}{2\Delta x}[\mathbf{H}(\mathbf{Q}^{n}_{j+1/2,-}) - \mathbf{H}(\mathbf{Q}^{n}_{j-1/2,+})] - \frac{\Delta t}{2}\mathbf{B}(\mathbf{Q}^{n}_{j-1/2,+}) \,, \tag{4.106}
$$

$$
\mathbf{Q}^{n+1/2}_{j-1/2,-} = \mathbf{Q}^{n}_{j-1/2,-} - \frac{\Delta t}{2\Delta x}[\mathbf{H}(\mathbf{Q}^{n}_{j-1/2,-}) - \mathbf{H}(\mathbf{Q}^{n}_{j-3/2,+})] - \frac{\Delta t}{2}\mathbf{B}(\mathbf{Q}^{n}_{j-1/2,-}) \,. \tag{4.107}
$$

Later the result obtained by using these three different approaches will be compared for a nonlinear scalar conservation law.

At the corrector step, we solve the Riemann problem at the point $x_{j-1/2}$ with piecewise constant initial data $\mathbf{Q}^{n+1/2}_{j-1/2,\pm}$:

$$
\begin{cases}
\mathbf{Q}_t + (\mathbf{H}(\mathbf{Q}))_x = \mathbf{0} \,, \quad x \in \mathbb{R}, \quad t > t_{n+1/2} \\
\mathbf{Q}(x,t_{n+1/2}) = \begin{cases} \mathbf{Q}^{n+1/2}_{j-1/2,-} \,, & x < x_{j-1/2} \\ \mathbf{Q}^{n+1/2}_{j-1/2,+} \,, & x > x_{j-1/2} \,. \end{cases}
\end{cases} \tag{4.108}
$$

That is, we must still solve Riemann problems at the cell interfaces as in the Godunov method, but these are now between modified states $\mathbf{Q}^{n+1/2}_{j-1/2,+}$ and $\mathbf{Q}^{n+1/2}_{j-1/2,-}$ rather than between $\bar{\mathbf{Q}}^{n}_{j-1}$ and $\bar{\mathbf{Q}}^{n}_{j}$. Note that, as in the Godunov method, the source terms are set to zero. Now suppose that we can solve the Riemann problem with left and right states $\mathbf{Q}^{n+1/2}_{j-1/2,+}$ and $\mathbf{Q}^{n+1/2}_{j-1/2,-}$. Just as in the first-order method, we can accomplish this by finding an intermediate state $\hat{\mathbf{Q}}_{j-1/2}$ such that $\mathbf{Q}^{n}_{j-1/2,+}$ and $\hat{\mathbf{Q}}_{j-1/2}$ are connected by a discontinuity satisfying the Rankine-Hugoniot condition and so are $\hat{\mathbf{Q}}_{j-1/2}$ and $\mathbf{Q}^{n}_{j-1/2,-}$.

The most interesting question is how do we choose the slopes $\mathbf{\Gamma}^{n}_{j}$? We choose the slopes such that the monotonicity condition is satisfied [14]. Methods of this type were first introduced by van Leer in a series of papers [14]. The monotonicity condition says that, when a monotonic initial-value distribution is numerically advanced, the resulting distribution must be monotonic again. Therefore, if $\bar{q}_j^n$ lies between $\bar{q}_{j-1}^n$ and $\bar{q}_{j+1}^n$, then $\bar{q}_j^{n+1}$ must lie between $\bar{q}_{j-1}^{n+1}$ and $\bar{q}_{j+1}^{n+1}$. However, as it is expressed by van Leer [14], " in practise it is easier to deal with the following sufficient requirement: if $\bar{q}_j^n$ lies between $\bar{q}_{j-1}^n$ and $\bar{q}_{j+1}^n$, then $\bar{q}_j^{n+1}$ must lie between $\bar{q}_{j-1}^n$ and $\bar{q}_{j+1}^n$". It is clear that in order to preserve the monotonicity of a sequence of cell averages, the linear functions $q^n(x)$ given in (4.73) must not take values outside the range spanned by the neighbouring cell averages. That is, the onset of numerical oscillations in a monotonic sequence of cell averages are prevented by putting a limit to the slope of the distribution in each cell.

The slopes $\mathbf{\Gamma}_j^n$ are also determined by prediction-correction steps. In the prediction step we can use central differencing to define the predictor

$$\mathbf{\Gamma}_j^n = (\bar{\mathbf{Q}}_{j+1}^n - \bar{\mathbf{Q}}_{j-1}^n)/2 \,. \tag{4.109}$$

In the correction step we limit the slope componentwise in order to ensure that a monotone sequence of the cell averages can be produced. Therefore, we limit the slopes such that the linear distribution $q(x, t_n)$ $(x_{j-1/2} < x < x_{j+1/2})$ does not take values outside the range spanned by $\bar{q}_{j-1}^n$ and $\bar{q}_{j+1}^n$. Additionally, if the cell average is an extremum with respect to the neighboring cell averages, the slope must be set equal to zero. Finally, if the sign of the slope is not the same as the sign of the finite-difference slope that follows from the neighboring cell averages, the slope must be set equal to zero again. These three different rules of limiting also guarantee that q, if initially positive, remains positive. As a result of these observations, the slopes are given in the van Leer scheme as follows

$$\Gamma_j^n = \begin{cases} \min\,\{|a_j^n|, 2|b_{j-1/2}^n|, 2|c_{j+1/2}^n|\} \times \mathrm{sgn}(a_j^n)\,, & \\ & \text{if} \quad \mathrm{sgn}(a_j^n) = \mathrm{sgn}(b_{j-1/2}^n) = \mathrm{sgn}(c_{j+1/2}^n) \\ 0\,, & \text{otherwise} \end{cases} \tag{4.110}$$

where Γ_j^n represents any component of $\mathbf{\Gamma}_j^n$ and

$$2a_j^n = \bar{q}_{j+1}^n - \bar{q}_{j-1}^n \ , \qquad b_{j-1/2}^n = \bar{q}_j^n - \bar{q}_{j-1}^n \ , \qquad c_{j+1/2}^n = \bar{q}_{j+1}^n - \bar{q}_j^n \ . \tag{4.111}$$

This slope limiter is very popular in the literature and it has been used through many examples to show that the slope limiter is very important in practice. We now want to discuss how we can derive such a slope limiter. Note that equation (4.109) takes the following form $\Gamma_j^n = a_j^n$ for any component of $\mathbf{\Gamma}_j^n$. In other words, in the absence of any restriction the slopes are taken as a_j^n. If the sign of the slope is not the same as the sign of the slopes of the neighboring cells, then the slope must be set equal to zero. That is, we have $\Gamma_j^n = 0$ if the condition $\mathrm{sgn}(a_j^n) = \mathrm{sgn}(b_{j-1/2}^n) = \mathrm{sgn}(c_{j+1/2}^n)$ is not satisfied. We now consider the case where this condition is satisfied, that is, a_j^n, $b_{j-1/2}^n$ and $c_{j+1/2}^n$ have the same sign. Omitting the time superscript n we consider the following cases:

Case A: Suppose that $\bar{q}_{j-1} \leq \bar{q}_{j+1}$. Note that in the present case $-b_{j-1/2} \leq c_{j+1/2}$ and $a_j \geq 0$ which gives $b_{j-1/2} \geq 0$ and $c_{j+1/2} \geq 0$. The monotonicity condition requires that $\bar{q}_{j-1} \leq q(x, t_n) \leq \bar{q}_{j+1}$ for $x_{j-1/2} < x < x_{j+1/2}$. This restriction takes the following form

$$\bar{q}_{j-1} \leq \bar{q}_j + \frac{\Gamma_j}{\Delta x}(x - x_j) \leq \bar{q}_{j+1} \ , \qquad x_{j-1/2} < x < x_{j+1/2}$$

or

$$-b_{j-1/2} \leq \frac{\Gamma_j}{\Delta x}(x - x_j) \leq c_{j+1/2} \ , \qquad x_{j-1/2} < x < x_{j+1/2}$$

if (4.73) is used. The limits $x \to x_{j-1/2}+0$ and $x \to x_{j+1/2}-0$ give the conditions

$$-2c_{j+1/2} \leq \Gamma_j \leq 2b_{j-1/2} \qquad \text{and} \qquad -2b_{j-1/2} \leq \Gamma_j \leq 2c_{j+1/2} \ ,$$

respectively. Recalling that $b_{j-1/2} \geq 0$ and $c_{j+1/2} \geq 0$, we can rewrite these two conditions in the form

$$-2b_{j-1/2} \leq \Gamma_j \leq 2b_{j-1/2} \qquad \text{and} \qquad -2c_{j+1/2} \leq \Gamma_j \leq 2c_{j+1/2} \ , \tag{4.112}$$

If we choose Γ_j such that

$$\Gamma_j = \min\left\{a_j, 2b_{j-1/2}, 2c_{j+1/2}\right\} \ , \tag{4.113}$$

the above conditions are satisfied.

Case B: Suppose that $\bar{q}_{j+1} \leq \bar{q}_{j-1}$. Note that in the present case $c_{j+1/2} \leq -b_{j-1/2}$ and $a_j \leq 0$ which gives $b_{j-1/2} \leq 0$ and $c_{j+1/2} \leq 0$. The monotonicity condition requires that $\bar{q}_{j+1} \leq q(x, t_n) \leq \bar{q}_{j-1}$ for $x_{j-1/2} < x < x_{j+1/2}$. This restriction takes the following form

$$\bar{q}_{j+1} \leq \bar{q}_j + \frac{\Gamma_j}{\Delta x}(x - x_j) \leq \bar{q}_{j-1} \ , \qquad x_{j-1/2} < x < x_{j+1/2}$$

or

$$c_{j+1/2} \leq \frac{\Gamma_j}{\Delta x}(x - x_j) \leq -b_{j-1/2} \ , \qquad x_{j-1/2} < x < x_{j+1/2}$$

if (4.73) is used. The limits $x \to x_{j-1/2}+0$ and $x \to x_{j+1/2}-0$ give the conditions

$$2b_{j-1/2} \leq \Gamma_j \leq -2c_{j+1/2} \qquad \text{and} \qquad 2c_{j+1/2} \leq \Gamma_j \leq -2b_{j-1/2} \ ,$$

respectively. Recalling that $b_{j-1/2} \leq 0$ and $c_{j+1/2} \leq 0$, we can rewrite these two conditions in the form

$$2b_{j-1/2} \leq \Gamma_j \leq -2b_{j-1/2} \qquad \text{and} \qquad 2c_{j+1/2} \leq \Gamma_j \leq -2c_{j+1/2} \ . \tag{4.114}$$

If we choose Γ_j such that

$$\Gamma_j = \min\left\{-a_j, -2b_{j-1/2}, -2c_{j+1/2}\right\} \ , \tag{4.115}$$

the above conditions are satisfied. We now combine equations (4.113) and (4.115) as follows

$$\Gamma_j = \min\left\{|a_j|, 2|b_{j-1/2}|, 2|c_{j+1/2}|\right\} \times \operatorname{sgn}(a_j) \ . \tag{4.116}$$

In other words, when the condition $\operatorname{sgn}(a_j^n) = \operatorname{sgn}(b_{j-1/2}^n) = \operatorname{sgn}(c_{j+1/2}^n)$ is not satisfied, we choose Γ_j^n such that (4.116) is satisfied, As a result, in general we choose Γ_j^n such that equation (4.110) is satisfied.

4.6 A Numerical Experiment

In this section, as an example of how the numerical technique introduced above can be applied to nonlinear scalar inhomogeneous equations we consider the inhomogeneous Burgers equation. The inhomogeneous Burgers equation has the advantage of being relatively simple equation where the results can be obtained analytically. Furthermore the results can be easily explained and interpreted physically. We first discuss the solution of the Cauchy problem associated with the inhomogeneous Burgers equation:

$$\begin{cases} q_t + qq_x = \alpha q \ , & x \in \mathbb{R} \ , \qquad t > 0 \\ q(x,0) = q_0(x) \end{cases} \tag{4.117}$$

where $\alpha > 0$ and $q_0(x)$ is a continuous differentiable function of x. In this case it follows from (4.18) that a characteristic curve passing through the point $(x_0, 0)$ is obtained as a solution of the differential system

$$\frac{dx}{dt} = q(x(t), t), \qquad x(0) = x_0 \ . \tag{4.118}$$

Along such a curve, we have

$$\frac{dq}{dt} = \alpha q \ . \tag{4.119}$$

Then the solution of the Cauchy problem (4.117) is

$$q(x,t) = q(x_0(x,t), t) = q_0(x_0(x,t))e^{\alpha t} \ , \tag{4.120}$$

and the characteristic curve passing through the point $(x_0, 0)$ is given by

$$x = x_0 + \frac{q_0(x_0)}{\alpha}(e^{\alpha t} - 1) \ . \tag{4.121}$$

Note that for each (x,t) we solve (4.121) for x_0 and substitute the result into (4.120). Also note that the slopes of the lines tangent to the characteristic curves are equal to $1/q$.

We now discuss the solution of the Riemann problem associated with the inhomogeneous Burgers equation:

$$\begin{cases} q_t + qq_x = \alpha q \ , & x \in \mathbb{R} \ , \qquad t > 0 \\ q(x,0) = \begin{cases} q_L & x < x_m \\ q_R & x > x_m \end{cases} \end{cases} \tag{4.122}$$

where the initial jump is positioned at $x = x_m$. This Riemann problem was proposed by Chalabi [17]. It follows from (4.121) that the characteristic curve passing through the point $(x_0, 0)$ is given by

$$x(x_0,t) = \begin{cases} x_0 + \frac{q_L}{\alpha}(e^{\alpha t} - 1) \,, & x_0 < x_m \\ x_0 + \frac{q_R}{\alpha}(e^{\alpha t} - 1) \,, & x_0 > x_m \,. \end{cases} \tag{4.123}$$

Then we have

$$x_0 = \begin{cases} x - \frac{q_L}{\alpha}(e^{\alpha t} - 1) \,, & x < x_m + \frac{q_L}{\alpha}(e^{\alpha t} - 1) \\ x - \frac{q_R}{\alpha}(e^{\alpha t} - 1) \,, & x > x_m + \frac{q_R}{\alpha}(e^{\alpha t} - 1) \,, \end{cases} \tag{4.124}$$

and

$$q(x,t) = \begin{cases} q_L e^{\alpha t} \,, & x < x_m + \frac{q_L}{\alpha}(e^{\alpha t} - 1) \\ q_R e^{\alpha t} \,, & x > x_m + \frac{q_R}{\alpha}(e^{\alpha t} - 1) \,. \end{cases} \tag{4.125}$$

It is obvious that the characteristic curves do not intersect if $q_L \leq q_R$. That is, the solution of the Riemann problem is a rarefaction wave if $q_L < q_R$. Note that, if $q_L < q_R$, (4.125) does not include the solution corresponding to the interval $x_m + \frac{q_L}{\alpha}(e^{\alpha t} - 1) < x < x_m + \frac{q_R}{\alpha}(e^{\alpha t} - 1)$. On the other hand, the solution of the Riemann problem is a shock wave if $q_L > q_R$. Note that, if $q_L > q_R$, the solution given in (4.125) must be modified such that multivalued solutions are avoided. Furthermore, we emphasize that the value of the solution increases exponentially in time due to the source term and that the left and right values of the solution are modified depending on the value of α. The propagation speed s of the shock was calculated by Chalabi [17] from the Rankine-Hugoniot jump condition (4.31) in the form

$$s = (q_L + q_R)e^{\alpha t}/2 \,, \tag{4.126}$$

which shows that the propagation speed of the shock depends on the value of α. For the homogeneous Burgers equation where $\alpha = 0$ the propagation speed of the shock reduces to that given in (4.55). Furthermore the shock speed satisfies the entropy condition (4.47) since $c_1(q) = q$ for the present problem.

We now test the numerical method on the Riemann problem (4.122). The initial data are taken as

$$q_L = 3 \,, \qquad q_R = 0.5, \qquad x_m = 0.15 \,. \tag{4.127}$$

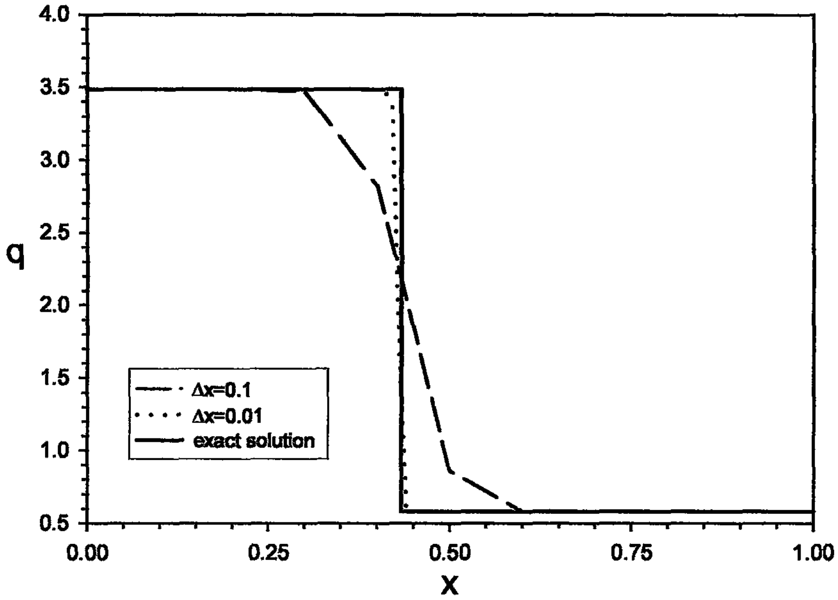

Figure 4.4: At time $t = 0.15$, the exact and numerical solutions of the Riemann problem for the inhomogeneous Burgers equation. The numerical solutions are obtained using the second-order Godunov method.

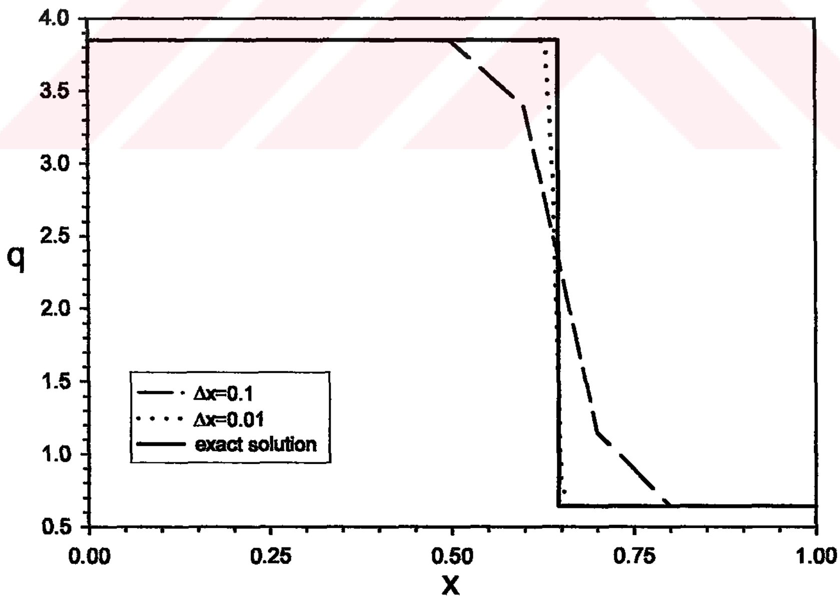

Figure 4.5: At time $t = 0.25$, the exact and numerical solutions of the Riemann problem for the inhomogeneous Burgers equation. The numerical solutions are obtained using the second-order Godunov method.

The computational domain is [0, 1] which is subdivided into cells with $x_1 = \Delta x/2$ and $x_M = 1 - \Delta x/2$ so that $\Delta x = 1/M$. The solution is computed up to $T = 0.25$ for $\alpha = 1$. We apply the second-order Godunov method discussed above to the Riemann problem. Recall that in Section 4.5 three different ways are used to update the state variables at the cell boundaries and that these three approaches used to obtain the approximations at the midpoint in time are called as Case A, Case B and Case C. We first use the numerical scheme corresponding to Case C and compare the numerical results obtained for two different grids: a coarse one and a finer one. In the first case we apply the numerical scheme with $M = 10$ and $N = 25$ which corresponds to $\Delta x = 0.1$ and $\Delta t = 0.01$, respectively. In the second case we apply the numerical scheme with $M = 100$ and $N = 250$ which corresponds to $\Delta x = 0.01$ and $\Delta t = 0.001$, respectively. Note that in both cases the CFL condition given in (4.68) is satisfied. Figure 4.4. shows the numerical solutions corresponding to these two cases at time $t = 0.15$. Figure also shows the exact solution for comparison purposes. Similarly, Figure 4.5 shows the numerical and exact solutions at time $t = 0.25$. As it is expected, the numerical results obtained using the finer grid are more accurate than those obtained using the coarser grid. We observe that the shock positions estimated by the numerical scheme are correct. Furthermore, the second-order numerical method achieves almost the same sharp resolution as the exact solution if the number of the grid points is sufficiently high. We also point out that the numerical method does not give an overshoot at the shock. This is due to the van Leer slope limiter we used. In conclusion, the numerical solution obtained using the second-order Godunov method converges to the exact solution as the grid is refined.

We now compare the accuracy of the second-order Godunov method with the accuracy of the corresponding first-order Godunov method for $M = 10$ and $N = 25$. Figures 4.6 and 4.7 show the numerical results corresponding to these two different methods at time $t = 0.15$ and $t = 0.25$, respectively. The results presented in Figures 4.6 and 4.7 show that the first-order Godunov method smears the shock more than the corresponding second-order method and that

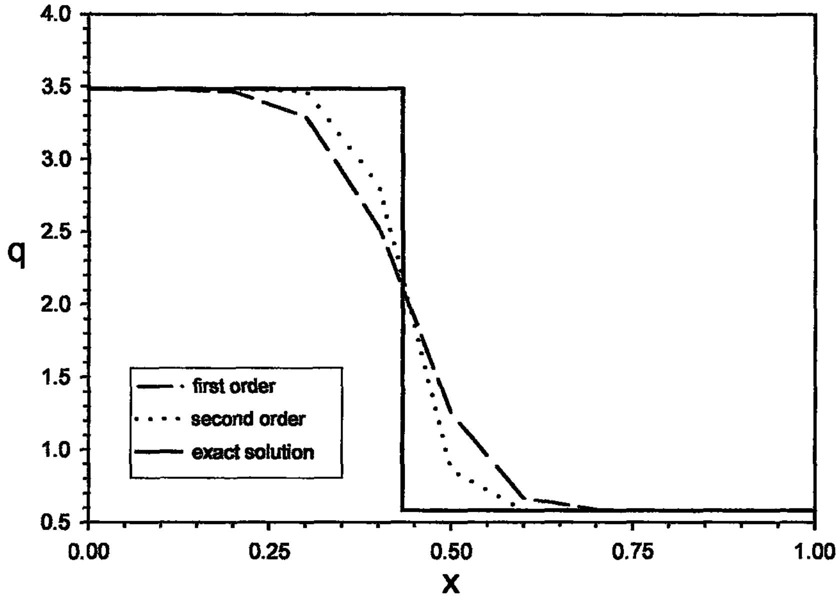

Figure 4.6: At time $t = 0.15$, the exact and numerical solutions of the Riemann problem for the inhomogeneous Burgers equation. The numerical solutions are obtained using the first-order and second-order Godunov methods.

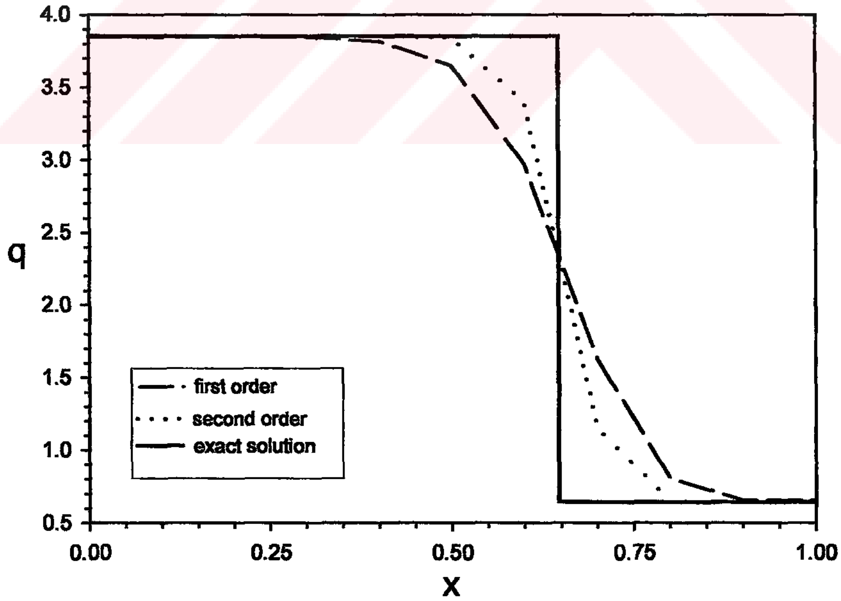

Figure 4.7: At time $t = 0.25$, the exact and numerical solutions of the Riemann problem for the inhomogeneous Burgers equation. The numerical solutions are obtained using the first-order and second-order Godunov methods.

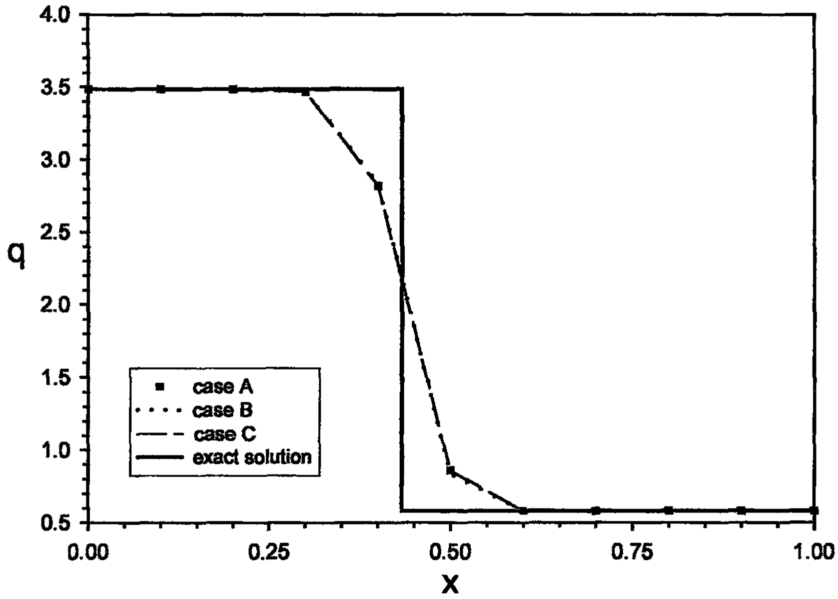

Figure 4.8: At time $t = 0.15$, the exact and numerical solutions of the Riemann problem for the inhomogeneous Burgers equation. The numerical solutions are obtained using the second-order Godunov method. The state variables at the cell boundaries are calculated using three different approaches: Case A, Case B and Case C

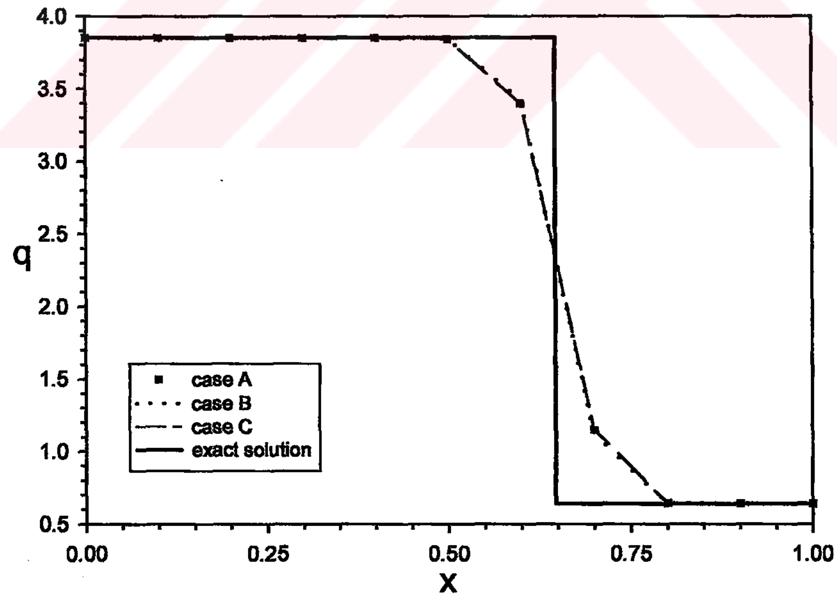

Figure 4.9: At time $t = 0.25$, the exact and numerical solutions of the Riemann problem for the inhomogeneous Burgers equation. The numerical solutions are obtained using the second-order Godunov method. The state variables at the cell boundaries are calculated using three different approaches: Case A, Case B and Case C

the second- order method seems to work well in identifying the shock.

We now compare the accuracy of the numerical scheme corresponding to Case C with the accuracy of the numerical schemes corresponding to Case A and Case B for $M = 10$ and $N = 25$. Figures 4.8 and 4.9 show the numerical results corresponding to these three different cases at time $t = 0.15$ and $t = 0.25$, respectively. The numerical solutions are obtained using the second-order Godunov method. The numerical schemes corresponding to Case A, Case B and Case C produce rather similar results for the present problem. We point out that the numerical scheme corresponding to Case C will be used in the next chapter.

5. WAVE PROPAGATION IN A NON-LINEAR HYPERELASTIC TUBE

5.1 Introduction

In this chapter we study wave propagation in a circular cylindrical nonlinear elastic tube when the tube was subjected to dynamic extension. One end of the tube was fixed and the other end was subjected to a dynamic extension. The tube was considered as a hyperelastic, isotropic, homegeneous, incompressible membrane. Numerical results were given for Mooney-Rivlin and neo-Hookean materials. The same problem has been studied by Tait and Zhong [5]. They have considered a numerical technique based on the method of characteristics. The present discussion of the problem is set in a framework which differs in two aspects from that studied by Tait and Zhong [5]. First we derive the governing equations using an alternative, but equivalent, approach to that used in [5]. In particular we use the membrane theory derived in Chapter 1 of the present thesis by using an asymptotic expansion technique, whereas they formulate membrane theory following the direct approach of Green, Naghdi and Wainwright [18] and regard the mebrane as an elastic surface in three dimensional space. The equivalence of the membrane theories, obtained by using the direct theory and by using an asymptotic expansion technique is not the subject of the present study. For a discussion about the equivalence of these membrane theories we refer to [2]. Second, for the numerical solution of the governing equations we employ the second-order Godunov method which was introduced in the previous chapter. In another study [6] Tait and Zhong also considered the same tube and, in addition to the extension, imposed a dynamical twist at the moving end.

In Section 5.2 we formulate the problem of dynamic extension of a membrane tube made of an incompressible hyperelastic material. In Section 5.3 we present the numerical results obtained by using the numerical method of the previous chapter for membrane tubes made of an incompressible hyperelastic material. In particular we present the numerical results corresponding to the neo-Hookean and Mooney-Rivlin materials. We also discuss how the results of Tait and Zhong [5] are related to those obtained in Section 5.3. In Section 5.4 we present the numerical results for membrane tubes made of a compressible hyperelastic material. In particular we present the numerical results corresponding to the Blatz-Ko and neo-Hookean compressible materials.

5.2 Governing Equations for the Loading Problem

We consider a circular cylindrical membrane of homogeneous incompressible isotropic nonlinearly elastic material. In its (undeformed, stress free) natural configuration the membrane tube is defined by

$$R_i \leq R \leq R_i + H, \qquad 0 \leq \Theta < 2\pi, \qquad 0 \leq Z \leq L \tag{5.1}$$

where (R, Θ, Z) are cylindrical polar coordinates with corresponding unit vectors $\mathbf{E}_R, \mathbf{E}_\Theta, \mathbf{E}_Z$. That is, R_i is the inner radius, H is the thickness and L is the length of the membrane before deformation. We suppose that the ends of the tube in the natural configuration are attached to rigid rings or discs of radius R_i. We also suppose that the end of the tube at $Z = L$ is kept fixed and the end originally at $Z = 0$ is displaced in the negative direction.

The axially symmetric deformation of the membrane at time t is defined by

$$r = r(Z,t), \qquad \theta = \Theta, \qquad z = z(Z,t) \tag{5.2}$$

where (r, θ, z) are cylindrical polar coordinates associated with the deformed configuration. Here we use the membrane theory developed in Chapter 3 for the case of axisymmetric deformations. We introduce nondimensional quantities by setting

$$\bar{t} = t(\frac{\mu}{\rho_0})^{1/2}/R_i, \qquad \bar{Z} = Z/R_i, \qquad f = z/R_i, \qquad g = r/R_i,$$

$$\bar{W} = W/\mu, \qquad \bar{T}_1 = T_1/\mu, \qquad \bar{T}_2 = T_2/\mu, \qquad \bar{L} = L/R_i \tag{5.3}$$

where ρ_0 is the density, μ is a constant with appropriate dimension to be defined later, W is the strain energy function and T_1 and T_2 are the principal Biot stresses. As in Chapter 3 we drop the bars. Following Chapter 3 we now write the governing equations of the membrane tube as follows. We drop the superscript 0 which is used to denote the zeroth-order quantities. It follows from (3.43) and (3.71) that the principal stretches $\lambda_1(Z,t)$ and $\lambda_2(Z,t)$ are given by

$$\lambda_1 = [(f')^2 + (g')^2]^{1/2}, \qquad \lambda_2 = g \tag{5.4}$$

where prime denotes differentiation with respect to the dimensionless axial coordinate Z. Also we have

$$g' = \lambda_1 \cos\beta, \qquad f' = \lambda_1 \sin\beta \tag{5.5}$$

where β denotes the angle measured from the outward radius vector to the tangent to deformed profile, taken in the positive sense. It follows from (3.97) that the Biot principle stresses T_1 and T_2 are given by

$$T_1 = \left.\frac{\partial W}{\partial \Lambda_1}\right|_{\Lambda_k=\lambda_k}, \qquad T_2 = \left.\frac{\partial W}{\partial \Lambda_2}\right|_{\Lambda_k=\lambda_k} \qquad k = 1,2,3 \tag{5.6}$$

where $W = W(\Lambda_1, \Lambda_2)$. In the absence of the normal and tangential surface tractions (that is, $P_n = P_t \equiv 0$), the equations of motion given in (3.88) and (3.89) take the following form

$$\frac{\partial}{\partial Z}(T_1 \cos\beta) - T_2 = \frac{\partial^2 g}{\partial t^2}, \tag{5.7}$$

$$\frac{\partial}{\partial Z}(T_1 \sin\beta) = \frac{\partial^2 f}{\partial t^2}. \tag{5.8}$$

If we set

$$u = \frac{\partial g}{\partial t}, \qquad v = \frac{\partial f}{\partial t} \tag{5.9}$$

we can write the following compatibility equations

$$\frac{\partial(\lambda_1 \cos\beta)}{\partial t} = \frac{\partial u}{\partial Z}, \qquad \frac{\partial(\lambda_1 \sin\beta)}{\partial t} = \frac{\partial v}{\partial Z}, \qquad \frac{\partial \lambda_2}{\partial t} = u\,. \tag{5.10}$$

If these compatibility equations are combined with the equations of motion given by (5.7) and (5.8), the governing equations may be rewritten in the vector form

$$\frac{\partial \mathbf{Q}}{\partial t} + \frac{\partial \mathbf{H}(\mathbf{Q})}{\partial Z} + \mathbf{B}(\mathbf{Q}) = \mathbf{0}, \tag{5.11}$$

where

$$\begin{aligned}
\mathbf{Q} &= \{\lambda_1 \cos\beta, \lambda_1 \sin\beta, \lambda_2, u, v\}^{\mathrm{T}}, \\
\mathbf{H} &= -\{u, v, 0, T_1\cos\beta, T_1\sin\beta\}^{\mathrm{T}}, \\
\mathbf{B} &= -\{0, 0, u, -T_2, 0\}^{\mathrm{T}} .
\end{aligned} \tag{5.12}$$

Here the superposed T denotes the transpose. The above system can be written in the form

$$\frac{\partial \mathbf{Q}}{\partial t} + \mathbf{A}(\mathbf{Q})\frac{\partial \mathbf{Q}}{\partial Z} + \mathbf{B} = \mathbf{0}, \tag{5.13}$$

where

$$\mathbf{A}(\mathbf{Q}) = \partial \mathbf{H}(\mathbf{Q})/\partial \mathbf{Q} \tag{5.14}$$

is the 5×5 Jacobian matrix with the non-zero entries given by

$$\begin{aligned}
&A_{14} = -1, \qquad A_{25} = -1, \qquad A_{41} = -\frac{\partial T_1}{\partial \lambda_1}\cos^2\beta - \frac{T_1}{\lambda_1}\sin^2\beta, \\
&A_{42} = A_{51} = -\left(\frac{T_1}{\lambda_1} - \frac{\partial T_1}{\partial \lambda_1}\right)\sin\beta\cos\beta, \qquad A_{43} = -\frac{\partial T_1}{\partial \lambda_2}\cos\beta, \\
&A_{52} = -\frac{\partial T_1}{\partial \lambda_1}\sin^2\beta - \frac{T_1}{\lambda_1}\cos^2\beta, \qquad A_{53} = -\frac{\partial T_1}{\partial \lambda_2}\sin\beta .
\end{aligned} \tag{5.15}$$

The eigenvalues of $\mathbf{A}$ are

$$\Delta_0 = 0, \qquad \Delta_{\pm 1} = \pm C_L, \qquad \Delta_{\pm 2} = \pm C_T, \tag{5.16}$$

where the wave speeds C_L and C_T are given by

$$C_L^2 = \frac{\partial T_1}{\partial \lambda_1}, \qquad C_T^2 = \frac{T_1}{\lambda_1} . \tag{5.17}$$

We require that the wave speeds are real. The corresponding left eigenvectors can be given as

$$\begin{aligned}
\mathbf{L}_0 &= (0, 0, 1, 0, 0), \\
\mathbf{L}_{\pm 1} &= (C_L\cos\beta, C_L\sin\beta, C_L^{-1}\frac{\partial T_1}{\partial \lambda_2}), \\
\mathbf{L}_{\pm 2} &= (C_T\sin\beta, -C_T\cos\beta, 0, \mp\sin\beta, \pm\cos\beta) .
\end{aligned} \tag{5.18}$$

The boundary and initial conditions for the problem can be given as follows. Since the initial configuration is the reference configuration

$$g(Z,0)=1\ , \qquad f(Z,0)=Z\ , \tag{5.19}$$

one can write the initial conditions in the form

$$\lambda_1(Z,0)=\lambda_2(Z,0)=1\ , \qquad \beta(Z,0)=\pi/2\ , \qquad u(Z,0)=v(Z,0)=0\ , \tag{5.20}$$

for $0 \le Z \le L$. The boundary conditions for the present problem are

$$\begin{gathered}\lambda_2(0,t)=1, \qquad u(0,t)=0, \qquad v(0,t)=-v_0, \qquad t>0 \\ \lambda_1(L,t)=\lambda_2(L,t)=1,\ \ \beta(L,t)=\pi/2,\ \ u(L,t)=0,\ \ v(L,t)=0,\ \ t>0\ .\end{gathered} \tag{5.21}$$

Here we assume that the waves do not arrive in the end $Z=L$ over the time interval considered.

Up to this point the strain energy function W has remained arbitrary. It is not clear whether the wave speeds are real. In order to obtain precise results we consider a Mooney-Rivlin strain energy function. It follows from (2.48) that the nondimensional form of the Mooney-Rivlin strain energy function is

$$W(\Lambda_1,\Lambda_2)=\frac{1}{2}[\gamma(\Lambda_1^2+\Lambda_2^2+\Lambda_1^{-2}\Lambda_2^{-2}-3)+(1-\gamma)(\Lambda_1^{-2}+\Lambda_2^{-2}+\Lambda_1^2\Lambda_2^2-3)] \tag{5.22}$$

where $0<\gamma\le 1$. Now the constant μ used above represents the shear modulus for infinitesimal deformation from the undeformed state. Recall that (5.22) reduces to the strain energy function of the neo-Hookean material for $\gamma=1$. Using equations (5.6), the Biot principal stresses, T_1 and T_2, are given by

$$T_1=[\gamma+(1-\gamma)\lambda_2^2](\lambda_1-\lambda_1^{-3}\lambda_2^{-2}) \tag{5.23}$$

$$T_2=[\gamma+(1-\gamma)\lambda_1^2](\lambda_2-\lambda_1^{-2}\lambda_2^{-3})\ . \tag{5.24}$$

It follows from (5.17) that

$$C_L^2=[\gamma+(1-\gamma)\lambda_2^2](1+3\lambda_1^{-4}\lambda_2^{-2}) \tag{5.25}$$

$$C_T^2=[\gamma+(1-\gamma)\lambda_2^2](1-\lambda_1^{-4}\lambda_2^{-2})\ . \tag{5.26}$$

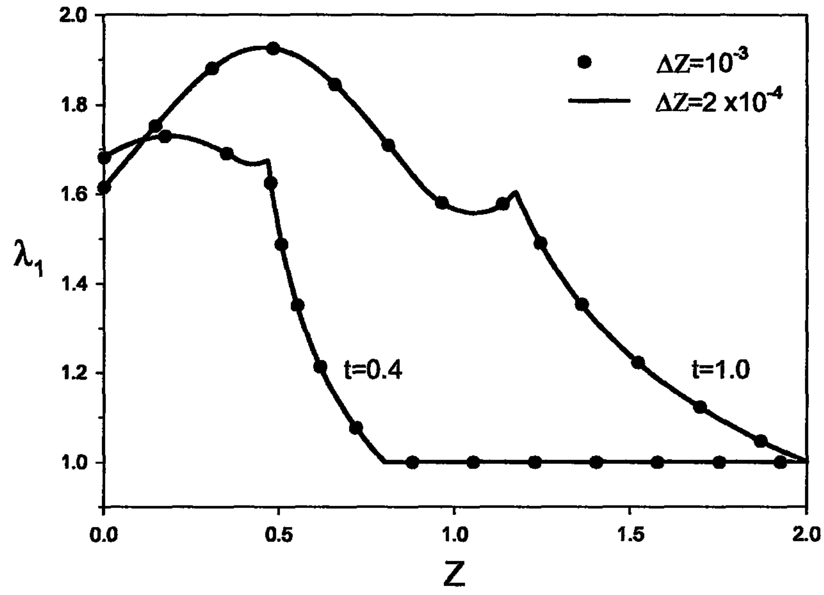

Figure 5.1: λ_1 as a function of Z at $t = 0.4$ and $t = 1$. The solid curve represents the numerical solution obtained for the fine grid ($\Delta Z = 2 \times 10^{-4}$, $\Delta t = 0.5 \times 10^{-4}$). The dotted curve represents the numerical solution obtained for the coarse grid ($\Delta Z = 10^{-3}$, $\Delta t = 0.25 \times 10^{-3}$). $L = 2$, $v_0 = 1$, $\gamma = 0.25$.

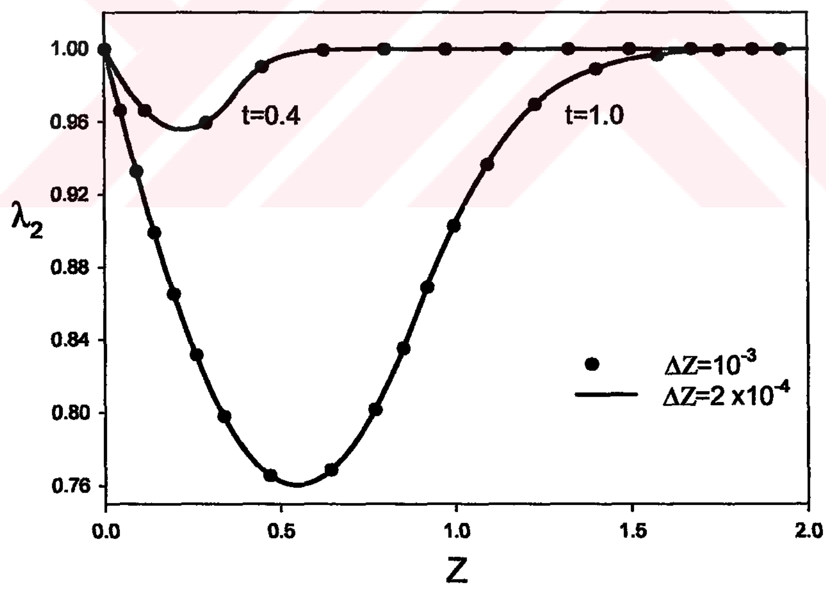

Figure 5.2: λ_2 as a function of Z at $t = 0.4$ and $t = 1$. The solid curve represents the numerical solution obtained for the fine grid ($\Delta Z = 2 \times 10^{-4}$, $\Delta t = 0.5 \times 10^{-4}$). The dotted curve represents the numerical solution obtained for the coarse grid ($\Delta Z = 10^{-3}$, $\Delta t = 0.25 \times 10^{-3}$). $L = 2$, $v_0 = 1$, $\gamma = 0.25$.

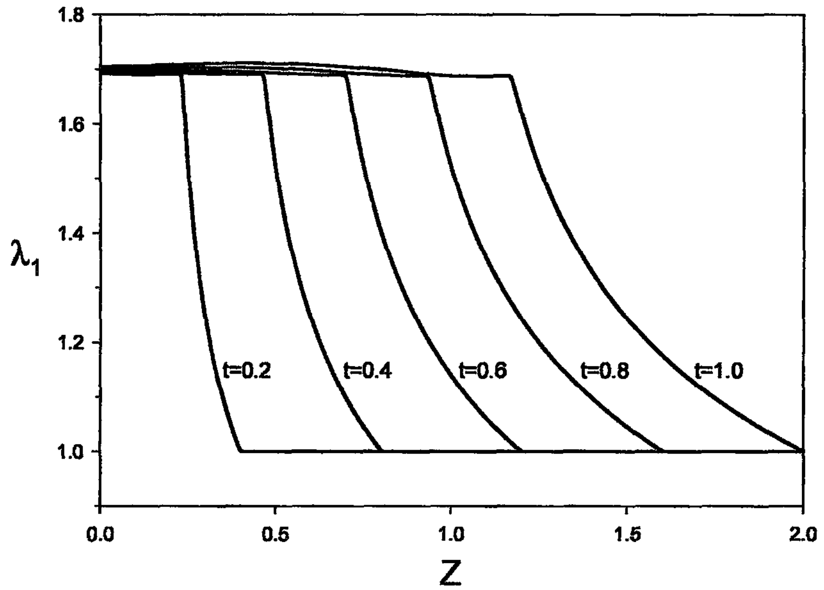

Figure 5.3: λ_1 as a function of Z at various times. $\Delta Z = 10^{-3}$, $\Delta t = 0.25 \times 10^{-3}$, $L = 2$, $v_0 = 1$, $\gamma = 1$.

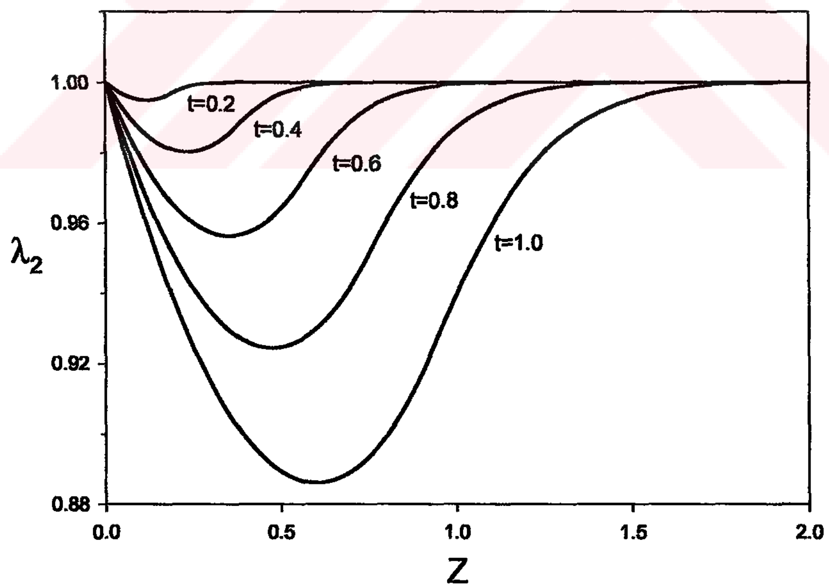

Figure 5.4: λ_2 as a function of Z at various times. $\Delta Z = 10^{-3}$, $\Delta t = 0.25 \times 10^{-3}$, $L = 2$, $v_0 = 1$, $\gamma = 1$.

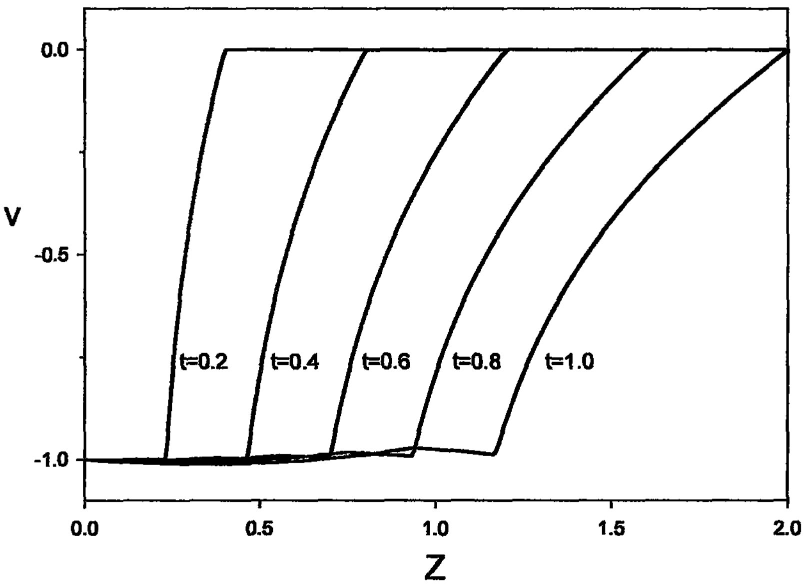

Figure 5.5: v as a function of Z at various times. $\Delta Z = 10^{-3}$, $\Delta t = 0.25 \times 10^{-3}$, $L = 2$, $v_0 = 1$, $\gamma = 1$.

It is obvious from (5.25) that $C_L^2 > 0$. Also it follows from (5.26) that $C_T^2 > 0$ provided

$$\lambda_1^2 \lambda_2 > 1 \ . \tag{5.27}$$

There exist four waves propagating in the tube and two of them propagate in the positive direction along the tube whereas the remaining two propagate in the negative direction. Since

$$C_L^2 - C_T^2 = 4[\gamma + (1-\gamma)\lambda_2^2)]\lambda_1^{-4}\lambda_2^{-4} > 0 \tag{5.28}$$

we have $C_L^2 > C_T^2 > 0$ whenever $\lambda_1^2\lambda_2 > 1$. Therefore the eigenvalues of **A** are all real and distinct whenever $\lambda_1^2\lambda_2 > 1$. That is, the system (5.11) is strictly hyperbolic and there is no degeneracy.

5.3 Numerical Results: The Incompressible Problem

We use the second-order Godunov method discussed in Chapter 4 for the solution of the impact problem described in the previous section. To update the state

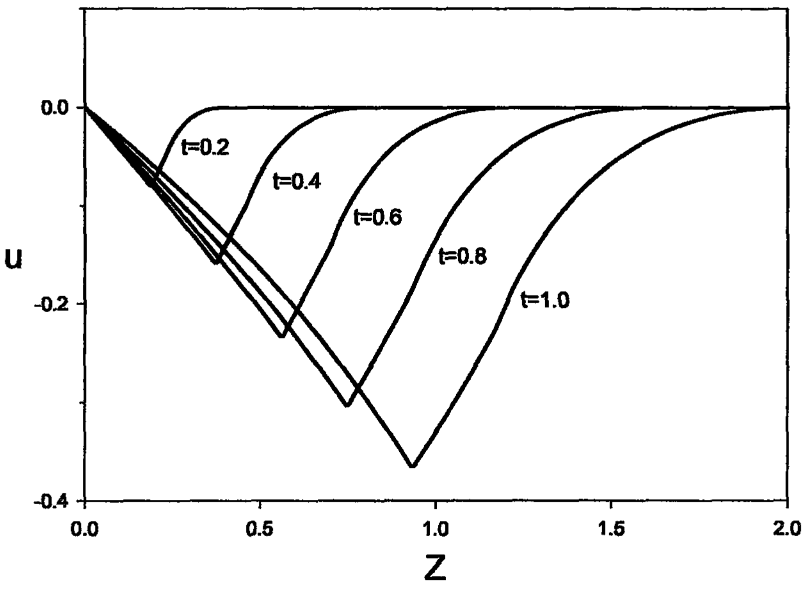

Figure 5.6: u as a function of Z at various times. $\Delta Z = 10^{-3}$, $\Delta t = 0.25 \times 10^{-3}$, $L = 2$, $v_0 = 1$, $\gamma = 1$.

variables at the cell boundaries we use the approximations corresponding to Case C for the values of the state variables at the midpoint in time. The computational domain is subdivided into cells with

$$Z_1 = \frac{1}{2}\Delta Z\,,\ \ldots\,, Z_K = (K - \frac{1}{2})\Delta Z\,,\ \ldots\ , Z_M = L - \frac{1}{2}\Delta Z\,, \tag{5.29}$$

so that $\Delta Z = L/M$. That is, the ends of the tube originally at $Z = 0$ and $Z = L$ correspond to the cell interfaces at $Z = Z_{1/2}$ and $Z = Z_{M+1/2}$, respectively.

In all the numerical experiments considered in this section we apply the numerical scheme for the parameter values given by

$$L = 2\,, \qquad v_0 = 1\,. \tag{5.30}$$

The solution is computed up to time $t = 1$. We first compare the numerical results obtained for two different grids: a coarse one and a finer one. In these experiments we consider a tube made of the Mooney-Rivlin material where $\gamma = 0.25$ is used. In the first case we apply the numerical scheme with $M = 2000$ and $N = 4000$ which correspond to $\Delta Z = 10^{-3}$ and $\Delta t = 0.25 \times 10^{-3}$,

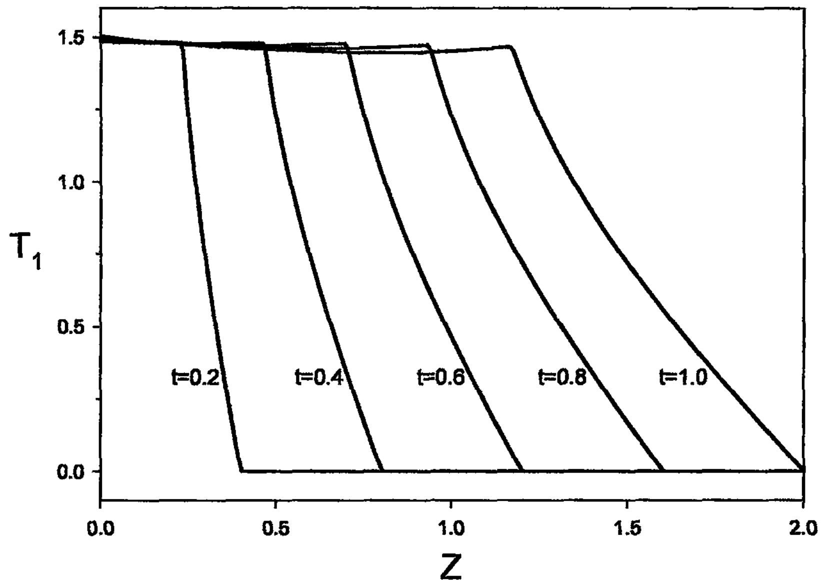

Figure 5.7: T_1 as a function of Z at various times. $\Delta Z = 10^{-3}$, $\Delta t = 0.25 \times 10^{-3}$, $L = 2$, $v_0 = 1$, $\gamma = 1$.

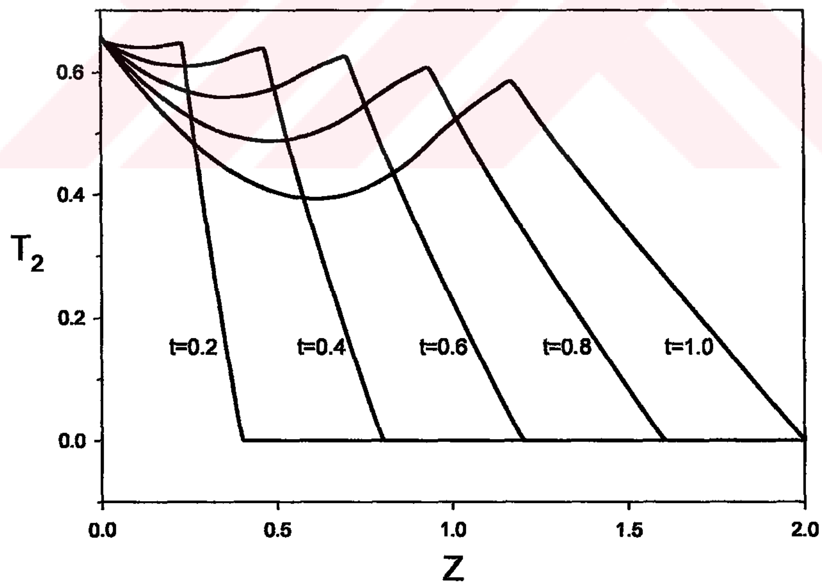

Figure 5.8: T_2 as a function of Z at various times. $\Delta Z = 10^{-3}$, $\Delta t = 0.25 \times 10^{-3}$, $L = 2$, $v_0 = 1$, $\gamma = 1$.

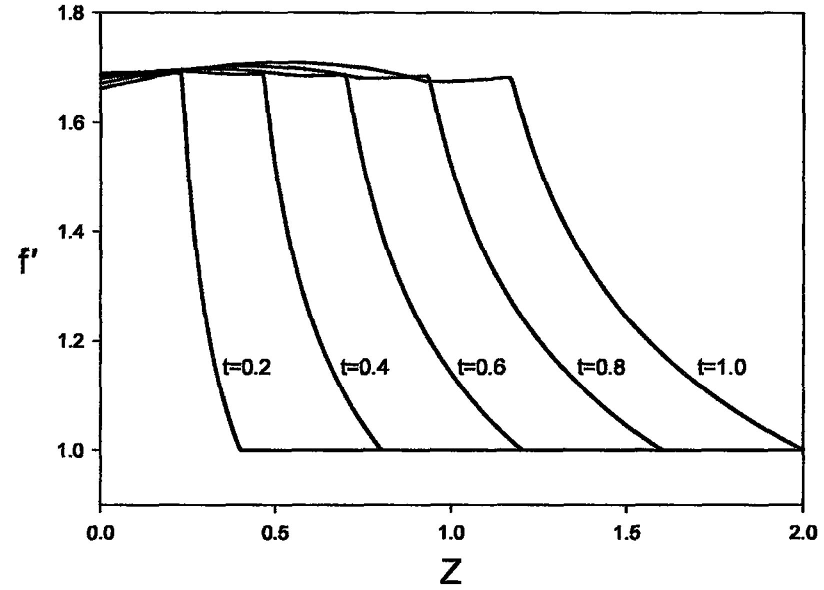

Figure 5.9: f' as a function of Z at various times. $\Delta Z = 10^{-3}$, $\Delta t = 0.25 \times 10^{-3}$, $L = 2$, $v_0 = 1$, $\gamma = 1$.

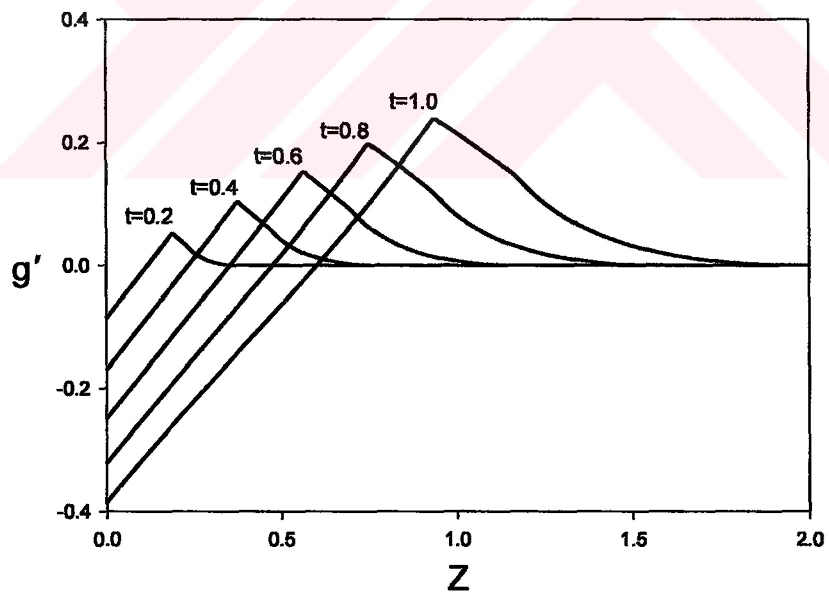

Figure 5.10: f' as a function of Z at various times. $\Delta Z = 10^{-3}$, $\Delta t = 0.25 \times 10^{-3}$, $L = 2$, $v_0 = 1$, $\gamma = 1$.

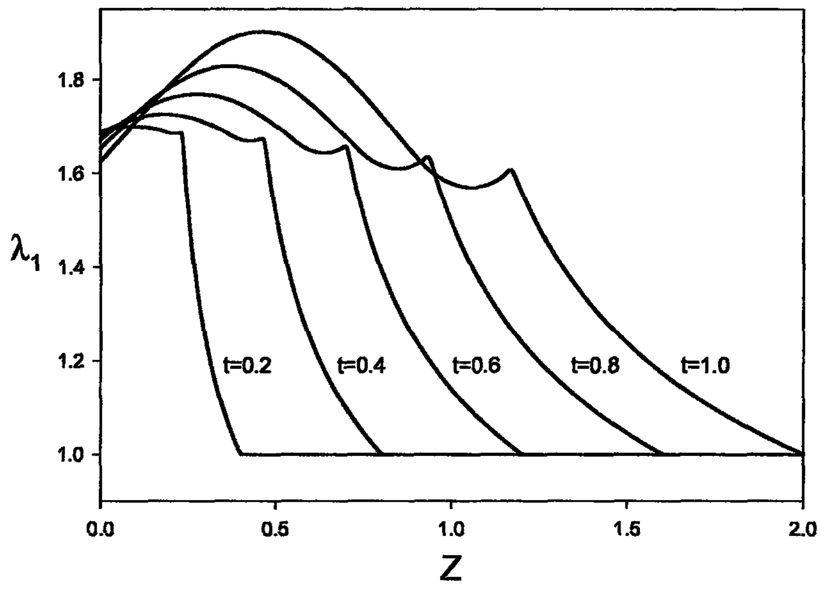

Figure 5.11: λ_1 as a function of Z at various times. $\Delta Z = 10^{-3}$, $\Delta t = 0.25 \times 10^{-3}$, $L = 2$, $v_0 = 1$, $\gamma = 0.3$.

respectively. In the second case we apply the numerical scheme with $M = 10000$ and $N = 20000$ which correspond to $\Delta Z = 10^{-4}$ and $\Delta t = 0.5 \times 10^{-4}$, respectively. Since, in the present problem, $(C_L)_{max} \leq 2$, in both cases the CFL condition given by (4.68) is satisfied. Figures 5.1 and 5.2 show the numerical results corresponding to these two cases.

In Fig. 5.1 we show the behaviour of the stretch λ_1 as a function of Z at $t = 0.4$ and $t = 1.0$. In Fig. 5.2 we show the behaviour of the stretch λ_2 as a function of Z at $t = 0.4$ and $t = 1.0$. We observe from these two figures that the numerical results obtained using the finer grid are not distinguishable from those obtained using the coarser grid. Therefore we present the numerical results obtained using the coarser grid in the remaining part of this section.

We first represent the numerical results corresponding to a tube made of the neo-Hookean material in which $\gamma = 1$. Figures 5.3 - 5.10 show the values of λ_1, λ_2, v, u, T_1, T_2, f' and g' as a function of Z at various times. Recall that we take the undeformed configuration as the initial configuration. Therefore

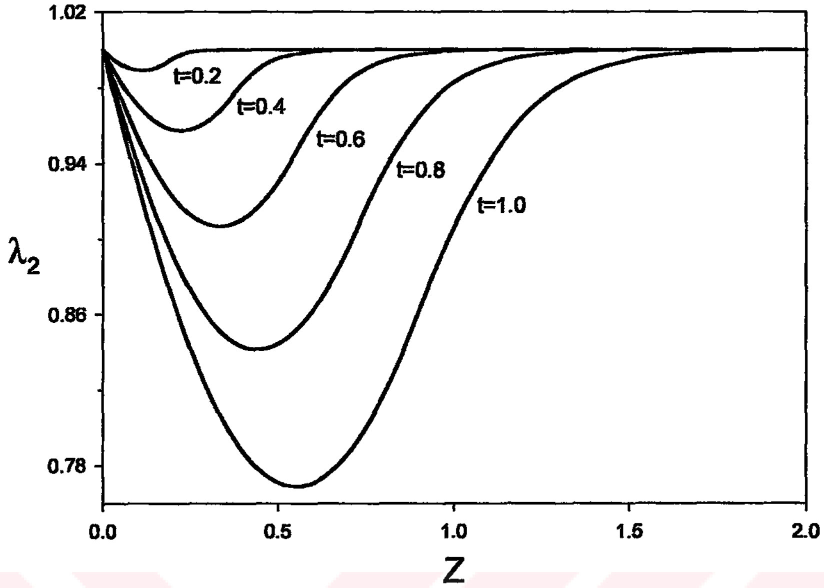

Figure 5.12: λ_2 as a function of Z at various times. $\Delta Z = 10^{-3}$, $\Delta t = 0.25 \times 10^{-3}$, $L = 2$, $v_0 = 1$, $\gamma = 0.3$.

the membrane is undisturbed ahead of the fastest wave. We observe that the fastest wave is a pure stretching expansion wave, that is, a f' (or v) wave. The leading edge of the f' wave travels at speed $C_L|_{\lambda_1=\lambda_2=1} = 2$. Behind the wavefront associated with the f' wave, interaction takes place and a g' (or u) wave propagates. We also observe from Figures 5.3 - 5.10 that there are jumps in $\frac{\partial \lambda_1}{\partial Z}$, $\frac{\partial v}{\partial Z}$, $\frac{\partial u}{\partial Z}$, $\frac{\partial T_1}{\partial Z}$, $\frac{\partial T_2}{\partial Z}$, $\frac{\partial f'}{\partial Z}$ and $\frac{\partial g'}{\partial Z}$ but no jump in $\frac{\partial \lambda_2}{\partial Z}$. There is an effect due to these discontinuities. The f' (or v) wave exhibits a perturbation as it passes through the $\frac{\partial g'}{\partial Z}$ (or $\frac{\partial u}{\partial Z}$) discontinuity. Similarly, the g' (or u) wave exhibits a perturbation as it passes through the $\frac{\partial f'}{\partial Z}$ (or $\frac{\partial v}{\partial Z}$) discontinuity. It may be difficult to distinguish these perturbations from the figures for the neo-Hookean material. However these perturbations become stronger for the Mooney-Rivlin material considered below and they become more visible.

Tait and Zhong [19] observed similar perturbations for the impact problem

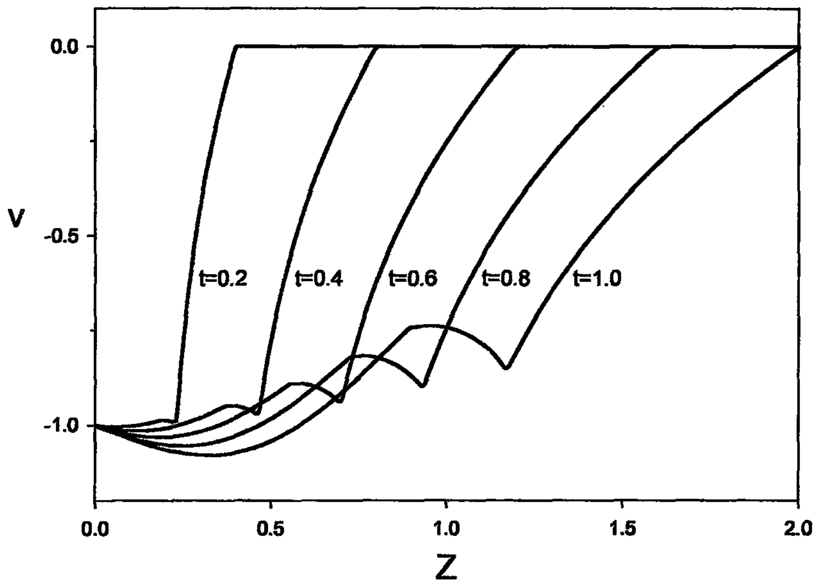

Figure 5.13: v as a function of Z at various times. $\Delta Z = 10^{-3}$, $\Delta t = 0.25 \times 10^{-3}$, $L = 2$, $v_0 = 1$, $\gamma = 0.3$.

of a nonlinear elastic string, where they used a first-order Godunov method. They pointed out that " the refinement of the numerical technique would be of interest". It is surprising that the present second-order Godunov method also provides a similar physical picture.

We now present the numerical results corresponding to a tube made of the Mooney-Rivlin material in which $\gamma = 0.3$. Figures 5.11 - 5.19 show the values of λ_1, λ_2, v, u, T_1, T_2, f', g' and β as a function of Z at various times. The only qualitative differences between the results for the neo-Hookean material and the Mooney-rivlin material are evident for λ_1, v, T_1, and f' behind the edge of the expansion wave, where the variations of these quantities with respect to Z become stronger for the Mooney-Rivlin material. As in the previous case, the f' (or v) wave exhibits a perturbation as it passes through the $\frac{\partial g'}{\partial Z}$ (or $\frac{\partial u}{\partial Z}$) discontinuity. Similarly, the g' (or u) wave exhibits a perturbation as it passes through the $\frac{\partial f'}{\partial Z}$ (or $\frac{\partial v}{\partial Z}$) discontinuity. It is evident from the figures that these perturbations become stronger for the Mooney-Rivlin material. Tait and Zhong

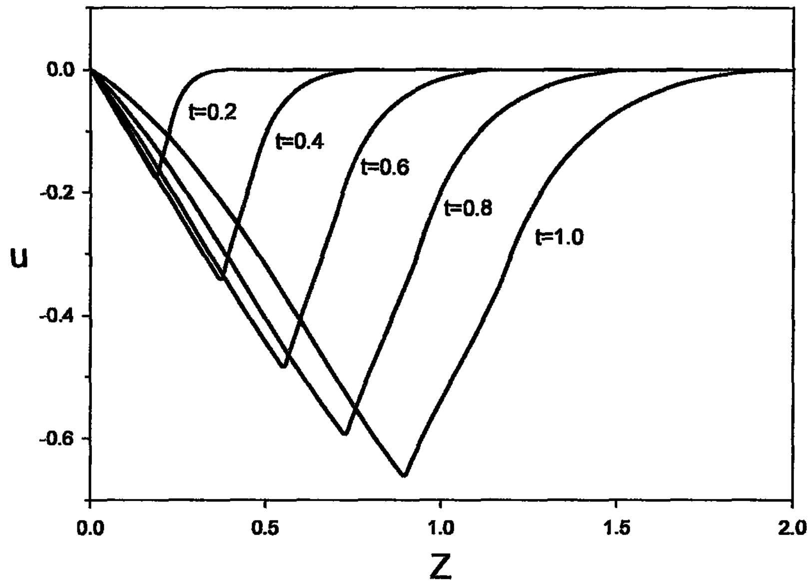

Figure 5.14: u as a function of Z at various times. $\Delta Z = 10^{-3}$, $\Delta t = 0.25 \times 10^{-3}$, $L = 2$, $v_0 = 1$, $\gamma = 0.3$.

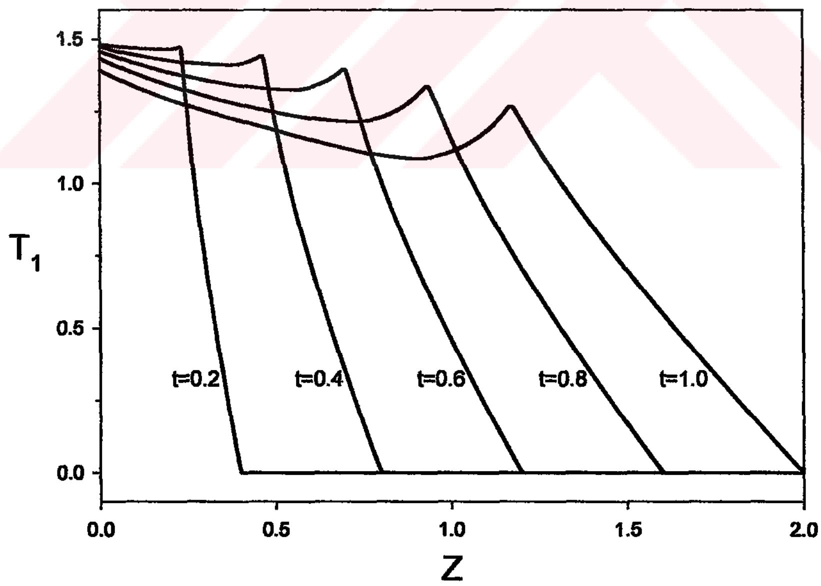

Figure 5.15: T_1 as a function of Z at various times. $\Delta Z = 10^{-3}$, $\Delta t = 0.25 \times 10^{-3}$, $L = 2$, $v_0 = 1$, $\gamma = 0.3$.

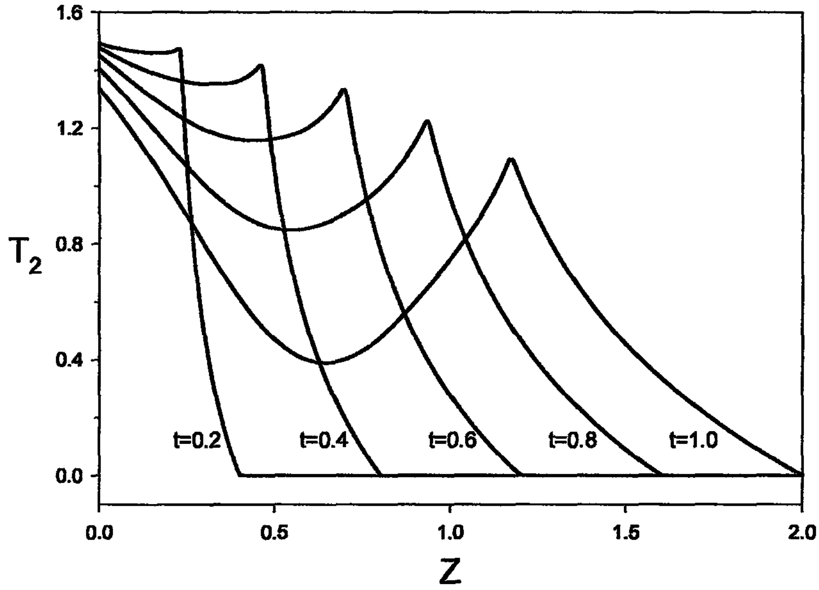

Figure 5.16: T_2 as a function of Z at various times. $\Delta Z = 10^{-3}$, $\Delta t = 0.25 \times 10^{-3}$, $L = 2$, $v_0 = 1$, $\gamma = 0.3$.

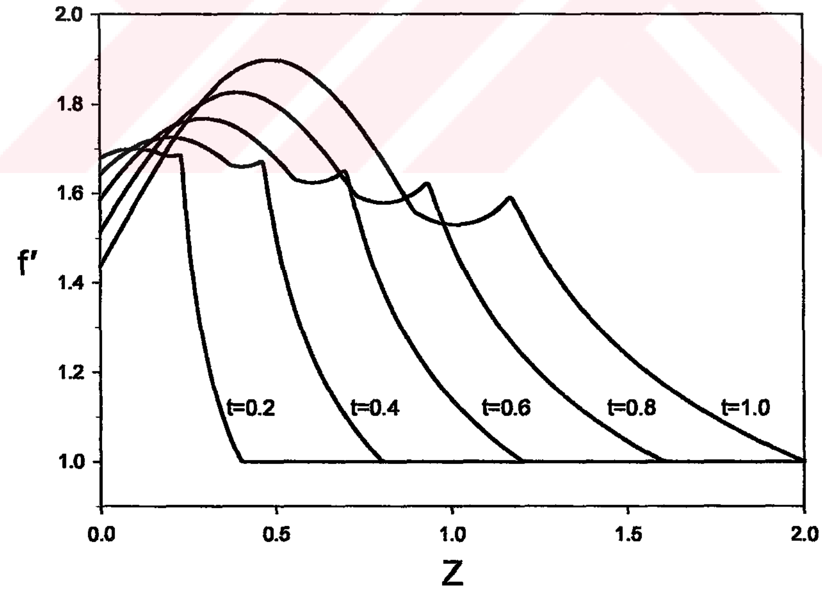

Figure 5.17: f' as a function of Z at various times. $\Delta Z = 10^{-3}$, $\Delta t = 0.25{\times}10^{-3}$, $L = 2$, $v_0 = 1$, $\gamma = 0.3$.

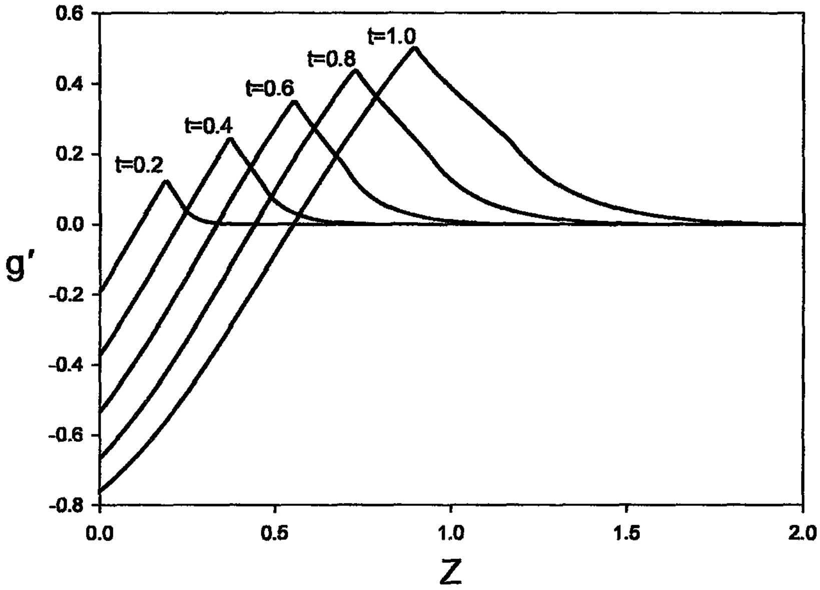

Figure 5.18: g' as a function of Z at various times. $\Delta Z = 10^{-3}$, $\Delta t = 0.25\times10^{-3}$, $L = 2$, $v_0 = 1$, $\gamma = 0.3$.

[5] present the numerical results for λ_1 and λ_2 only in the case of Mooney-Rivlin material. A comparison of the numerical results corresponding to λ_1 and λ_2 shows good agreement between the numerical results in the present study and those given in [5].

5.4 Numerical Results: The Compressible Problem

In this section, we extend the approach in the previous two sections to the case of compressible hyperelastic materials. We consider the problem of dynamic extension of a membrane tube made of a compressible hyperelastic material and solve the problem numerically by using the second-order Godunov method. Since the resulting equations, except those related to the constitutive relations, are equivalent to those in Section 5.2, we do not repeate them here. In short, equations (5.1)-(5.21) are also valid for the compressible problem. We present the numerical results corresponding to both the neo-Hookean compressible material and the Blatz-Ko compressible material.

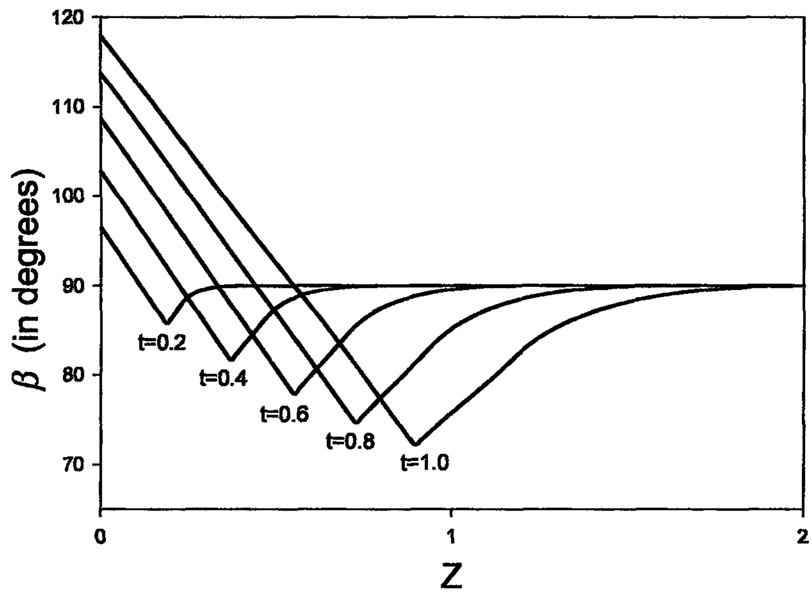

Figure 5.19: β as a function of Z at various times. $\Delta Z = 10^{-3}$, $\Delta t = 0.25\times 10^{-3}$, $L = 2$, $v_0 = 1$, $\gamma = 0.3$.

Te nondimensional form of the strain-energy function corresponding to the neo-Hookean compressible material is

$$W(\Lambda_1, \Lambda_2, \Lambda_3) = \frac{1}{2}(\Lambda_1^2 + \Lambda_2^2 + \Lambda_3^2 + \Lambda_1^{-2}\Lambda_2^{-2}\Lambda_3^{-2} - 4). \tag{5.31}$$

from which the principal Biot stresses T_1 and T_2 given by (5.6) are calculated as

$$T_1 = \lambda_1 - \lambda_1^{-3}\lambda_2^{-2}\lambda_3^{-2}\,, \quad T_2 = \lambda_2 - \lambda_1^{-2}\lambda_2^{-3}\lambda_3^{-2}\,. \tag{5.32}$$

We now use the restriction given by (3.108) to eliminate λ_3 from these equations. For the neo-Hookean compressible material, (3.108) gives λ_3^2 in the form

$$\lambda_3^2 = \lambda_1^{-1}\lambda_2^{-1}\,. \tag{5.33}$$

Then we can rewrite

$$T_1 = \lambda_1 - \lambda_1^{-2}\lambda_2^{-1}\,, \quad T_2 = \lambda_2 - \lambda_1^{-1}\lambda_2^{-2}\,. \tag{5.34}$$

It follows from (5.17) that

$$C_L^2 = 1 + 2\lambda_1^{-3}\lambda_2^{-1}\,, \quad C_T^2 = 1 - \lambda_1^{-3}\lambda_2^{-1}\,. \tag{5.35}$$

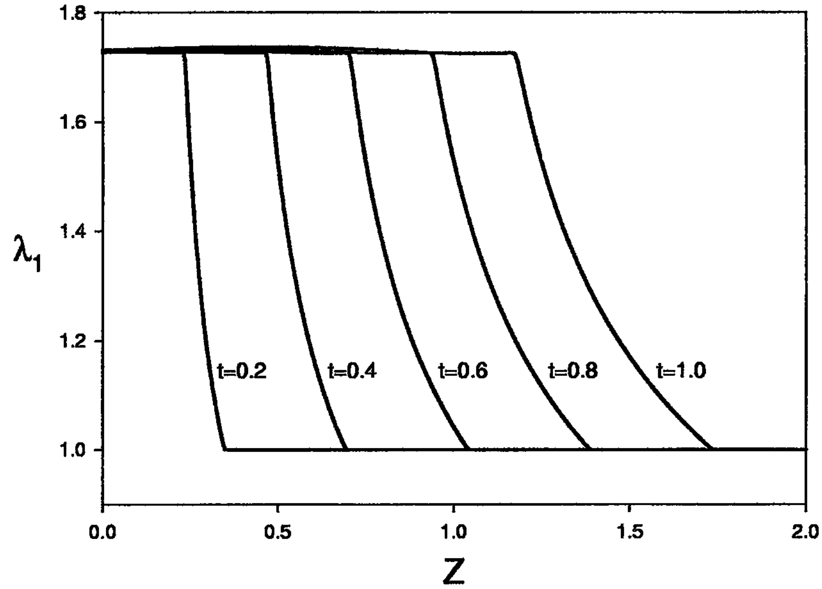

Figure 5.20: λ_1 as a function of Z at various times for the neo-Hookean compressible material. $\Delta Z = 10^{-3}$, $\Delta t = 0.25 \times 10^{-3}$, $L = 2$, $v_0 = 1$.

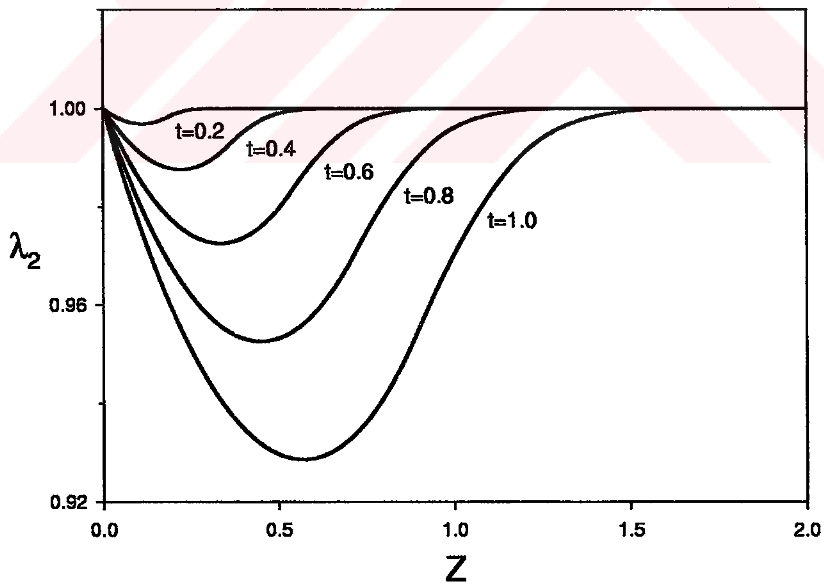

Figure 5.21: λ_2 as a function of Z at various times for the neo-Hookean compressible material. $\Delta Z = 10^{-3}$, $\Delta t = 0.25 \times 10^{-3}$, $L = 2$, $v_0 = 1$.

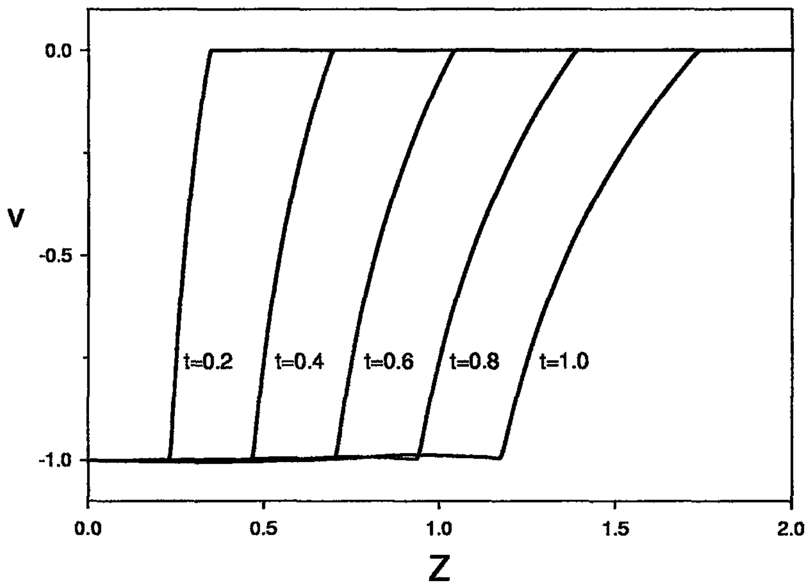

Figure 5.22: v as a function of Z at various times for the neo-Hookean compressible material. $\Delta Z = 10^{-3}$, $\Delta t = 0.25 \times 10^{-3}$, $L = 2$, $v_0 = 1$.

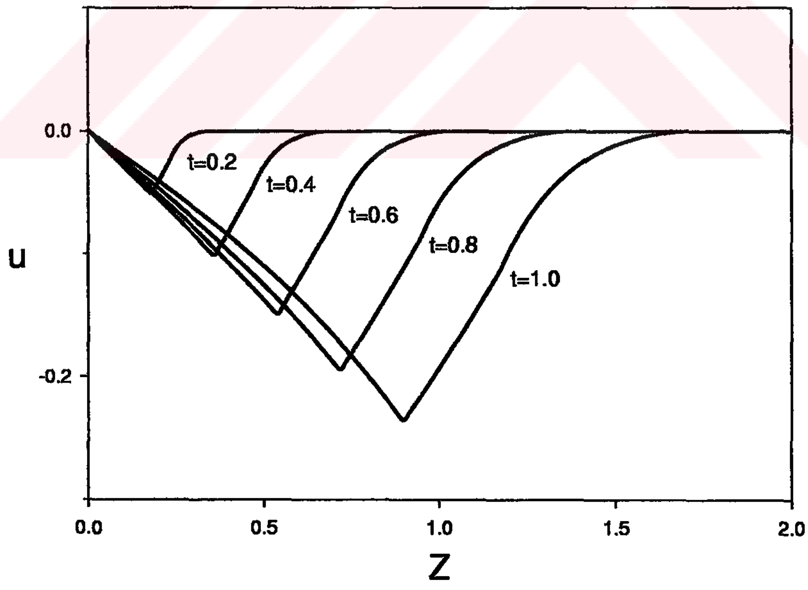

Figure 5.23: u as a function of Z at various times for the neo-Hookean compressible material. $\Delta Z = 10^{-3}$, $\Delta t = 0.25 \times 10^{-3}$, $L = 2$, $v_0 = 1$.

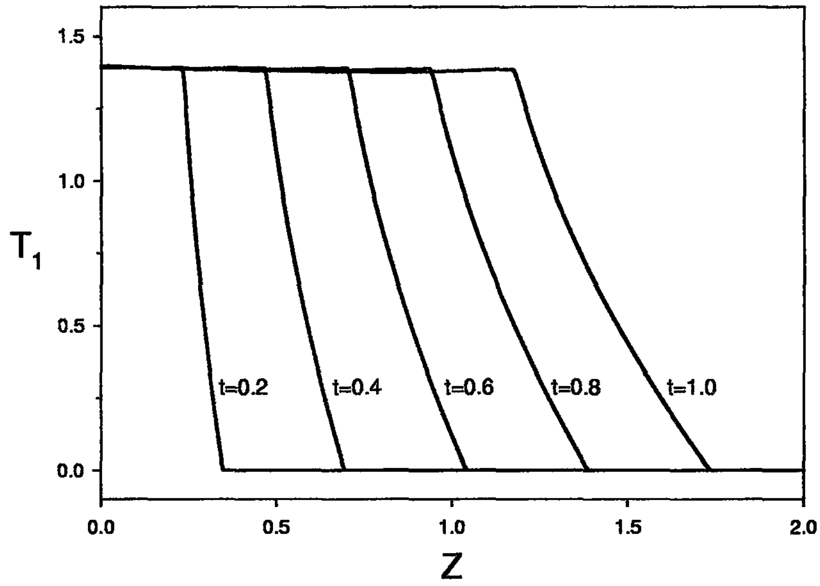

Figure 5.24: T_1 as a function of Z at various times for the neo-Hookean compressible material. $\Delta Z = 10^{-3}$, $\Delta t = 0.25 \times 10^{-3}$, $L = 2$, $v_0 = 1$.

It is obvious from (5.35) that $C_L^2 > 0$. Also it follows from (5.35) that $C_T^2 > 0$ provided

$$\lambda_1^3 \lambda_2 > 1 \ . \tag{5.36}$$

As in the incompressible problem, there exist four waves propagating in the tube and two of them propagate in the positive direction along the tube whereas the remaining two propagate in the negative direction. Since

$$C_L^2 - C_T^2 = 3\lambda_1^{-3}\lambda_2^{-1} > 0 \ , \tag{5.37}$$

we have $C_L^2 > C_T^2 > 0$ whenever $\lambda_1^3\lambda_2 > 1$. Therefore the eigenvalues of $\mathbf{A}$ are all real and distinct whenever $\lambda_1^3\lambda_2 > 1$. That is, the system (5.11) is strictly hyperbolic and there is no degeneracy. We now apply the numerical scheme for the parameter values given by

$$L = 2 \ , \qquad v_0 = 1 \ , \tag{5.38}$$

again. Figures 5.20 - 5.27 show the values of λ_1, λ_2, v, u, T_1, T_2, f' and g' as a function of Z at various times. As is seen from these figures the remarks

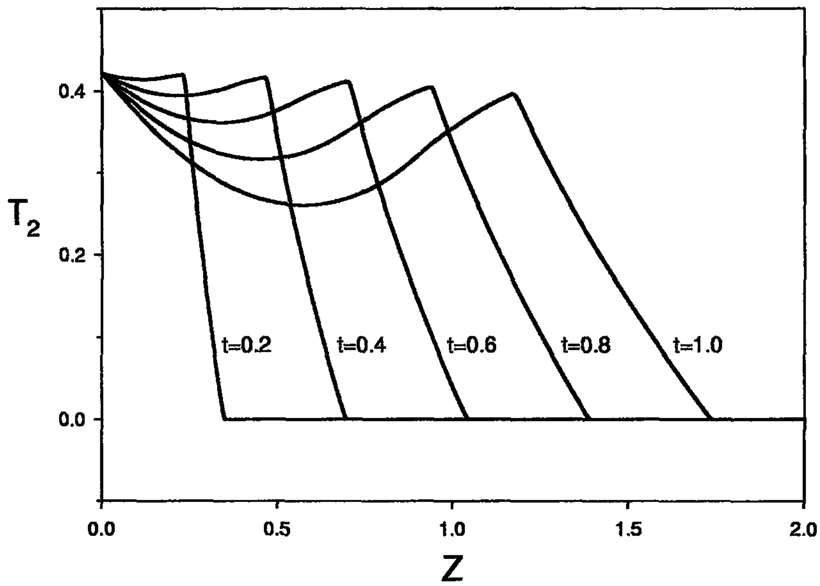

Figure 5.25: T_2 as a function of Z at various times for the neo-Hookean compressible material. $\Delta Z = 10^{-3}$, $\Delta t = 0.25 \times 10^{-3}$, $L = 2$, $v_0 = 1$.

made above for the neo-Hokean incompressible material are qualitatively valid for the neo-Hookean compressible material too. Recall that we take the undeformed configuration as the initial configuration. Therefore, the membrane is undisturbed ahead of the fastest wave. We observe that the fastest wave is again a pure stretching expansion wave, that is, a f' (or v) wave. The leading edge of the f' wave travels at speed $C_L|_{\lambda_1=\lambda_2=1} = \sqrt{3}$. Behind the wavefront associated with the f' wave interaction takes place and a g' (or u) wave propagates. We also observe from Figures 5.20 - 5.27 that there are jumps in $\frac{\partial \lambda_1}{\partial Z}$, $\frac{\partial v}{\partial Z}$, $\frac{\partial u}{\partial Z}$, $\frac{\partial T_1}{\partial Z}$, $\frac{\partial T_2}{\partial Z}$, $\frac{\partial f'}{\partial Z}$ and $\frac{\partial g'}{\partial Z}$ but no jump in $\frac{\partial \lambda_2}{\partial Z}$. As in the incompressible problem, there is an effect due to these discontinuities. The f' (or v) wave exhibits a perturbation as it passes through the $\frac{\partial g'}{\partial Z}$ (or $\frac{\partial u}{\partial Z}$) discontinuity. Similarly, the g' (or u) wave exhibits a perturbation as it passes through the $\frac{\partial f'}{\partial Z}$ (or $\frac{\partial v}{\partial Z}$) discontinuity. It may be difficult to distinguish these perturbations from the figures for the compressible neo-Hookean material as it is for the incompressible neo-Hookean material.

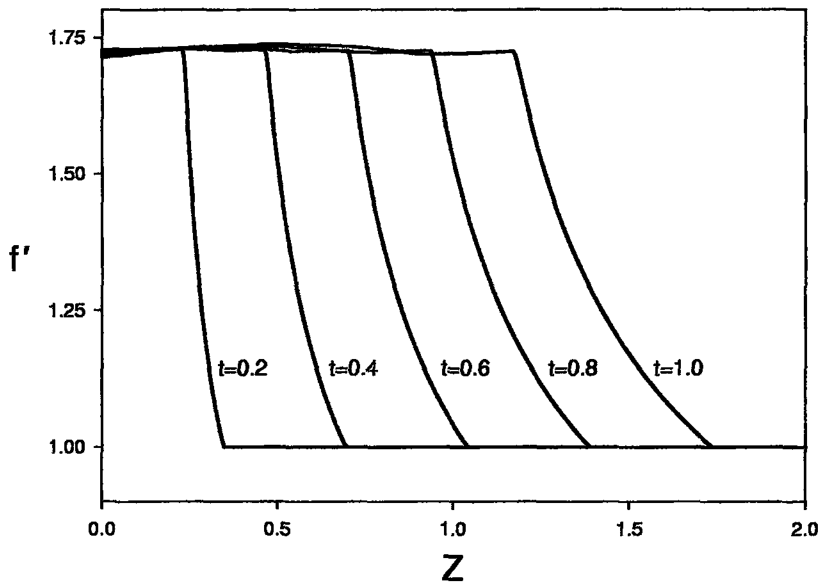

Figure 5.26: f' as a function of Z at various times for the neo-Hookean compressible material. $\Delta Z = 10^{-3}$, $\Delta t = 0.25 \times 10^{-3}$, $L = 2$, $v_0 = 1$.

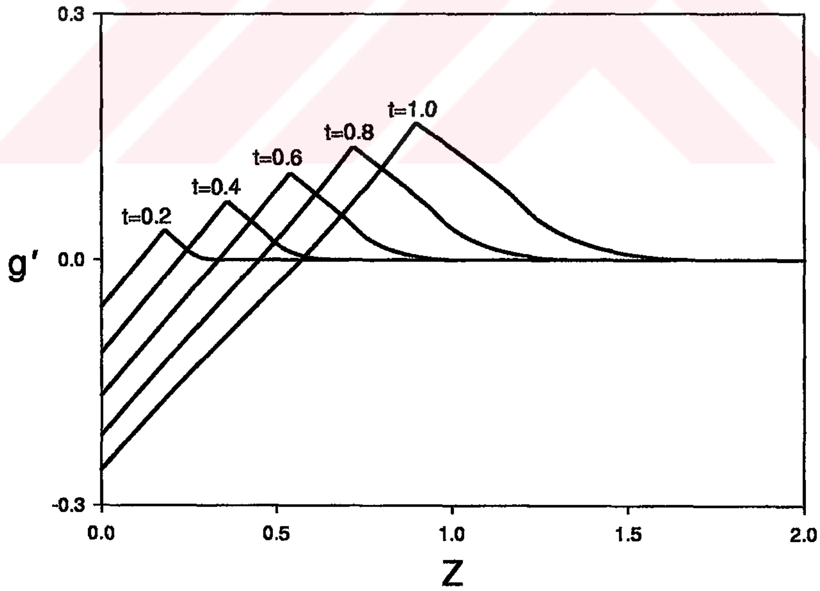

Figure 5.27: g' as a function of Z at various times for the neo-Hookean compressible material. $\Delta Z = 10^{-3}$, $\Delta t = 0.25 \times 10^{-3}$, $L = 2$, $v_0 = 1$.

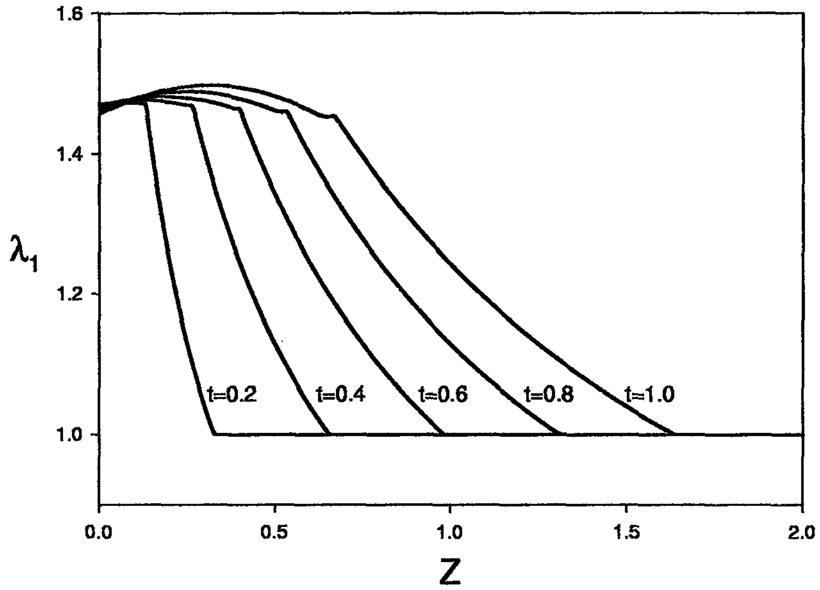

Figure 5.28: λ_1 as a function of Z at various times for the Blatz-Ko material. $\Delta Z = 10^{-3}$, $\Delta t = 0.25 \times 10^{-3}$, $L = 2$, $v_0 = 0.5$.

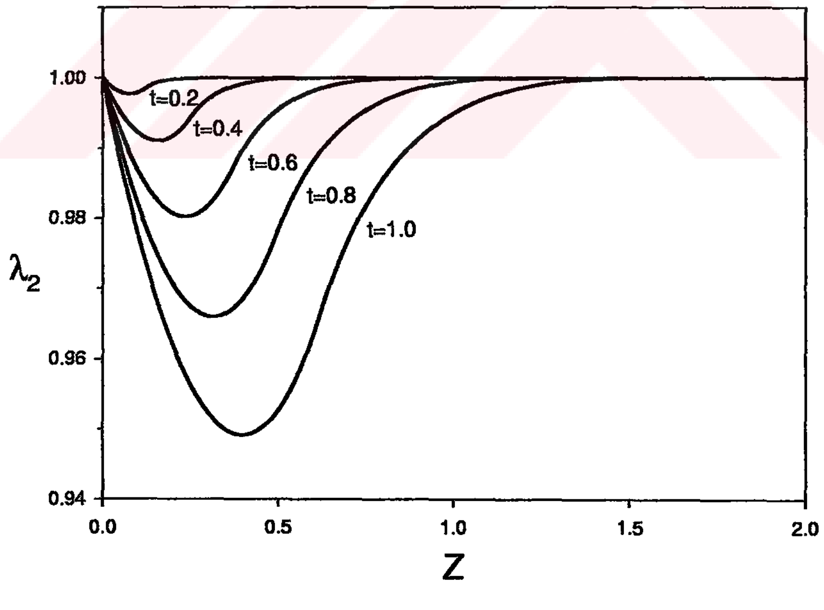

Figure 5.29: λ_2 as a function of Z at various times for the Blatz-Ko material. $\Delta Z = 10^{-3}$, $\Delta t = 0.25 \times 10^{-3}$, $L = 2$, $v_0 = 0.5$.

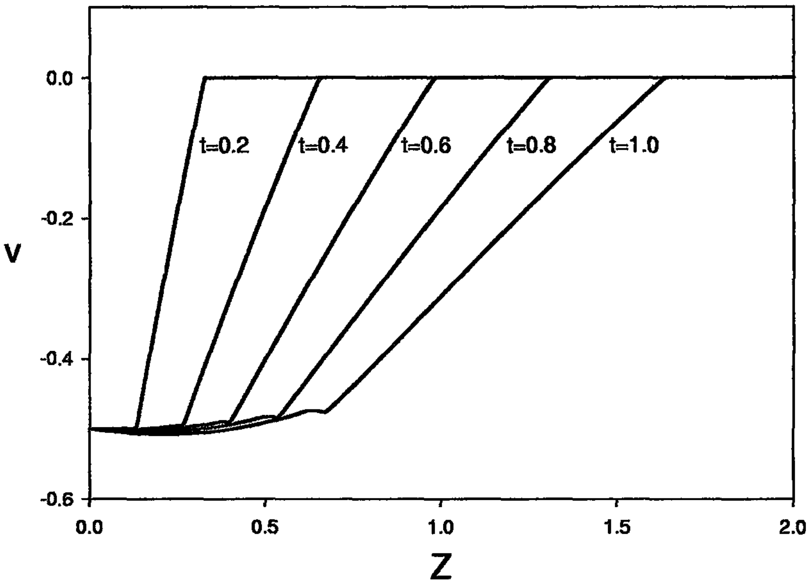

Figure 5.30: v as a function of Z at various times for the Blatz-Ko material. $\Delta Z = 10^{-3}$, $\Delta t = 0.25 \times 10^{-3}$, $L = 2$, $v_0 = 0.5$.

We now represent the numerical results corresponding to a membrane tube made of the Blatz-Ko compressible material. The nondimensional form of the strain-energy function corresponding to the Blatz-Ko compressible material is

$$W(\Lambda_1, \Lambda_2, \Lambda_3) = \frac{1}{2}(\Lambda_1^{-2} + \Lambda_2^{-2} + \Lambda_3^{-2} + 2\Lambda_1\Lambda_2\Lambda_3 - 5), \tag{5.39}$$

from which the principal Biot stresses T_1 and T_2 given by (5.6) are computed as

$$T_1 = -\lambda_1^{-3} + \lambda_2\lambda_3 \ , \quad T_2 = -\lambda_2^{-3} + \lambda_1\lambda_3 \tag{5.40}$$

We now use the restriction given by (3.108) to eliminate λ_3 from these equations. For the Blatz-Ko material, (3.108) gives λ_3 in the form

$$\lambda_3 = (\lambda_1\lambda_2)^{-1/3} \tag{5.41}$$

Then we can express T_1 and T_2 as

$$T_1 = -\lambda_1^{-3} + \lambda_1^{-1/3}\lambda_2^{2/3} \ , \quad T_2 = -\lambda_2^{-3} + \lambda_1^{2/3}\lambda_2^{-1/3} \ . \tag{5.42}$$

It follows from (5.17) that

$$C_L^2 = -\frac{1}{3}\lambda_1^{-4/3}\lambda_2^{2/3} + 3\lambda_1^{-4} \ , \quad C_T^2 = \lambda_1^{-4/3}\lambda_2^{2/3} - \lambda_1^{-4} \ . \tag{5.43}$$

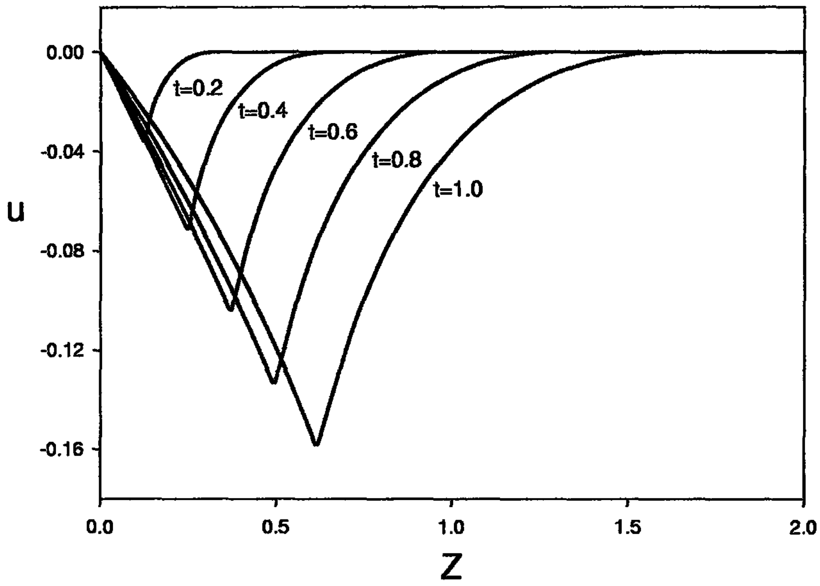

Figure 5.31: u as a function of Z at various times for the Blatz-Ko material. $\Delta Z = 10^{-3}$, $\Delta t = 0.25 \times 10^{-3}$, $L = 2$, $v_0 = 0.5$.

If we introduce a new function $\alpha(\lambda_1, \lambda_2)$ through the relation

$$\alpha(\lambda_1, \lambda_2) = \lambda_1^{-4} - \frac{1}{3}\lambda_1^{-4/3}\lambda_2^{2/3} , \tag{5.44}$$

we can easily deduce that

$$C_L^2 = 2\lambda_1^{-4} + \alpha , \quad C_T^2 = 2\lambda_1^{-4} - 3\alpha , \quad C_L^2 - C_T^2 = 4\alpha . \tag{5.45}$$

Then we observe that $C_L^2 > C_T^2 > 0$ whenever

$$0 < \alpha(\lambda_1, \lambda_2) < \frac{2}{3}\lambda_1^{-4} \tag{5.46}$$

That is, if this condition is satisfied, the eigenvalues of $\mathbf{A}$ are all real and distinct, and consequently the system (5.11) is hyperbolic. After some numerical experiments we observe that this condition is satisfied if $v_0 \leq 0.714$. Therefore, we apply the numerical scheme for the parameter values given by

$$L = 2 , \qquad v_0 = 0.5 , \tag{5.47}$$

in the case of the Blatz-Ko material. Figures (5.28)-(5.35) show the values of λ_1, λ_2, v, u, T_1, T_2, f' and g' as a function of Z at various times. It is obvious

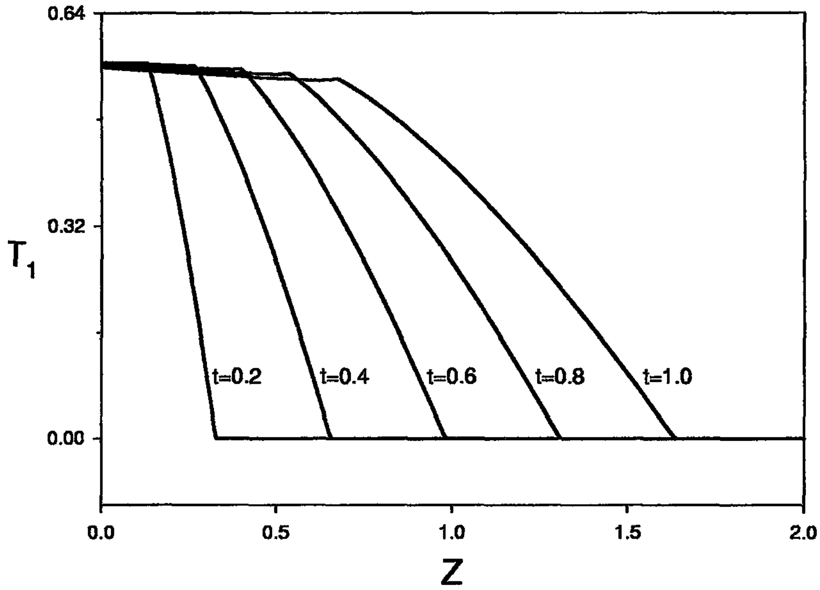

Figure 5.32: T_1 as a function of Z at various times for the Blatz-Ko material. $\Delta Z = 10^{-3}$, $\Delta t = 0.25 \times 10^{-3}$, $L = 2$, $v_0 = 0.5$.

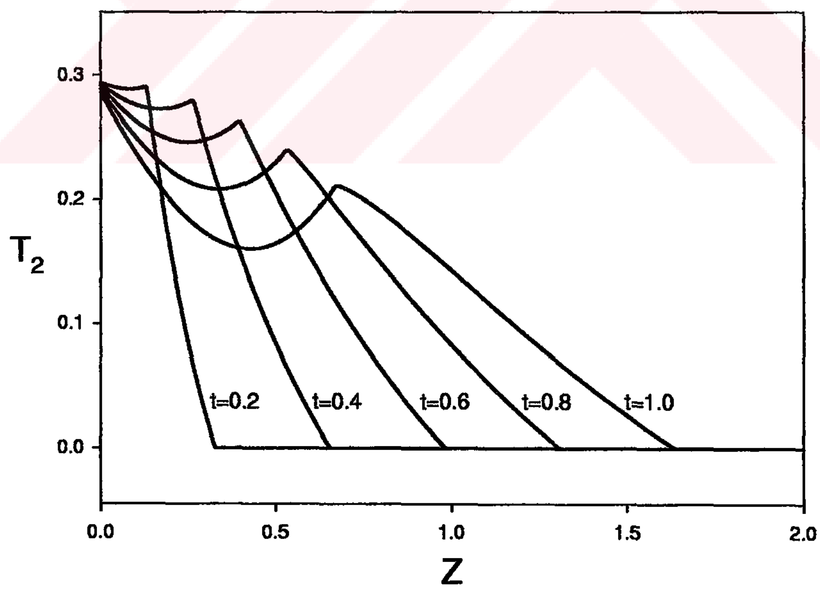

Figure 5.33: T_2 as a function of Z at various times for the Blatz-Ko material. $\Delta Z = 10^{-3}$, $\Delta t = 0.25 \times 10^{-3}$, $L = 2$, $v_0 = 0.5$.

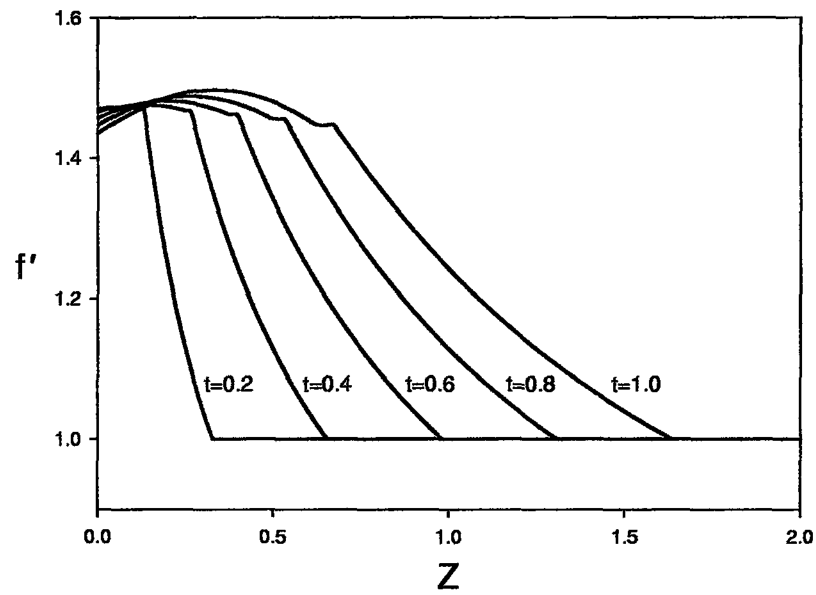

Figure 5.34: f' as a function of Z at various times for the Blatz-Ko material. $\Delta Z = 10^{-3}$, $\Delta t = 0.25 \times 10^{-3}$, $L = 2$, $v_0 = 0.5$.

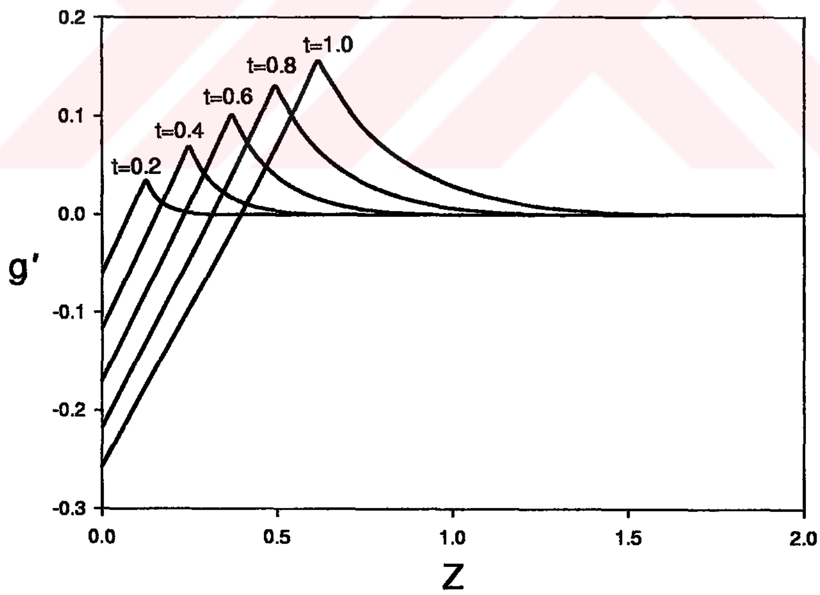

Figure 5.35: g' as a function of Z at various times for the Blatz-Ko material. $\Delta Z = 10^{-3}$, $\Delta t = 0.25 \times 10^{-3}$, $L = 2$, $v_0 = 0.5$.

from these figures that the remarks made above for the neo-Hookean compressible material are qualitatively valid for the Blatz-Ko compressible material too. Since the undeformed configuration is taken as the initial deformation, the membrane tube is undisturbed ahead of the fastest wave. The fastest wave is again a pure streching expansion wave, that is, a f' (or v) wave. The leading edge of the f' wave travels at speed $C_L|_{\lambda_1=\lambda_2=1} = 2\sqrt{\frac{2}{3}}$. Behind the wavefront associated with the f' wave, interaction takes place and a g' (or u) wave propagates. As in the case of the compressible neo-Hookean material, there are jumps in $\dfrac{\partial \lambda_1}{\partial Z}$, $\dfrac{\partial v}{\partial Z}$, $\dfrac{\partial u}{\partial Z}$, $\dfrac{\partial T_1}{\partial Z}$, $\dfrac{\partial T_2}{\partial Z}$, $\dfrac{\partial f'}{\partial Z}$ and $\dfrac{\partial g'}{\partial Z}$ but no jump in $\dfrac{\partial \lambda_2}{\partial Z}$.

6. CONCLUSIONS

In this thesis, an asymptotic theory for membrane equations of thin hyperelastic tubes is developed and the lowest order equations of the asymptotic expansion are studied in detail. Also the propagation of finite amplitude waves in a circular cylindrical hyperelastic membrane when its one end is subjected to dynamic extension is studied numerically by using a Godunov-type finite volume method.

The present discussion of membrane theory is set in a framework which differs in three aspects from that used in the literature. First, finite axisymmetric dynamic deformations of general nonlinearly elastic circular cylindrical membranes were considered in the present work whereas finite static deformations were considered in the literature. Second, the case in which the inner surface of the tube is subjected to both time-dependent normal and tangential tractions was considered whereas the case in which the inner surface is subjected to only normal tractions was considered in the literature. Finally, in the present work the membrane equations are derived in terms of the components of the nominal stress tensor instead of those of the Cauchy stress tensor used in the literature.

The present investigation of the impact problem defined in Chapter 5 is set in a framework which differs in three aspects from that studied by Tait and Zhong [5]. First, in the present work the membrane theory developed in Chapter 3 was used. Secondly, a second-order Godunov method was used to solve numerically the corresponding initial and boundary value problem whereas a numerical technique based on the method of characteristics was used by Tait and Zhong. Finally, the numerical results corresponding to the membrane tubes made of a compressible hyperelastic material were also presented whereas the study of Tait and Zhong was restricted to the membrane tubes made of an incompressible hyperelastic material.

In the present thesis, no attempt was made to consider the case where one end of the membrane tube is subjected to a dynamic radial expansion instead of a dynamic extension, but it is hoped that we may do so in a later study.

REFERENCES

[1] **Ogden, R.W.**, 1984. Non-linear Elastic Deformations, Ellis Horwood Limited, Chichester.

[2] **Haughton, D.M.**, 2001. Elastic membranes in Nonlinear Elasticity: Theory and Applications, LMS lecture notes No.283, ed. Ogden, R.W, Fu, Y.B., pp. 233-267, Cambridge University Press, Cambridge.

[3] **Erbay, H.A.**, 1997. On the asymptotic membrane theory of thin hyper-elastic plates, *Int. J. Eng. Sci.*, **35**, 151-170.

[4] **Erbay, H.A. and Demiray, H.**, 1995. Finite axisymmetric deformations of elastic tubes: An approximate method, *J. Eng. Math.*, **29**, 451-472.

[5] **Tait, R.J. and Zhong, J.L**, 1994. Wave propagation in a non-linear e-lastic tube, *Bull. Tech. Univ.*, **47**, 127-150.

[6] **Tait, R.J. and Zhong, J.L**, 1992. Motion of mass on a non-linear elastic string, *J. Non-Linear Mech.*, **27**, 2, 139-148.

[7] **Narasimhan, Maysore N.L.**, 1993. Principles of Continuum Mechanics, John Wiley, New York.

[8] **Leveque, R.J.**, 1992. Numerical Methods for Conservation Laws, Second edition, Birkhauser, Basel .

[9] **Godlewski, E. and Raviart, P.A.**, 1996. Numerical Approximation of Hyperbolic Systems of Conservation Laws, Springer-Verlag, New York.

[10] **Kröner, D.**, 1997. Numerical Schemes for Conservation Laws, Wiley, West Sussex.

[11] **Lax, P.D.**, 1957. Hyperbolic systems of conservation laws, II., *Comm. Pure Appl. Math.*, **10**, 537-566.

[12] **Godunov, S.K.**, 1959. A finite difference method for the numerical computation of discontinuous solutions of the equations of fluid dynamics, *Mat. Sb.*, **47**, 271-290.

[13] **Lax, P.D. and Wendroff, B.**, 1960. Systems of conservation laws, *Comm. Pure Appl. Math.*, **13**, 217-237.

[14] **van Leer, B.**, 1979. Towards the ultimate conservative difference scheme. V. A second-order sequel to Godunov's method, *J. Comput. Phys.*, **32**, 101-136.

[15] **Osher S.**, 1985. Convergence of generalized MUSCL schemes, *SIAM J. Num. Anal.* **22**, 217-235.

[16] **Haddow, J.B. and Jiang, L.**. Finite amplitude azimuthal shear waves in a compressible hperelastic solid, *ASME J. Appl. Mech.*, in press.

[17] **Chalabi, A.**, 1992. Stable upwind schemes for hyperbolic conservation laws with source terms, *IMA J. Num. Anal.*, **12**, 217-241.

[18] **Green, A.E., Naghdi, P.M., Wainwright, W.L.**, 1965. A general theory of Cosserat surface, *Arch. for Rat. Mech. and Anal.*, **2**, 287-308.

[19] **Tait, R.J. and Zhong, J.L**, 1993. Perturbation methods for the impact problem of a non-linear elastic string, *J. Non-Linear Mech.*, **28**, 6, 713-730.

AUTOBIOGRAPHY

Born on the 15th of April, 1977 in Ankara. Completed primary education at 19 Mayıs Primary School in 1988, and secondary education at Antalya Gazi high school in 1994. Attended Istanbul Technical University, Faculty of Sciences and Letters, Mathematics Department, engineering mathematics program between 1994-1999, and earned her B.Sc. in June 1999. The same year started the M.Sc. program at the Mathematics Department, Istanbul Technical University.

T.C. YÜKSEKÖĞRETİM KURULU
DOKÜMANTASYON MERKEZİ